Aus dem Institut für Anatomie und Zellbiologie
der Philipps-Universität Marburg
Abteilung Molekulare Neurowissenschaften
Direktor: Professor Dr. E. Weihe

Cellular and molecular basis of TNFα, IL-1β and LPS mediated signaling in rat dorsal root ganglion

Inaugural Dissertation
zur Erlangung des Doktorgrades der Humanbiologie
(Dr. rer. physiol.)

dem Fachbereich Humanmedizin
der Philipps-Universität Marburg
vorgelegt

von
Yanzhang Li
aus Henan, V. R. China

Marburg 2004

Angenommen vom Fachbereich Humanmedizin
der Philipps-Universität Marburg am 19.05. 2004
Gedruckt mit Genehmigung des Fachbereichs
Dekan: Prof. Dr. Bernhard Maisch
Referent: Prof. Dr. Eberhard Weihe
Korreferent: Prof. Dr. Michael Lohoff

Contents

1. Introduction

1.1 Role of primary sensory neurons of the dorsal root ganglion

The dorsal root ganglion (DRG) is embedded within the vertebral column along the dorsolateral side of the neural tube. The DRG contains primary sensory neurons and non-neuronal cells such as Schwann cells, satellite cells, macrophages, microglia-like cells and mast cells. DRG neurons are pseudounipolar. One process projects a long distance to peripheral tissues such as the skin, where it detects sensory stimuli. The other branch relays this information to the dorsal horn of spinal cord or to the brain stem (1, 2).

Individual DRG neurons respond selectively to specific types of stimuli because of morphological and molecular specialization of their peripheral terminals. There is functional specialization among DRG neurons on the basis of what environmental stimulus they detect. Distinct classes of these neurons recognize painful stimuli (nociception), innocuous stimuli such as light touch (mechanoreception), and positional information (proprioception) (1).

Nociceptive (pain) neurons detect noxious thermal, mechanical (high-threshold) or chemical stimuli. Among the pain sensing neurons, there is further biochemical and functional diversity. Some DRG neurons are classified as peptidergic, releasing neuropeptides such as calcitonin gene-related peptide (CGRP) and substance P (SP) in response to noxious thermal stimuli and inflammation (1, 3, 4). All SP-positive DRG neurons are known to contain CGRP and these neurons are considered to be a part of nociceptive population of sensory neurons (5, 6). Some neurons are classified as vanilloid receptor 1 (VR1, also referred to as TRPV1) expressing neurons, which is essential for the development of inflammatory thermal hyperalgesia (7-9). VR1, a member of the transient receptor potential (TRP) channel family, is an non-selective ion channel on sensory neurons that is activated by temperatures exceeding 43.8°C, and by capsaicin, the main pungent ingredient in hot chili peppers as well as by protons (7-9). VR1 is expressed predominantly by small-size to medium-size sensory neurons (8).

One very important function of the primary sensory neurons is to provide the information about the occurrence or threat of injury. The perception of pain contributes to this function. Inflammation is the major cause of pain (10). During inflammation proinflammatory cytokines such as tumor necrosis factor alpha (TNFα) and interleukin-1 beta (IL-1β) are released by a variety of cells (e.g., macrophages) to

regulate the inflammatory responses (11). Studies in animals have demonstrated mechanical and thermal hyperalgesia after systemic or local injection of TNFα, IL-1β or lipopolysaccharide (LPS) (12-15). Overexpression of proinflammatory cytokines can lead to systemic syndromes such as septic shock. Therefore, the responses to TNFα, IL-1β or LPS must be controlled. The question how these molecules signal to primary sensory neurons of DRG has not yet been resolved.

1.2 TNFα in the dorsal root ganglion

TNFα is a multipotent proinflammatory cytokine that induces a wide variety of responses including apoptosis in some cells and proliferation in others (16). The principal physiological function of TNFα is to stimulate the recruitment of neutrophils and monocytes to the site of infection and to activate these cells to eradicate microbes. TNFα is the principal mediator of the acute inflammatory response to Gram-negative bacteria and other infectious microbes and is responsible for many systemic responses of severe infections such as septic shock, which is characterized by vascular collapse, disseminated intravascular coagulation, and metabolic disturbances (17). The activated mononuclear phagocytes are the major cellular source of TNFα. In addition, T cells can also be a cellular source of TNFα during the immune response (18). In the nervous system, microglia and astrocytes are believed to be the primary source of TNFα (19-23). In the peripheral nervous system, TNFα has been shown to be produced in macrophages and Schwann cells (24, 25). Recent reports have described the presence of TNFα in primary sensory neurons and its axonal transport in the intact and injured rat sciatic nerve (26-29). TNFα immunoreactivity has been detected in a subpopulation of rat DRG neurons and was reported to be upregulated after chronic constriction injury of the sciatic nerve (28, 29). However, whether TNFα is truly synthesized by primary sensory neurons has not yet been demonstrated.

1.3 TNF receptor subtypes and their expression in primary sensory neurons of the dorsal root ganglion

The ability of TNFα to influence cellular functions depends on the expression of TNF receptors and activation of specific intracellular signaling pathways. There are two distinct TNF receptors of 55 kD (type I TNF receptor-TNFR1, or p55) and 75 kD (type II TNF receptor-TNFR2, or p75). The majority of TNFα effects are transmitted

through TNFR1. However, recent studies of knockout mice indicate that TNFR2 plays an important role in neurodegeneration (30).

Analysis of mice lacking TNFR1 or TNFR2 indicates that TNFR2 is critical to proliferation of oligodendrocyte progenitors and remyelination (30). In retinal ischemia, TNFR1 augments neuronal death, whereas TNFR2 promotes neuroprotection (31). Complementary DNAs coding for human and mouse TNFR2 have been reported (32-34). The gene structures of the human and mouse TNFR2 gene have been determined (35, 36). However, except of one previous report describing three transcripts of the rat TNFR2 gene in microglia (37), the full length cDNA and the structure of the rat TNFR2 gene have not yet been fully characterized.

TNFR1 and TNFR2 have been localized in rat DRG neurons by immunohistochemistry (27, 29, 38, 39), but proof of their neuronal biosynthesis by demonstrating their mRNAs is still missing. In DRG cultures containing both neurons and non-neuronal cells, Pollock and coworkers demonstrated positive immunofluorescence on neurons for both TNF receptors (38). However, a cellular expression analysis of TNFR1 and TNFR2 at the mRNA level has not been performed. One previous report has described TNFR1 and TNFR2 transcripts in neurons of mouse trigeminal ganglia (40), but the neuronal signals for TNFR2 are extremely low, close to background. Therefore, it is of critical importance to further investigate the cell-specific expression of TNF receptors in rat primary afferents at the mRNA level.

1.4 TNFα and nociception

Several studies have shown that TNFα is involved in the generation of inflammatory pain, neuropathic pain and hyperalgesia through its actions in the periphery and in the central nervous system (CNS) (14, 15, 41-53). Intracerebroventricular (i.c.v.) injection of TNFα induces thermal hyperalgesia in rats (54). Intrathecal administration of TNFα not only produces hyperalgesia but also changes the spinal cord neuronal responses to nociceptive stimuli in the rat (50). Acutely administered TNFα to the nerve trunk elicits an acute mechanical hyperalgesia in the awake rat (45). Endoneural injection of TNFα has been also shown to induce axonal degeneration, demyelination and thermal hyperalgesia and to evoke ectopic activity in isolated nerve fibers when applied topically (44). Recombinant TNFα can excite nociceptors and induce heat-evoked release of CGRP from the peripheral nerve terminals in the rat skin model (55). In chronic constriction injury (CCI), an animal model of injury-induced painful mononeuropathy, inhibition of the synthesis, release,

or functional neutralization of TNFα results in reduced pain-associated behavior (46-48). Thalidomide, a selective blocker of TNFα production can reduce thermal hyperalgesia and mechanical allodynia in animals with CCI (53). Neutralizing antibodies against TNFα can reduce pain-related behavior in CCI and partial sciatic nerve transection (PST) (47, 48). Administration of soluble TNFR1 attenuates mechanical allodynia in a rat model of neuropathic pain. TNFα-induced hyperalgesia seems to depend on TNFR1 (46, 56). Epineural injection of neutralizing antibodies against TNFR1 in mice subjected to CCI reduces thermal hyperalgesia and mechanical allodynia, while application of neutralizing antibodies against TNFR2 does not (46). Antisense oligodeoxyribonucleotides against TNFR1 reduces hyperalgesia (56). However, whether and which TNF receptor is involved in nociceptive responses is not fully understood. Thus, it needs to be investigated which category of primary sensory neurons is responsible for the TNFα-induced nociception.

1.5 IL-1β and IL-1R1 and their expression in the dorsal root ganglion

IL-1 is a 17 kDa polypeptide produced by a large variety of cells including macrophages, fibroblasts, keratinocytes, synoviocytes, mast cells, glial cells, and neurons (57, 58). The activated mononuclear phagocytes are the major cellular source of IL-1. IL-1 production by mononuclear phagocytes is induced by bacterial products such as LPS and by other cytokines such as TNFα. Biologically active IL-1 consists of two distinct forms called IL-1α and IL-1β, respectively. The principal function of IL-1 is as a mediator of the host inflammatory response to infections and other inflammatory stimuli. IL-1 is a pleiotropic proinflammatory cytokine. In addition to its immune functions, IL-1 is involved in nociceptive behavior (19, 59) and seems to play a role in neural regeneration after axotomy in rat DRG (60). In cultured DRG cells, IL-1β has been shown to induce the release of SP (61, 62).

The ability of IL-1 to influence cellular functions depends on the expression of the appropriate receptor. Two different membrane receptors for IL-1 have been characterized. The type 1 receptor (IL-1R1) is the major receptor for IL-1-mediated biologic responses. The type 2 receptor (IL-1R2) does not transmit any signal and its major function is to act as a decoy receptor that competitively inhibits IL-1 binding to the type I signaling receptor (57, 58, 63-67). IL-1R1 knockout mice no longer respond to intraperitoneal or intracerebroventricular injected IL-1 (68-71). In the same way,

IL-1R1 inhibition by a neutralizing antibody injected in the lateral ventricle of the brain abrogates the behavioral effects of intracerebroventricular applied IL-1β (72). In contrast, inhibition of IL-1R2 potentiates this effect (73).

The constitutive expression of IL-1 receptors has been described on both glia and neurons in several brain regions (66, 72, 74-81). So far only one study by Copray and coworkers (82) reported the expression of IL-1β and IL-1R1 in rat DRG neurons. Based on in situ hybridization using non-radioactive labeled probes or immunocytochemistry these authors have suggested that both IL-1β mRNA and IL-1R1 mRNA are expressed in DRG neurons (82). They further suggested that IL-1β acts on primary sensory neurons in an autocrine or paracrine manner (82). However, non-neuronal cells in the DRG including macrophages which represent the most likely source of IL-1β synthesis have not been shown to synthesize IL-1β. Therefore, it is necessary to further investigate neuronal and non-neuronal expression pattern of IL-1β and IL-1R1 in DRG with more sensitive methods including in situ hybridization with radioactive labeled probes and laser capture microdissection (LCM) in combination with RT-PCR.

1.6 IL-1β and pain

IL-1 has been shown to be involved in nociceptive behavior (19, 59). When administered centrally or peripherally, IL-1β has been found to induce hyperalgesia in diverse animal pain models (59). The nociceptive responses to IL-1β in rats have been reported after central administration by various routes. Intracerebroventricular (i.c.v.) injection of IL-1β in rats exerts biphasic effects on thermal and mechanical nociception; lower doses cause hyperalgesia but higher doses induce analgesia as assessed by the hot-plate test and paw-pressure test (19, 83-86). I.c.v. injection of low doses of IL-1β enhances the response of wide dynamic range (WDR) neurons in the trigeminal nucleus caudalis to noxious pinch (84). Furthermore, it has been demonstrated that IL-1β is hyperalgesic when microinjected into discrete regions of the hypothalamus and neighboring brain areas (87, 88). When delivered intrathecally, IL-1β enhances dorsal horn neuronal responses, including the acute responses to C-fiber stimulation, wind-up and post-discharge and also causes the development of mechanical allodynia and hyperalgesia (50, 89, 90).

Peripheral administration of IL-1β in rats does affect nociceptive behavior in mice and rats. Intraperitoneal (i.p.) injection of IL-1β has been shown to produce

hyperalgesia as assessed by the tail-flick and the hot-plate test (14, 91). Intra-plantar (i. pl.) injection of IL-1β has revealed its central role in the pathophysiology of inflammatory pain and hyperalgesia (92, 93). When administered subcutaneously, IL-1β is able to produce a dose-dependent increase in the sensitivity of rat paws to mechanical stimulation (13, 92-94). Cutaneous hyperalgesia induced after a plantar injection of IL-1β to the hind-paw skin has been investigated by recording action potentials of the rat dorsal root in response to mechanical and thermal stimuli. It has been demonstrated that small diameter cutaneous nerves are activated (92). However, which category of primary sensory neurons is responsible for IL-1β-induced nociception is not known. In particular, it is not known how IL-1R1 is related to presumed nociceptive neurons expressing CGRP, SP or VR1.

1.7 Effects of LPS on primary sensory neurons of the dorsal root ganglion

Lipopolysaccharide (LPS) is a constant component of the outer cell membrane of gram-negative bacteria, which can activate monocytes/macrophages to produce a number of proinflammatory cytokines such as TNFα, IL-1β, and IL-6 (95). Over-response to LPS can lead to systemic inflammatory syndrome or septic shock (95). Therefore, the responses to infection or LPS must be controlled. However, whether the primary sensory neurons can directly detect an infectious state by sensing LPS is not known. A recent report has revealed that circulating cytokines and endotoxin are not necessary for the activation of the sickness or corticosterone response produced by peripheral E. coli challenge (96). Subcutaneous injection of replicating E. coli produces a robust fever and corticosterone response at a time when there are no detectable increases in circulating cytokines (TNFα, IL-β and IL-6) or endotoxin (96). This suggests the existence of a neural pathway for the detection of bacterial infection signaling from the periphery to the central nervous system. LPS has been shown to affect DRG neuronal activities in vivo and in vitro (97-99). Infusion of bacterial lipopolysaccharide close to the sciatic nerve caused an increase of NADPH-d-positive neurons in the rat L4 dorsal root ganglia on the treated side, whereas sham operation had no effect (97). In cultured DRG neurons, LPS can evoke CGRP release and increase [Ca(2+)](i) (98, 99).

1.8 LPS-related receptors

Recognition of LPS is a complex process. LPS is first bound to a serum protein LBP (LPS-binding protein) (100), which functions by transferring LPS monomers to CD14 (101). CD14 is a high affinity LPS receptor that can either be secreted into the serum (soluble CD14, sCD14) or be expressed on the surface of macrophages (membrane CD14, mCD14). However, mCD14 does not have a cytoplasmic signaling domain (101, 102). Recent studies suggest that toll like receptor 4 (TLR4) functions as the signal-transducing receptor for LPS (103-106). The effects of LPS on DRG neurons could be directly mediated by neuronal LPS receptors. However, it is not known whether TLR4 and/or CD14 are expressed in DRG neurons under in vivo conditions. Therefore, it is of particular interest to investigate the possible expression pattern of TLR4 and CD14, the receptors related to LPS signaling, in DRG.

1.9 LPS and inflammatory pain

Primary sensory neurons respond to noxious stimuli and thus provide a signal to alert the organism of potential injury (10). Pain is experienced predominantly and most severely when the inflamed site is mechanically stimulated by being moved or touched. This tenderness or lowered threshold is referred to as hyperalgesia. Inflammatory pain is a critical defensive and protective reaction to injury or infection. The process of inflammation is conducting the removal of the injured tissue and the eradication of bacteria (11). LPS has been shown to induce hyperalgesia associated with inflammation (14, 50, 91, 107-110). Nociceptive responses induced by LPS in rat and mouse have been reported following various routes of administration. Intrathecal administration of LPS has been found to produce thermal hyperalgesia as measured by the plantar test (111), whereas both thermal hyperalgesia and tactile allodynia were observed in the rat hind paw following intracerebroventricular (i.c.v.) administration (10, 50). The intraplantar (i.pl.) injection of LPS produced central sensitization thereby reducing the threshold for nociceptive stimuli in the tail-flick and hot-plate tests (94). Intraperitoneal (i.p.) administration of LPS produced hyperalgesia in rat hind paws as measured by thermal threshold (110). However, which category of primary sensory neuron is responsible for LPS-induced inflammatory pain is not known.

1.10 Aims

The aims of this thesis were the following:

1. **Characterization of the rat TNFR2 gene**

   To investigate the gene expression of rat TNF receptors, the basic information of rat TNFR2 gene needed to be obtained. Therefore, the cDNA sequence and the gene structure of rat TNFR2 had to be characterized first followed by the analysis of the tissue-specific expression and the regulation of rat TNFR2 gene by LPS.

2. **Characterization of the constitutive and LPS-induced cell specific expression pattern of TNF receptors in DRG**

   To examine the effects of systemic LPS on the expression of TNF receptors in rat DRG, RT-PCR and Northern blot analysis were performed on RNA extracts of control rats and of rats after LPS challenge. To prove the neuronal expression of TNF receptors in primary sensory neurons and to clarify which TNF receptor is expressed in DRG neurons, the cellular expression pattern of these receptors were analyzed by laser capture microdissection combined with RT-PCR and by in situ hybridization. The sensory cell line F11 was used as an in vitro model to investigate the neuronal expression of TNF receptors. To address the molecular basis of TNFα-induced nociceptive effects on primary sensory neurons, colocalization of anticipated neuronal TNF receptor in presumed nociceptive DRG neurons expressing CGRP, SP or VR1 was investigated using double labeling ISH.

3. **Investigation of the constitutive and LPS-induced expression pattern of TNFα in the DRG**

   To clarify whether TNFα is synthesized in primary sensory neurons or non-neuronal cells, the cellular expression pattern of TNFα was examined under unchallenged conditions and after LPS treatment using RT-PCR analysis on RNA extracts of microdissected cells and by in situ hybridization.

4. **Examination of the constitutive and LPS-induced expression pattern of IL-1β and IL-1R1 in DRG**

   To solve the controversial question as to whether IL-1β is synthesized in DRG neurons and to further prove the neuronal expression of IL-1R1, the expression of IL-1β and IL-1R1 mRNAs was investigated under unchallenged conditions and after LPS treatment using RT-PCR analysis of DRG RNA extracts and of RNA extracts from microdissected DRG neurons. To determine the cellular distribution

of IL-1β and IL-1R1 in DRG, in situ hybridization was performed using radioactive labeled probes. In order to confirm the neuronal expression of IL-1R1, Northern blot analysis was conducted on poly(A)$^+$ RNA isolated from F11 cells and from DRGs. To address the molecular basis of IL-1β-induced nociceptive effects on primary sensory neurons, colocalization studies of IL-1R1 in presumed nociceptive DRG neurons expressing CGRP, SP or VR1 were performed using double labeling ISH.

5. Analysis of toll-like receptor 4 and CD14 expression in DRG and the influence of LPS

To address the question whether primary sensory neurons can directly detect an infectious state by sensing LPS, the expression of the LPS related receptors, TLR4 and CD14 was investigated under unchallenged conditions and after LPS treatment using RT-PCR and Northern blot analysis of DRG total RNAs or poly(A)$^+$ RNA, and/or using RT-PCR analysis of the RNAs from the microdissected cells. To investigate the cellular distribution of TLR4 and CD14 in DRG, in situ hybridization was performed. In order to address the molecular basis of LPS-induced nociceptive effects on primary sensory neurons, colocalization studies of neuronal LPS receptors in presumed nociceptive DRG neurons expressing CGRP, SP or VR1 were carried out using double labeling ISH.

2 Materials and Methods

2.1 Materials

2.1.1 Equipment

β-γ Detector LB122 Berthold	Amersham, Braunschweig
Cell culture incubatorHERAcell	Heraeus, Hanau, Germany
CM 3050 Kryostat	Leica, Nussloch
DNA-Engine PTC-200	MJ Research, Watertown, USA
Gene Amp PCR System 9700	Perkin Elmer, Foster City, USA
Gel Doc 1000	BioRad, Hercules, USA
Mini-PROTEAN II electrophoresis cell	BioRad, Hercules, USA
HM 500 OM Kryostat	Microm, Walldorf
Hybridization oven	Bachofer, Reutlingen
MCID M5 Image analysis system	Imaging Research, St. Catharines, Canada
Microscope AX 70	Olympus Optical, Hamburg, Germany
PixCell II Laser-Capture-Microscope	Arcturus, San Diego, USA
Power supply units	BioRad, Hercules, USA
Mini Trans-Blot Electrophoretic Transfer Cell	BioRad, Hercules, USA
Turboblotter	Schleicher&Schuell, Dassel
UV Stratalinker 2400	Stratagene, Amsterdam, Netherlands
Wallac 1410, Liquid Scintillation Counter	Pharmacia, Freiburg

2.1.2 Chemicals and reagents

Acetic anhydride	Sigma, Deisenhofen
Acrylamide/Bisacrylamide	Roth, Karlsruhe
Agar	Fluka, Buchs
Agarose	Gibco-BRL, Neu Isenburg
Ammonium persulfate	Serva, Heidelberg
Ampicillin	Gibco-BRL, Karlsruhe
Antibiotic-Antimycotic (100 x)	Gibco-BRL, Karlsruhe
5-bromo-4-chloro-3-indolyl-phosphate-4-toluidine salt (BCIP)	Roche, Mannheim
Boric acid	Merck, Darmstadt
Bromphenol blue sodium salt	Serva, Heidelberg
Calcium Chloride	Merck, Darmstadt
Chloramphenicol	Sigma, Munchen
Chloroform	Merck, Darmstadt
Cresylviolet	Fluka, Buchs

D19 developer	Kodak, New Haven, USA
Denhardt's Reagent (50 x)	Sigma, Deisenhofen
DePex	Serva, Heidelberg
Deoxynucleoside triphosphate (dNTP)	Roche, Mannheim
Dextransulfate (Na-Salt)	Sigma, Deisenhofen
Digoxigenin RNA Labeling Mix	Roche, Mannheim
Dimethylformamide	Fluka, Buchs
Dimethyl sulfoxide (DMSO)	Sigma, Deisenhofen
Dithiothreitol (DTT)	Roche, Mannheim
Dulbecco's Minimal Essential Medium (DMEM)	Gibco-BRL, Karlsruhe
Diethyl pyrocarbonate (DEPC)	Roche, Mannheim
Ethanol	Merck, Darmstadt
Ethidium bromide	Roth, Karlsruhe
Ethylene diaminetetraacetic acid (EDTA)	Merck, Darmstadt
Fetal bovine serum (FBS)	Gibco-BRL, Karlsruhe
Formamide	Merck, Darmstadt
Formaldehyde, 37%	Merck, Darmstadt
Glacial acetic acid	Merck, Darmstadt
Glycerol	Merck, Darmstadt
Glycine	Roth, Karlsruhe
Guanidine hydrochloride	Roth, Karlsruhe
Ham's F10 Nutient Mixture	Sigma, Deisenhofen
HAT Supplement (100 x)	Gibco-BRL, Karlsruhe
(2-Hydroxyethyl)-1-piperazineethanesulphonic acid (HEPES)	Roth, Karlsruhe
Isopropanol	Sigma-Aldrich, Seelze
isopentane (2-methyl butane)	Fluka, Buchs
Isopropylthio-β-D-galactoside (IPTG)	Applichem, Darmstadt
K5, Autoradiography emulsion	Ilford, London, UK
L-glutamine 200 mM (100 x)	Gibco-BRL, Karlsruhe
β-mercaptoethanol	Sigma, Deisenhofen
Methanol	Sigma-Aldrich, Seelze
Methyl blue	Sigma, Deisenhofen
Na2-EDTA	Merck, Darmstadt
NaOH	Merck, Darmstadt
NBT (4-Nitroblue- Tetrazol - chloride)	Roche, Mannheim
NLS (normal lamb serum)	Sigma, Deisenhofen
Ethylphenyl-polyethylene glycol (NP-40)	USB, Cleveland, Ohio
Non-fat dried milk	Roche, Mannheim

NorthernMax Pre/Hybridization Buffer	Ambion, Austin, USA
NTB2, Autoradiography emulsion	Eastman Kodak, Rochester, NY
NTP (nucleoside triphosphate)	Roche, Mannheim
Phenol/chloroform/isopropanol(25 : 24 : 1)	Roth, Karlsruhe
Phenylmethylsulfonyl fluoride (PMSF)	Sigma, Deisenhofen
Pepstatin A	Sigma, Deisenhofen
Poly (dI-dC)	Sigma-Aldrich, Seelze
RNase inhibitor	MBI Fermentas, St.Leon-Rot, Germany
Roenteroll, developer for X-ray film	Tetenal, Norderstedt
Rotiphorese Gel 30	Roth, Karlsruhe
SDS (Sodium dodecyl sulfate)	Roth, Karlsruhe
Sodium acetate	Roth, Karlsruhe
Sodium azide	Merck, Darmstadt
Sodium acetate	Merck, Darmstadt
Sodium chloride	Merck, Darmstadt
Sonicated salmon sperm DNA	Sigma, Deisenhofen
Superfix, Fixer for X-ray film	Tetenal, Norderstedt
TEMED, tetramethyl ethylene diamine	Roth, Karlsruhe
Tissue-Tek O.C.T compound	Sakura, Zoetwerwounde, Netherlands
Triethanolamine (TEA)	Sigma, Deisenhofen
3-(Triethoxysilyl) propylamine	Merck, Darmstadt
Tris (hydroxymethyl) aminomethane	Roth, Karlsruhe
Triton X100	Sigma, Deisenhofen
TRIzol	Gibco-BRL, Karlsruhe
tRNA	Roche, Mannheim
Tryptone Peptone	DIFCO, Detroid, USA
Trypsin-EDTA solution (10x)	Gibco-BRL, Karlsruhe
Tween 20	Merck, Darmstadt
X-gal	peQLab, Erlangen
Xylene Cyanol	Sigma, Deisenhofen
Xylol	Roth, Karlsruhe
Yeast extract	DIFCO, Detroit, USA

2.1.3 Buffers and solutions

DEPC-treated H_2O

10% (v/v) DEPC in ethanol was diluted in H_2O to 0.1% (v/v).
incubated at 37°C overnight with shaking and autoclaved

20 × SSC

3 M NaCl

0.3 M sodium citrate

pH 7.0

Denhardt´s reagent

1% (w/v) Ficoll 400

1% (w/v) polyvinylpyrrolidone

1% (w/v) bovine serum albumin

10 x PBS (pH 6.75):

1.53 M NaCl

77 mM Na_2HPO4

23 mM NaH_2PO4

TE (pH 8.0)

10 mM Tris (pH 8.0),

1 mM EDTA (pH 8.0)

TAE (pH 8.0):

40 mM Tris-acetate

2 mM EDTA (pH 8.0)

10 x HEPES Buffer

200 mM HEPES (Sigma)

10 mM Na2-EDTA

pH 7.8, adjust with NaOH

Filter and autoclave

RNA Sample Buffer

1 ml 10 x HEPES

5 ml Formamide

1.6 ml 37% Formaldehyde

RNA Loading Buffer

50% glycerol

0.5% Bromophenol blue

0.5% Xylene Cyanol

RNA gel electrophoresis buffer

1 x HEPES buffer

6% Formaldehyde

In situ hybridization buffer

600 mM NaCl

10 mM Tris HCl pH 7.5

1 mM EDTA-Na2

0.05% (w/v) tRNA (20 mg/ml)

1 x Denhardt´s

10% (w/v) Dextransulphate

100 µg/ml Sonicated salmon sperm DNA

50% (v/v) Formamide

20 mM DTT

Cresyl violet solution

0.5% cresylviolet

60 mM sodium acetate

340 mM acetic acid

The solution is stirred in the dark for 7 days and filtered

RNase buffer

10 mM Tris HCl pH 8.0

0.5 M NaCl

1 mM EDTA

40 µg/ml RNase A (10 mg/ml in ddH2O)

1 U/ml RNase T1 (500,000 U/ml stocking solution)

4% PFA buffer (Formaldehyde/PBS solution)

Solution 1

40 g (60 g) paraformaldehyde (PFA)

500 ml (750 ml) ddH_2O (preheat water and cool to 50 - 55°C)

stirring in the hold and adding concentrated NaOH slowly until the solution cleared

Solution 2

100ml (150 ml) 10 x PBS + 400 ml (600 ml) ddH2O (1 : 5 dilute) and cooled on ice

Mix both solutions together and cool to RT

Adjust pH with concentrated HCl to 7.3 - 7.4

Filter the solution and store at 4°C

SDS sample buffer(2 ×)

1.0 ml glycerol

0.5 ml β-mercaptoethanol

3.0 ml 10% SDS

1.25 ml 1.0 M Tris-HCl pH 6.7

1-2 mg bromophenol blue

10 x Tris-glycine SDS electrophoresis buffer

250 mM Tris

2.5 M Glycine

1% SDS

pH8.3

Transfer buffer

25 mM Tris

192 mM glycine

20% (v/v) methanol

pH 8.3

TBS (Tris buffered saline)

10 mM Tris-HCl, pH 8.0

150 mM NaCl

Digoxigenin detection buffer

Buffer 1

100 mM Tris-HCl, pH 7.5

150 mM NaCl

Buffer 2

100 mM Tris-HCl, pH 9.5

100 mM NaCl

50 mM $MgCl_2$

Block-buffer

In buffer 1

10% NLS (normal Lambserum)

0.01% Triton X-100

Chromogensolution

10 ml buffer 2

45 µl NBT (4-Nitroblue-Tetrazol-chloride)

35 µl BCIP (5-bromo-4-chloro-3- indolyl-phosphate)

2.1.4 Cell lines

The rat dorsal root ganglion/mouse neuroblastoma hybridoma cell line F11 was provided by Dr. Mark C. Fishman (Massachusetts General Hospital - Harvard Medical School, Boston, Massachusetts, USA) (112).

2.1.5 Animals

Wistar rats (200 - 225g, male) were purchased from Charles River (Sulzfeld, Germany).

2.1.6 Radioactive nucleotides

[α-^{35}S] UTP (1000 Ci/mmol)	Amersham Biosciences, Freiburg
[α-^{35}S] CTP (1000 Ci/mmol)	Amersham Biosciences, Freiburg
[α-^{32}P] UTP (3000 Ci/mmol)	Amersham Biosciences, Freiburg

2.1.7 Antibodies

Goat anti rat TNFR1	Santa Cruz, California
Anti-Dig-Fab fragment	Roche, Mannheim
Anti-goat IgG secondary antibody	dianova, Hamburg

2.1.8 Kits

PolyATract mRNA Isolation System	Promega, Mannheim

QIAGEN Plasmid Maxi Kit	QIAGEN, Hilden
QIAprep Spin Miniprep Kit	QIAGEN, Hilden
QIAquick PCR Purifiation Kit	QIAGEN, Hilden
QIAquick Nucleotide Removal Kit	QIAGEN, Hilden
QIAquick Gel Extraction Kit	QIAGEN, Hilden
RNeasy Mini Kit	QIAGEN, Hilden
Advantage 2 PCR Kit	BD Biosciences Clontech, USA
Smart RACE cDNA Amplification Kit	BD Biosciences Clontech, USA
Avidin/Biotin Blocking Kit	Vector, Burlingame, CA

2.1.9 Enzymes

Taq DNA polymerase	Applied Biosystems, Foster City, USA
AmpliTaq Gold DNA Polymerase	Applied Biosystems, Foster City, USA
PfuTurbo high fidelity DNA polymerase	Stratagene, La Jolla, USA
RNA Polymerase (SP6, T7)	Roche, Mannheim
RNase A	Roche, Mannheim
RNase T1	Roche, Mannheim
Superscript II Reverse Transcriptase	Gibco-BRL, Karlsruhe
T4-DNA-Ligase	Promega, Mannheim
DNase I	Roche, Mannheim
AatII	Roche, Mannheim
NdeI	New England Biolab, Schwalbach/Taunus
NcoI	New England Biolab, Schwalbach/Taunus
NotI	New England Biolab, Schwalbach/Taunus
PstI	Roche, Mannheim
SacI	New England Biolab, Schwalbach/Taunus
SacII	New England Biolab, Schwalbach/Taunus
SpeI	New England Biolab, Schwalbach/Taunus
SphI	New England Biolab, Schwalbach/Taunus

2.1.10 Oligonucleotides

The PCR primers were designed using the online program Primer 3 (http://www-genome.wi.mit.edu/cgi-bin/primer/primer3_www.cgi) except the EST (expressed sequence tag) primers. All the oligonucleotides were synthesized by MWG-Biotech (Ebersberg, Germany). The optimal annealing temperature was calculated using the primer analysis software Oligo 6 (Molecular Biology Insights, West Cascade, USA).

Gene	GenBank #	Primer Name	Sequence	Annealing Tm	Product size
CD14	AF087943	rCD14F84	ttgttgctgttgcctttgac	60°C	1077 bp
		rCD14R1160	gagcaaagccaaagttcctg		
		r/mCD14F273	taccttctaaagcgtgtggaca	57°C	724 bp
		r/mCD14R996	tatccagcctgttgtaactgag		
TNFR1	M63122	rTNFR1F983	gggattcagctcctgtcaaa	56°C	400 bp
		rTNFR1R1382	atgaactccttccagcgtgt		
		RTNFR1F704	tcccctgtaaggagaaacagaa	60°C	1199 bp
		RTNFR1R1902	gctttttctccacaatcacctc		
TNFR2	U55849	RTNFR2F66	gttctctgacaccacatcatcc	57°C	456 bp
		rTNFR2R521	gtcaataggtgctgctgttcaa		
	AF142499	RTNFR2F28	aatggaaacgtgatatgcagtg	58°C	702 bp
		RTNFR2R727	gcatcgtgaacgtctgtagc		
		rTNFR2F1	ttcggagtggccagttcaaga		
		rTNFR2R405	gaagcaggtcgccagtcctaacatca		
	EST primers	rTNFR2F2814	atttataagcaggaattctgtccagca		
		rTNFR2F3569	ctgccttacccactgagccatcttgcc		
		rTNFR2F2174	ccttccttcagggaatctcagggactg		
		rTNFR2R2808	tgctggacagaattcctgcttataaat		
		rTNFR2R3569	ggcaagatggctcagtgggtaaggcag		
TNFα	NM_012675	rTNFαF15	catgatccgagatgtggaact	60°C	694 bp
		rTNFαR708	tcacagagcaatgactccaaag		
IL-1β	M98820	Upper primer 384	tctgtgactcgtgggatgatga	56°C	325 bp
		Down primer 708	atcttcttctttgggtattgtttgg		
IL-1R1	M95578	Upper-1162	gggtcggaaattgaatggg	54°C	526 bp
		Lower-1687	cctcgatggtatcttcccc		
TLR4	AF057025	Upper5’-328	aagcttgaatccctgcatagagg	53.8°C	1600 bp
		Lower3’-1927	tgtctctatgcgattgaaactgc		
		Upper5’-1431	aagcttgaatccctgcatagagg	60°C	499 bp
		Lower3’-1929	tgtctctatgcgattgaaactgc		
αCGRP	M11597	rCGRPA1U	acagataatagccccagaaagaag	60°C	345 bp
		rCGRPA322L	gctcacaagtgacaacattaacag		
VR1	AF029310	rVR1F15	ttgctccatttggggtgtgc	60°C	828 bp
		rVR1R842	cagggacaggggcagctcac		
GAPDH	AF106860	rGAPDHF119	cgacccctcattgacctcaactacatg	59°C	227 bp
		rGAPDHR345	ccccggccttctccatggtggtgaagac		

2.1.11 cDNA constructs

All the cDNA fragments were subcloned into the pGEMT vector. The plasmids which contain the specific gene fragments were linearized by different restriction enzymes. RNA polymerase using to produce sense or antisense RNA probes was indicated.

Gene	Insert	Enzyme	Probe	RNA polymerase
rTNFα	694 bp	NotI	sense	T7
		AatII	antisense	SP6
rTNFR1	1199 bp	NotI	sense	T7
		NcoI	antisense	SP6
rTNFR2	702 bp	NdeI	antisense	T7
		AatII	sense	SP6
rIL-1β	587 bp	NotI	antisense	T7
		NcoI	sense	SP6
rIL-1R1	526 bp	PstI	sense	T7
		KspI	antisense	SP6
rTLR4	1600 bp	AatII	sense	T7
		NdeI	antisense	SP6
rCD14	1077 bp	AatII	sense	T7
		SacI	antisense	SP6
rαCGRP	345 bp	SpeI	antisense	T7
		KspI	sense	SP6
rVR1	828 bp	SphI	sense	T7
		SpeI	antisense	SP6
rGAPDH	227 bp	SalI	sense	T7
		ApaI	antisense	SP6

2.1.12 DNA, RNA and protein size markers

0,25 - 9,5 kb RNA-ladder	Gibco-BRL, Karlsruhe
1 kb DNA-ladder	Gibco-BRL, Karlsruhe
100 bp DNA ladder	Gibco-BRL, Karlsruhe
1 kb DNA ladder	MBI Fermentas, St.Leon-Rot, Germany
100 bp DNA ladder	MBI Fermentas, St.Leon-Rot, Germany
Prestained SDS - PAGE standard	BioRad, Herculed, USA

2.1.13 Other supplies

BioMax Film	KODAK, USA
CapSure LCM Transfer Film TF-100	Arcturus, San Diego, USA
Eppendorf tubes	Eppendorf, Hamburg
Hybond PVDF	Amersham Biosciences,Freiburg
Hybond N Nylon membrane	Amersham Biosciences,Freiburg
Hyperfilm β-max	Amersham Biosciences,Freiburg
Hyperfilm ECL	Amersham Biosciences,Freiburg
Hyperfilm MP	Amersham Biosciences,Freiburg
Micro Bio-Spin P-30 Columns	BioRad, Hercules, USA
PAP-pen	Beckman Coulter, France
Sterile plastic ware for cell culture	Greiner, Germany
Tissue-Tek Cryomold	Miles, Elkhart, USA

2.2 Methods

2.2.1 Animal treatment

Animal care and procedures were conducted according to institutional guidelines. All rats were housed in clean plastic cages and had *ad libitum* access to food and water and kept on a 12 h-12 h light-dark cycle. The rats were injected intraperitoneally (i.p.) with a dose of 500 μg/kg BW of lipopolysaccharide (LPS) (serotype 0127: B8, Sigma, Munich, Germany). LPS was prepared at a concentration of 1 mg/ml in PBS. At different time points after the injection the rats were killed by exposure to 100% CO_2 and tissues were rapidly removed and either embedded in Tissue-Tek OCT compound (Sakura, Zoeterwoude, The Netherlands) by immersion in -50°C cold 2-Methylbutane (Fluka) on dry ice for cutting or frozen immediately in liquid nitrogen for RNA extraction.

2.2.2 Cell culture

F11 cells were grown in Ham's F12 medium, supplemented with 15% Hyclone defined fetal bovine serum (FBS), 1 x HAT Supplement, 1 x Antibiotic-Mix and 200 mM Glutamine at 37°C under 5% CO_2 in tissue culture flasks (Greiner Labortechnik GmbH, Germany). The cells were passaged with 0.05% Trypsin/0.02% EDTA at 80-90% confluences. Subcultures were cultivated in a ratio of 1:5 once a week using Trypsin/EDTA. The cells were harvested for RNA and protein extraction at 70-80% confluences.

2.2.3 Laser capture microdissection (LCM)

The DRG tissues were cut on a Leica cryostat (Leica, Nussloch, Germany) in 10 µm thick sections and mounted on glass slides. The sections were stored at –70°C. At room temperature, the frozen sections were air-dried for 15 min, stained with 0.5% cresyl violet for 15 min, washed in deionized water for 3 min, 2 min once in 70%, 96% and twice in 100% isopropanol alcohol, 5 min twice in Xylol and finally dried completely in air. Neuronal and non-neuronal cells were microdissected using the PixCell II LCM System (Arcturus, San Diego) with 7.5 µm Laser Spot Size, 70 mW Pulse Power, 0.6 ms Pulse Width. After capturing, the caps were plugged into the 0.5 ml plastic tubes (Eppendorf, Köln, Germany) containing 100 µl TRIzol (GibcoBRL, Karlsruhe, Germany). The tubes were inverted and stored at –20°C.

2.2.4 RNA isolation from tissues and F11 cells

Total RNA was isolated from different tissues and F11 cells using TRIzol Reagent according to the manufacturer's protocol. Total RNA was incubated with RNase-free DNase I (Roche Diagnostics, Mannheim, Germany) at 37°C for 30 min and purified using RNeasy Mini Kit (QIAGEN, Hilden, Germany). Poly(A)$^+$ RNA was prepared using Poly(A)$^+$ Tract mRNA Isolation system III (Promega, Mannheim, Germany) according to the manufacturer's instruction. The tubes with the LCM caps were vortexed vigorously and centrifuged briefly. Glycogen (Roche) was added as carrier to a final concentration of 250 µg/ml. The RNA pellet was dissolved in RNase-free deionized water and incubated with RNase-free DNase I at 37°C for 30 min. The reaction was extracted once with phenol-chloroform (ROTH, Karlsruhe, Germany). After precipitation and washing, the RNA pellet was dissolved in RNase-free water and stored at –70°C.

2.2.5 cDNA synthesis

2.2.5.1 Synthesis of cDNA for PCR

cDNA was synthesized using SUPERSCRIPT II reverse transcriptase (GibcoBRL) in total volume of 20 µl. About 2.5 µg DNase I treated total RNA was incubated with oligo(dT) 12-18 (1.25 µM, Amersham Pharmacia Biotech, Freiburg, Germany) at 70°C for 10 min in a volume of 11 µl and chilled on ice for 2 min. The reaction was performed in the presence of dithiothreitol (DTT) (10 mM), reverse transcriptase (200 U), dNTPs (500 µM), the first strand buffer (GibcoBRL) and incubated at 16°C for 10

min, at 42°C for 1 h and at 94°C for 5 min to inactivate the enzyme. The cDNA was diluted to 50 µl by adding 30 µl PCR grade water and stored at –20°C.

2.2.5.2 Synthesis of cDNA for RACE

For RACE cDNA synthesis the SMART^{TM} RACE cDNA Amplification Kit (CLONTECH Laboratories) was used. For 5'-RACE the cDNA was synthesized using a modified lock-docking oligo(dT) primer (termed the 5'-RACE cDNA Synthesis Primer or 5'-CDS) and the SMART II oligo. The 3'-RACE cDNA is synthesized using a traditional reverse transcription procedure, but with a special oligo(dT) primer. This 3'-RACE cDNA Synthesis Primer (3'-CDS) includes the lock-docking nucleotide positions as in the 5'-CDS primer and also has a portion of the SMART sequence at its 5'-end. The first strand cDNA for 5'- and 3'-RACE were synthesized using 1 µg DNase I treated spleen total RNA and Superscript II reverse transcriptase (GibcoBRL) according to the manufacturer's protocol modified with addition of $MnCl_2$ to a final concentration of 2 mM (113). After reverse transcription, the first strand product was diluted by adding 100 µl Tricine-EDTA buffer provided by the manufacturer. First-strand cDNA was stored at -20°C.

2.2.6 Polymerase chain reaction (PCR)

All PCR reactions were performed on a GeneAmp 9700 cycler or PTC-200 cycler using 5 µl cDNA in a total volume of 50 µl, containing forward and reverse primers (0.2 µM of each), 1 x PCR buffer, 1.5 mM $MgCl_2$, 200 µM dNTPs mixture and 1U AmpliTaq Gold (Roche) polymerase. All the PCR fragments were amplified by forward and reverse primers using following program: 1 cycle at 95°C for 5 min, 25 to 45 cycles (30 sec at 94°C, 30 sec at optimal annealing temperature, extension at 72°C for different time according to the length of the PCR fragments, 1 min/kb) and 10 min final extension at 72°C. As positive control glyceraldehydes phosphate dehydrogenase (GAPDH) was used as house keeping gene yielded a 227 bp PCR product (AF106860, nt. 119 – 345). Negative controls included RNA subjected to RT-PCR without reverse transcriptase, and PCR with water replacing cDNA. PCR products of 10 µl from each reaction were loaded and separated on 1.5% agarose gel containing ethidium bromide (EtBr). The gels were visualized under an ultraviolet transilluminator (BioRad). The PCR products were subcloned and sequenced. The sequence identity of the PCR products was confirmed by comparing with the GenBank database.

2.2.7 Rapid amplification of cDNA ends (RACE) of the rat TNFR2 gene

The first 5'-RACE PCR was carried out with the universal primer mix (UPM) provided by the manufacturer and a gene specific primer (RTNFR2R521) gtcaataggtgctgctgttcaa. The nested PCR for 5'-RACE was carried out with the Nested Universal Primer (NUP) provided with the kit and the gene specific nested primer (rTNFR2R405) gaagcaggtcgccagtcctaacatca. The first PCR for 3'-RACE was carried out with the gene specific primer (rTNFR2F2174) ccttccttcagggaatctcagggactg and (RTNFR2R2808) tgctggacagaattcctgcttataaat and UPM. The nested PCR for 3'-RACE was performed with the nested primer (rTNFR2R3569) ggcaagatggctcagtgggtaaggcag and NUP. The DNA polymerase is Advantage 2 Polymerase Mix (Clontech). The 5'- and 3'-RACE PCR products were subcloned into pGEMT vector and sequenced in Sequence Laboratories Goettingen (Goettingen, Germany).

2.2.8 DNA agarose gel electrophoresis

1.5% agarose gel was routinely used to separate DNA fragments in a size range of 100 to 10.000 bp (114). The appropriate amount of agarose was dissolved in 1 × TAE buffer by boiling for a few minutes in a microwave oven. When the gel solution had cooled down to about 60°C, ethidium bromide was added to a final concentration of 0.5 µg/ml. The solution was then poured into a gel mold. Suitable combs were used for generating the sample wells. The gel was allowed to harden for some 30 - 45 min. The gel was mounted in the electrophoresis chamber which was filled with 1 x TAE running buffer until the gel was just submerged. DNA samples and size standards were mixed with 0.1 volumes of 10 × loading buffer and applied to the wells. A voltage of 2 - 10 V/cm was applied until the bromophenol blue and xylene cyanol FF dyes had migrated an appropriate distance through the gel. After completion of the electrophoresis gel was examined under UV transilluminator and photographed using a gel documentation system (BioRad).

2.2.9 Cloning of PCR products into plasmid vectors

The QIAquick PCR Purification Kit (QIAGEN) was used to purify PCR products. The purified PCR fragments were ligated into pGEM-T Vector (Promega) followed by transformation into DH5α of *E. coli* according to manufacturer's instruction. The plasmids were isolated by using QIAfilter Plasmid Maxi Kit (QIAGEN) and sequenced

in Sequence Laboratories (Goettingen) with universal primer T7, SP6 and gene specific primers. Sequences were then confirmed by homology search using BLAST 2.0 (http://www.ncbi.nlm.nih.gov).

2.2.10 In vitro transcription

In vitro transcription reactions were carried out in a volume of 10 µl contained 1 µg linearized plasmids, 10 mM DTT (GibcoBRL), 20 - 40 U RNase inhibitor (MBI Fermentas, St.Leon-Rot, Germany), 1 x buffer, 200 U T7 or SP6 RNA polymerase (Roche), 0.5 mM NTPs mixture with ^{35}S-UTP or both ^{35}S-UTP and ^{35}S-CTP (>1000 Ci/mmol, Amersham Pharmacia Biotech, Freiburg, Germany) or digoxigenin-11-UTP (Roche) replaced UTP or both UTP and CTP. After 90 min incubation at 37°C, 10 U RNase-free DNase I was added into the reactions and incubated for another 15 min. After adding RNase-free water to 20 µl and 20 µl sodium carbonate buffer (pH 10.2, 80 mM $NaHCO_3$ – 120 mM Na_2CO_3), for limited hydrolysis the reactions were incubated at 60°C for the appropriate time (t = Lo - Lf/ K* Lo * Lf, Lo: the cDNA length, Lf: expected length of the probes (it is 250 bp in our laboratory), K is 0.11 in our case) (115, 116). The reactions were stopped by adding 2 µl 10% acetic acid. RNase-free water of 28 µl was added and probes were purified using Micro Bio-Spin P-30 columns (BioRad). To produce ^{32}P-UTP (>3000 Ci/mmol, Amersham) labeling antisense RNA probes for Northern blot same procedure except the step of sodium carbonate buffer at 60°C incubation was used.

2.2.11 In situ hybridization

2.2.11.1 Coating of glass slides

The glass slides were first washed with detergent at 60°C for 1 h with slightly shaking. The detergent was completely removed under running water. The slides were rinsed three times in deionized water. After 45 min washing in 70% ethanol with slightly shaking, the slides were dried by baking at 60°C. After immersion in 2% TESAP in acetone for 30 sec, the slides were soaked 30 sec twice in acetone and twice in deionized water. Slides were then dried completely by baking overnight at 42°C.

2.2.11.2 Preparation of tissue sections

Tissues were cut on a Leica cryostat (Leica) to 14 µm thick sections and thaw-mounted on adhesive slides and stored at -70°C.

2.2.11.3 Prehybridization

Frozen sections were removed from the freezer and air dried at room temperature for 15 min and fixed in 4°C pre-cooled 4% paraformaldehyde in phosphate-buffered-saline (PBS) for 60 min at room temperature. After three washes in 10 mM PBS (pH 7.4) for 10 min each and incubation in 0.4% Triton X-100 for 10 min, the slides were rinsed in deionized water and transferred to 0.1 M triethanolamine (pH 8.0) (Sigma). Acetic anhydride (Sigma) was added under stirring to a final concentration of 0.25% (v/v) and further incubated for 10 min. The slides were washed for 10 min in 10 mM PBS (pH 7.4) and rinsed in deionized water prior to dehydration in 50% and 70% isopropanol. Finally, the slides were air-dried at room temperature at least for 15 min and stored at -20°C.

2.2.11.4 Hybridization

In situ hybridization was performed as described previously (115, 116). Briefly, the frozen prehybridized sections were air dried and marked. The radioactive probes were diluted to 5 x 10^4 dpm/µl (single radioactive labeling) or 1 x 10^5 dpm/µl (double radioactive labeling) in hybridization solution. Appropriate amounts of hybridization solution containing radioactive antisense or sense RNA probes were applied to the sections. Slides were coverslipped and incubated at 60°C in humid box containing 50% formamide for 16 h. Sense probes were used as nonspecific controls.

2.2.11.5 Posthybridization and detection

Coverslips were removed and slides were washed in 2 x SSC and 1 x SSC for 20 min each followed by incubation in pre-heated to 37°C RNase buffer (10 mM Tris, pH 8.0, 0.5 M NaCl, 1 mM EDTA) containing 1 U/ml RNase T1 and 20 µg/ml RNase A (Roche) for 30 min at room temperature. Slides were washed at room temperature in 1 x, 0.5 x, and 0.2 x SSC for 20 min each, at 60°C in 0.2 x SSC for 60 min and at room temperature in 0.2 x SSC and deionized water for 15 min each. The tissue was dehydrated in 50% and 70% isopropanol and then air-dried.

Air-dried hybridized slides were exposed to Kodak BioMax MR Film (Amersham) for 6 h to 24 h. After exposure to X-ray film, the sections were coated with nuclear emulsion NTB-2 (Eastman Kodak, Rochester, NY). The coated slides were dried overnight in a dark box in the dark room. The dried slides were exposed for 3 to 42 days at 4°C. The slides were developed for 4 min in Kodak D-19 developer solution and fixed for 10 min in Tetenal Superfix25 solution (Tetenal Photowerk, Norderstedt, Germany) at room temperature. The developed slides were washed overnight in running tap water. After staining with 0.5% cresyl violet for 15 min, the slides were washed in deionized water for 3 min, once in 70% and 96% and twice in 100% isopropanol alcohol for 2 min each. After final incubation in Xylol twice for 5 min, the sections were coated with DePex and covered with glass coverslips. The sections were analyzed under an Olympus AX70 microscope (Olympus) and photographed under bright or dark field illumination.

2.2.12 Double in situ hybridization

For double ISH the digoxigenin labeled probes of αCGRP, SP, VR1 were added to a final concentration of 1 ng/µl in the hybridization solution containing radioactive probes. Hybridization and washing procedures were the same as described above except dehydration in alcohol was omitted. For the detection of non-radioactive hybrids, the slides were incubated for 1 h with blocking-buffer (buffer 1 containing 10% normal lamb serum, 0.01% Triton X-100). After rinsing in buffer 1, the slides were incubated with 1: 1000 diluted antibody (alkaline phosphatase-conjugated anti-DIG Fab fragments in 1: 10 diluted blocking buffer by buffer 1) overnight at 4°C and 1 h at 37°C. Excessive antibody was removed by washing in buffer 1 for 10 min twice. Slides were equilibrated in buffer 2 (100 mM Tris, pH 9.5, 100 mM NaCl; 50 mM $MgCl_2$) prior to color reaction. The color reaction was performed using the solution containing 5-bromo-4-chloro-3-indolyl phosphate (BCIP) and nitroblue tetrazolium salt (NBT) (Roche). The color development was controlled under the microscope. After 4 h for αCGRP and SP and after 10 h for VR1, respectively, slides were washed in deionized water for at least one day with several changes. For detection of ^{35}S-labeled probes, the slides were dipped in K5 Emulsion (ILFORD Imaging, Mobberley Chershire, UK), which was diluted 1: 1 in water. Sections were exposed at 4°C for various times. The cellular distribution of silver grains and the violet precipitate was studied under an

AX70 light microscope (Olympus). At high magnification, the number of double–labeled cells was determined. All digoxigenin-labeled cells were counted, regardless of their labeling intensity. Radioactive-labeled cells were counted at the same magnification in brightfield illumination. For each probe at least 3 sections were counted. The number of digoxigenin- and radioactive-labeled cells was counted twice to ensure accuracy. The percentage of double-labeled cells was calculated and expressed as the percentage of digoxigenin-labeled (αCGRP, SP, VR1 positive cells) and radioactive-labeled cells.

2.2.13 Northern Blot Analysis

2.2.13.1 RNA agarose gel electrophoresis

RNA was separated on a denatured formaldehyde agarose gel. 10 µl RNA was mixed with 10 µl RNA sample buffer and 2 µl RNA gel-loading buffers. After 10 min incubation at 65°C the RNA samples were placed on ice for 2 min. The RNA samples were vortexed and centrifuged briefly before loading into the wells of a 1.5% agarose gel prepared in 1 x HEPES electrophoresis buffer containing 6% formaldehyde. Electrophoresis was carried out at 5 V/cm in 1 x HEPES formaldehyde electrophoresis buffer (114).

2.2.13.2 RNA transfer

The separated RNAs were transferred from the agarose gel to a positively charged nylon membrane by downward capillary transfer (117) using the Turboblotter Rapid Downward Transfer Systems (Schleicher&Schuell, Dassel). After electrophoresis the RNA gel was rinsed in deionized water for four times 15 min each and maintained in deionized water prior to transfer. The nylon membrane was wetted by immersion in distilled water and then equilibrated in 20 x SSC buffer for 5 min. The transfer system was used according to the manufacturer's instruction. The transfer was performed overnight using 20 x SSC at room temperature. Following transfer, the membrane was gently washed in 2 x SSC for 5 min and placed briefly on a sheet of Whatman paper to remove any excess of 2 x SSC buffer. RNA was covalently bound to the membrane by crosslinking the molecules to the matrix under UV light (254nm) for a total dose of 120 mJ/cm^2 using a UV Stratalinker.

2.2.13.3 Detection of 18S and 28S RNA or RNA markers

Membranes were incubated in a solution of 0.02% Mehtyl blue in 0.3M Na-acetate pH5.5 for 2-3 min and washed 3 times in ddH_2O for 2-5 min each. Air-dry the Membranes were air-dried and photographed to document the bands for 18S RNA and 28S RNA or for the RNA markers.

2.2.13.4 Hybridization of blot and detection of mRNAs

Membranes were prehybridized with NorthernMax solution (Ambion, Cambridgeshire, UK) at 68°C for 30 min and hybridized for 14-20 h with 1- 4 x 10^6 cpm/ml ^{32}P-labeled antisense RNA probes at 68°C. After washing in preheated 2 x SSC containing 0.1% SDS for 5 min twice and washing with preheated 0.1 x SSC containing 0.1% SDS for 15 min twice at 68°C, membranes were exposed to Hyperfilm-MP (Amersham Pharmacia Biotech, Freiburg, Germany) for 20 min to 24 h. X-ray films digitized and analyzed using NIH image.

2.2.14 Western blot analysis

2.2.14.1 SDS polyacrylamide gel electrophoresis

SDS polyacrylamide gel electrophoresis was carried out in a discontinuous gel system using Mini-PROTEAN II Cell (BioRad) according to manufacturer's instruction. The 12% resolving gel solution was poured into the assembled gel mold between two glass plates separated by 1 mm thick spacers leaving some 2 cm space for the stacking gel. The gel surface was overlaid with water in order to prevent inhibition of polymerization by oxygen. After polymerization was completed (30 min), the stacking gel (always 4%) was poured on top of the resolving gel, and the comb was inserted. After polymerization of the stacking gel (30 min) the comb was removed and the gel mounted in the electrophoresis chamber. Both electrode reservoirs were filled with 1 x SDS electrophoresis buffer, the wells were cleaned and samples loaded. Electrophoresis was performed at 200 V constant voltages setting until the bromophenol blue dye had reached the bottom of the gel.

2.2.14.2 Protein transfer and detection

The cellular protein was extracted using TRIzol reagent after total RNA isolation according to the manufacturer's protocol. The vacuum dried protein was dissolved in

1% SDS solution and the concentration was measured using the Bradford method (Bio-Rad Protein assay, BioRad). The protein was boiled in 1 x SDS sample buffer for 4 min. The denatured samples were loaded in 30 µg protein per lane, separated on 12% SDS-PAGE and transferred to Hybond PVDF membrane (Amersham) using Mini Trans-Blot Electrophoretic Transfer Cell (BioRad) according to manufacturer's instruction. Transfer was performed overnight at 4°C, 30 V. After overnight blocking with 3% BSA (SERVA, Heidelberg, Germany) in Tris-buffered saline with 0.1% Tween-20 (TBST) at 4°C, membranes were incubated with Avidin/Biotin Blocking Kit (Vector, Burlingame, CA) to block endogenous avidin and biotin. Membranes were then incubated with goat anti-rat TNFRp55 polyclonal antibody (Santa Cruz) for 1 hour at room temperature in a dilution of 1: 50000 in TBST. After 5 washes for 5 min each, the membranes were incubated for 1 h with Biotin-Sp-donkey anti-goat IgG secondary antibody (dianova, Hamburg, Germany) in a dilution of 1: 5000 in TBST at room temperature. After 5 washes in TBST for 5 min each, the membranes were incubated with ABC complex (Vector) for 1 h at room temperature. Detection was perormed using ECL (enhanced chemiluminescence) reagents according to manufacturer's instruction and exposed 1 min to Hyperfilm ECL (Amersham).

3 Results

3.1 Characterization of the rat TNFR2 gene

3.1.1 Full length cloning of rat TNFR2 cDNA

In order to investigate the gene expression of TNFR2 in rat DRG, the full coding sequence and the gene structure of rat TNFR2 had to be obtained first. To obtain the full length cDNA of rat TNFR2 gene, rat expressed sequence site tags (EST) with homology to the mouse TNFR2 (M59378) were searched in the GenBank database. Using the EST sequence information, the reverse primers (rTNFR2F3569) ctgccttacccactgagccatcttgcc and (rTNFR2F2814) atttataagcaggaattctgtccagca were designed. Based on a partial cDNA sequence of rat TNFR2 (AF142499), a forward primer (rTNFR2F1) ttcggagtggccagttcaaga was designed. Using these pair primers and Pfu DNA polymerase, two PCR fragments of a 2353 bp (primer rTNFR2F1 + rTNFR2F2814) and of a 3429 bp (primer rTNFR2F1 + rTNFR2F3569) were obtained from RNA extracts of rat spleen. Based on these cDNA sequences the primers for 5'- and 3'-RACE PCR reactions were designed. The RACE PCR fragments were subcloned into pGEMT vector and sequenced. All the sequences from PCR fragments, 5'- and 3'-RACE fragments were integrated using the GeneTool software. Three cDNA sequences were obtained and submitted to GenBank (GenBank Acc. Nr.: AF498039, 2924 bp; AY191268, 4194 bp and AY191269, 5328 bp). To minimize coding sequence mistakes, a primer pair (rTNFR2F15) cagctagagcgcagcagag and (rTNFR2R1555) ctcagaaaaagtcatgaagttcca spanning the full coding region was used to perform RT-PCR with Pfu DNA polymerase. The same coding region was found in all the three cDNAs. The full coding sequence of rat TNFR2 gene had 90.3% and 74.1% sequence homology with that of mouse and human, respectively.

3.1.2 Alignment of rat TNFR2 putative amino acids with that of mouse and human

The nucleotide sequence of rat TNFR2 contains an open reading frame of 1422 nucleotides that codes for a protein of 474 amino acids, which shares a homology of 86% and 60% with that of mouse and human, respectively. As shown in Fig. 1, the putative peptide begins with a signal peptide of 22 amino acids. A potential 29-amino acid transmembrane domain separates the 235-amino acid extracellular domain and the

188-amino acid intracellular domain. The putative extracellular region contains a cysteine-rich region. The amino acids of the extracellular domain show 55% identity with that of hTNFR2 and 83% identity with that of mTNFR2. The amino acids of the intracellular region show 70% identity with that of hTNFR2 and 87 % identity with that of mTNFR2; however, the intracellular region of rTNFR2, which has the same number of amino acids as that of mTNFR2, has an additional 13 amino acids at its C terminus as compared with hTNFR2.

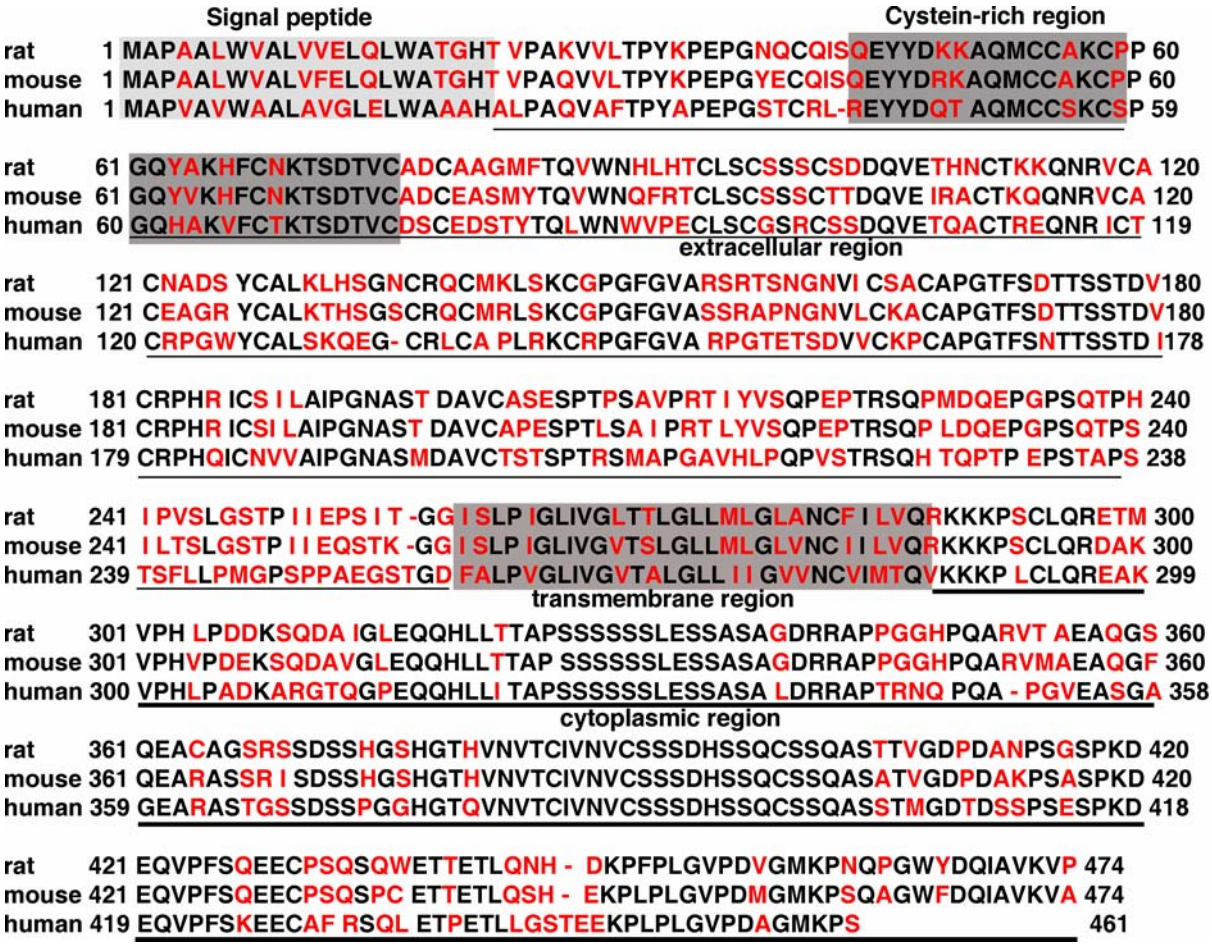

Fig. 1 Amino acid alignment of rTNFR2 with mTNFR2 and hTNFR2

The putative TNFR2 peptide contains 474 amino acids including a signal peptide (position 1-22), an extracellular region (position 23-258), a transmembrane region (position 259-288) and a cytoplasmic region (position 289-474). The extracellular region contains a cysteine-rich region (position 45-76). Identical residues of rTNFR2, mTNFR2 and hTNFR2 are indicated by black letters.

3.1.3 Structure of the rat TNFR2 gene

The gene structure of rat TNFR2 was elucidated by comparing rat TNFR2 cDNA sequences with the rat genome database in GenBank. The rat TNFR2 gene contains 10 exons that are located on chromosome 5q36. The coding region is divided into 10 exons and 9 introns, covering approximately 41 kb of sequence. The intron/exon boundaries

were located by comparing rTNFR2 cDNAs with the rat genome database. Exon size ranges from 35 bp (exon 8) to 4116 bp (exon 10) truncated by 9 introns ranging from 16443 bp (intron 1) to 263 bp (intron 5). Position, size, and splice junctions of each exon and intron are listed in Table 1. All the splice junctions conform to the GT/AG consensus sequences. The rat TNFR2 coding sequence starts at base 70 of exon 1 and extends to the initial 314 bp of exon 10, which includes 3'-untranslated region (3'-UTR). As shown in Fig. 2, exon 1 comprises the 5'-UTR, signal peptide and the N-terminus of the mature TNFR2 protein. The extracellular domain is encoded by exons 2 to 6, the transmembrane region by exons 6 and 7, and the intracellular region by exons 8 to 10.

Table 1 Exon/Intron Organization of the rat TNFR2 gene

Exon	Exon size(bp)	cDNA position	Splice donor	Splice acceptor	Intron	Intron size(bp)
1	147	1-147	AAG**gt**gggtgactcttga	cttattgccttcc**ag**GTT	1	16443
2	103	1148-250	CTG**gt**gagaggcagctgc	tccttgcttcctc**ag**GCC	2	1960
3	129	251-379	ATG**gt**gagtggcctgagc	ctttccatcctct**ag**ACC	3	1105
4	153	380-532	CAA**gt**aaggacccttctt	gattttctcttca**ag**GAA	4	517
5	94	533-626	CAT**gt**gagtgttgactcc	atcttcctccctc**ag**TTG	5	263
6	233	627-859	TTG**gt**aagtccccagtct	ctgtcttcttccc**ag**GTC	6	743
7	78	860-937	AAA**gt**aaggttctggtcc	ctctcttcattgt**ag**AGA	7	332
8	35	938-972	GTG**gt**gagtatctctgtg	ccctttttcttccc**ag**CCT	8	2921
9	208	973-1180	CAG**gt**aagaggcaggaac	tcttgtacttcac**ag**ATT	9	3766
10	4116	1181-5296				

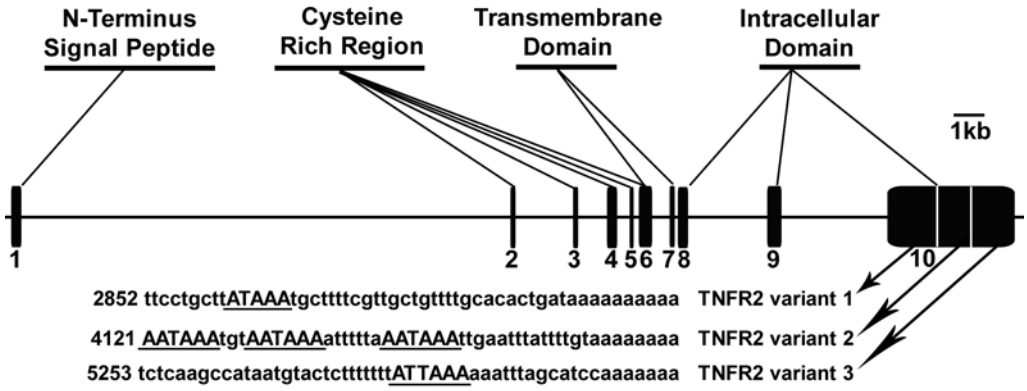

Fig. 2 Organization of rat TNFR2 gene

Schematic diagram illustrating the gene structure of rat TNFR2. The rat TNFR2 gene contains 10 exons and 9 introns. Exons and introns are drawn to scale. Putative protein domains are indicated. The poly(A) signal sequences used by the different rat TNFR2 transcripts are capitalized and underlined.

3.1.4 Tissue-specific distribution of rat TNFR2 transcripts

To examine whether rat TNFR2 transcripts are expressed in a tissue-specific manner, Northern blot analysis was performed on different rat tissues using specific antisense RNA probes spanning exon 5 to exon 10 (GenBank: AF498039, nt. 541-1242). As shown in Fig. 3A, three TNFR2 transcripts were observed in all the tissues examined. Weak signals for the three TNFR2 transcripts were detected in neural tissues including brain, spinal cord and DRG. Strong signals for the three transcripts were observed in peripheral tissues including lung, spleen and kidney. The highest levels of TNFR2 transcripts were found in spleen and lung. No evidence for tissue-specific transcription was found. The three rat TNFR2 transcripts consisted of a major band of 4.4 kb and two minor bands of 3.1 kb and 5.4 kb. As shown in Fig. 3B, the 4.4 kb transcript was the most abundant followed by the 3.1 kb transcript and the 5.4 kb transcript.

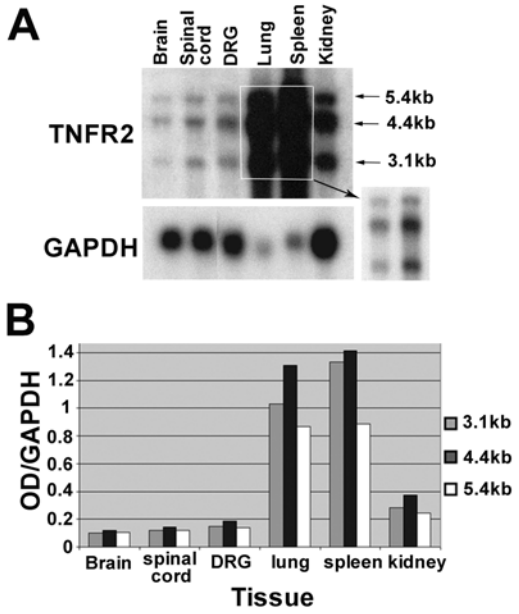

Fig. 3 Northern blot analysis of TNFR2 transcripts in rat tissues

(**A**) Three alternative transcripts of the rat TNFR2 gene were observed in different tissues. Note abundant expression of TNFR2 in spleen and lung. Two microgram poly(A)$^+$ RNA aliquots from different tissues were hybridized with rat TNFR2 antisense RNA probes. The membrane was exposed to X-ray film for 16 h. The same membrane was hybridized with GAPDH antisense RNA probes and exposed to X-ray film for 30 min. The GAPDH signals were used to normalize sample loading. (**B**) The amount of three transcripts is different. The transcripts with the size of 4.4 kb are expressed stronger than that of 3.1 kb and 5.4 kb in all tissues tested.

3.1.5 LPS-induced regulation of TNFR2 gene in rat spleen

LPS is known to enhance TNFR2 mRNA expression in macrophages and monocytes (118). To examine the kinetics of LPS-induced transcription of the TNFR2 gene, rats were treated with LPS (500 μg/kg BW) for 1 to 12 h and TNFR2 mRNA levels in rat spleen were evaluated by Northern blot analysis. The analysis of the X-ray film revealed that the systemic injection of LPS increased the expression of TNFR2 transcripts in the spleen. As shown in Fig. 4, LPS stimulation caused an increase of all

three TNFR2 transcripts already 1 h after injection. The levels of TNFR2 mRNAs peaked at 3 h after LPS treatment and were reduced to control levels at 12 h after LPS injection (Fig. 4A). Densitometry revealed a 2.4-fold increase of TNFR2 transcripts at 3 h after systemic LPS as compared with the controls. The 3.1 kb transcript increased up to 2.9 fold, the 5.4 kb transcript up to 2.5 fold and the 4.4 kb transcript up to 1.9 fold. The 3.1 kb transcript increased more than the other two transcripts (Fig. 4B).

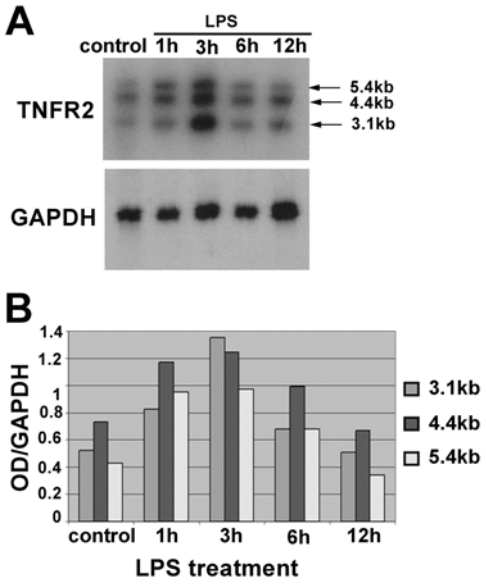

Fig. 4 Northern blot analysis of TNFR2 transcripts in rat spleen

(**A**) Three TNFR2 transcripts were detected in control and peaked at 3 h after systemic LPS. GAPDH as house keeping gene was detected to normalize the samples loading. Exposure time: 1 h for TNFR2 and 0.5 h for GAPDH. One microgram poly(A)$^+$ RNA was loaded per lane. (**B**) Densitometry revealed that TNFR2 transcripts increased up to 2.4 fold 3 h after systemic LPS as compared with the controls. Systemic LPS caused an increase of the 3.1 kb transcripts up to 2.9 fold. The 5.4 kb transcripts and the 4.4 kb transcripts increased up to 2.5 fold and 1.9 fold, respectively.

3.2 Expression of TNF receptors in rat dorsal root ganglion

3.2.1 RT-PCR detection of TNF receptors in RNA extracts of rat dorsal root ganglion

To investigate the expression of TNF receptors in rat DRG under basal conditions and after systemic LPS, RT-PCR analysis was performed on total RNA extracts using gene-specific primers. As shown in Fig. 5, after 35 cycles of PCR amplification, TNFR1 transcripts, which could be detected in RNA extracts of DRGs from an untreated rat, appeared to be slightly increased at 6 h after LPS treatment. In contrast, in RNA extracts of DRGs from an untreated rat only a faint band representing TNFR2 mRNA could be detected, which peaked at 3 h after LPS injection and was already decreased at 6 h after LPS injection.

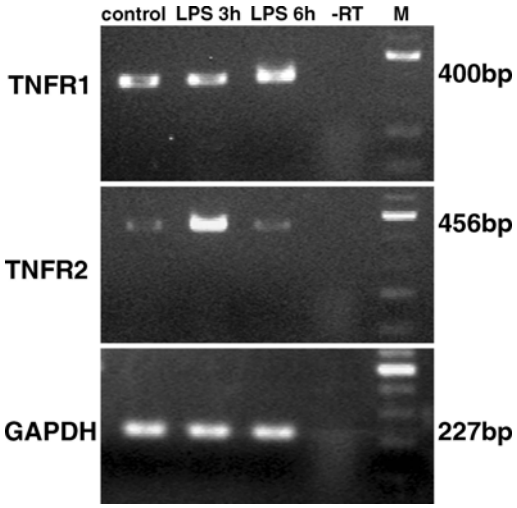

Fig. 5 RT-PCR analysis of TNF receptor transcripts in RNA extracts of DRGs from control rats and from rats after systemic LPS

RT-PCR with total RNA of rat DRG: control, 3 h after LPS treatment and 6 h after LPS treatment. TNFR1 (upper panel) could be detected in all samples with a subtle increase at 6 h after LPS. TNFR2 (middle panel) was detected at very low levels in the control, but increased to peak levels at 3 h after LPS treatment and decreased to control levels at 6 h after LPS. GAPDH as house-keeping gene exhibited no difference between the samples (lower panel). –RT: RT-PCR without reverse transcriptase as negative control. M: 100bp ladder.

3.2.2 Northern blot analysis of TNF receptor expression in rat dorsal root ganglion: effects of LPS

To determine LPS effects on the expression of TNF receptor transcripts in rat DRG Northern blot analysis was performed. For TNFR1 a single transcript of 2.3 kb was observed, while for TNFR2 three mRNA species of 5.4 kb, 4.4 kb and 3.1 kb were detected. Densitometry revealed a 2.5-fold increase of TNFR1 mRNA in DRG at 6 h after LPS (Fig. 6A). In contrast, TNFR2 mRNA levels increased about 2.7 fold already at 3 h after LPS treatment (Fig. 6B).

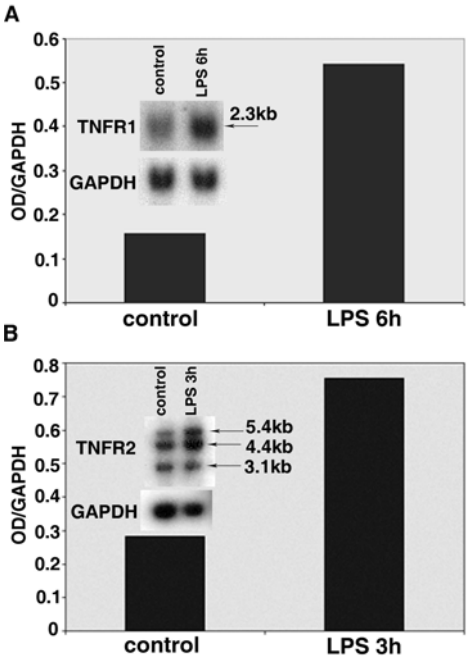

Fig. 6 Northern blot analysis of TNF receptor transcripts in rat DRG

(**A**) For the detection of TNFR1 mRNA 10 µg total RNA was loaded per lane. A single transcript of 2.3 kb was observed. Densitometry revealed a 2.5-fold increase of TNFR1 mRNA at 6 h after LPS as compared with control. GAPDH as house keeping gene was detected. Exposure time: 16 h for TNFR1 and 2 h for GAPDH. (**B**) For the detection of TNFR2 mRNA 2 µg poly(A)$^+$ RNA was loaded per lane. Three transcripts of 5.4 kb, 4.4 kb and 3.1 kb were observed. Densitometry revealed a 2.7-fold increase of TNFR2 mRNA at 3 h after LPS as compared with control. Exposure time: 16 h for TNFR2, 20 min for GAPDH.

3.2.3 RT-PCR analysis of TNF receptor expression in microdissected dorsal root ganglion neurons

To determine which type of TNF receptors is expressed in DRG neurons, the method of laser capture microdissection (LCM) in combination with RT-PCR was employed. Perikarya of primary afferents were microdissected from rat DRG sections (Fig. 7A, B, C) and total RNA was isolated. As shown in Fig. 7D, TNFR1 mRNA but not TNFR2 mRNA could be detected in RNA extracts of microdissected DRG neurons after 45 cycles of amplification by RT-PCR.

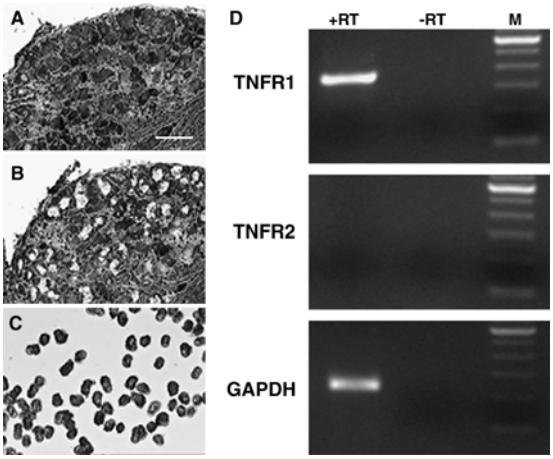

Fig. 7 Detection of TNF receptor transcripts in microdissected DRG neurons

(**A**) Before laser-capture microdissection (LCM). (**B**) After LCM. (**C**) Microdissected material. About 150 laser pulses were carried out. (**D**) RT-PCR analysis on the RNA extracts of microdissected DRG neuronal perikarya showed specific amplicons for TNFR1 but no PCR products for TNFR2. –RT: RT-PCR without reverse transcriptase. M: 100 bp ladder. The scale bar in A: 100 μm.

3.2.4 TNF receptor expression in the F11 cell line

To lend further support to the arising concept that TNFR1 rather than TNFR2 can mediate TNFα effects on primary sensory neurons, the expression of TNFR1 and TNFR2 were tested in the primary sensory cell line F11. As shown in Fig. 8A, RT-PCR analysis revealed that TNFR1 mRNA but not TNFR2 mRNA was constitutively expressed in F11 cells. In addition, using Western blot analysis a specific band of 55 kDa representing TNFR1 protein could be demonstrated in protein extracts of F11 cells as shown in Fig. 8B (a). After incubation with the secondary antibody alone no immunostaining was seen as shown in Fig. 8B (b).

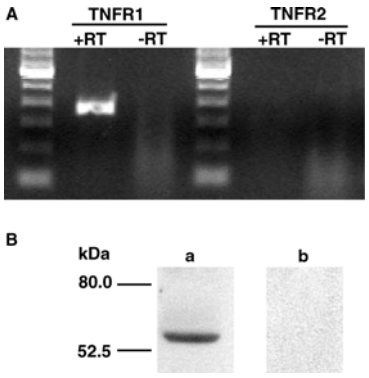

Fig. 8 RT-PCR and Western blot analysis of TNF receptors in F11 cell line

(**A**) In RNA extracts of F-11 cells constitutive expression of TNFR1 but not of TNFR2 mRNA was detected by RT-PCR. (**B**) Western blotting showed a single band of 55 kDa representing TNFR1 protein (**a**). Incubation with the secondary antibody alone revealed no immunostaining (**b**).

3.2.5 Cellular distribution of TNF receptor mRNAs in rat dorsal root ganglion and regulation of their expression after LPS

To identify the cells expressing TNF receptors in the rat DRG ISH studies were performed. Serial sections through the lumbar (L4) dorsal root ganglion were hybridized with specific riboprobes for TNFR1 and TNFR2, respectively. Hybridization signals representing TNFR1 were observed over large and small perikarya (Fig. 9A, B, E and F). High resolution microscopic analysis of emulsion coated slides revealed that silver grains representing TNFR1 mRNA were present in all of DRG neurons (Fig. 9E) and also in some DRG non-neuronal cells (Fig. 9E). Systemic LPS treatment caused an increase of TNFR1 mRNA levels not only in DRG neurons but also in non-neuronal cells (Fig. 9F). TNFR2 mRNA was detected at low levels in DRG of control rats (Fig. 9C). However, strong scattered signals for TNFR2 were detected in DRG of rats 3 h after LPS treatment (Fig. 9D). Under high resolution bright field illumination the silver grains for TNFR2 transcripts were exclusively observed over non-neuronal cells (Fig. 9G and H).

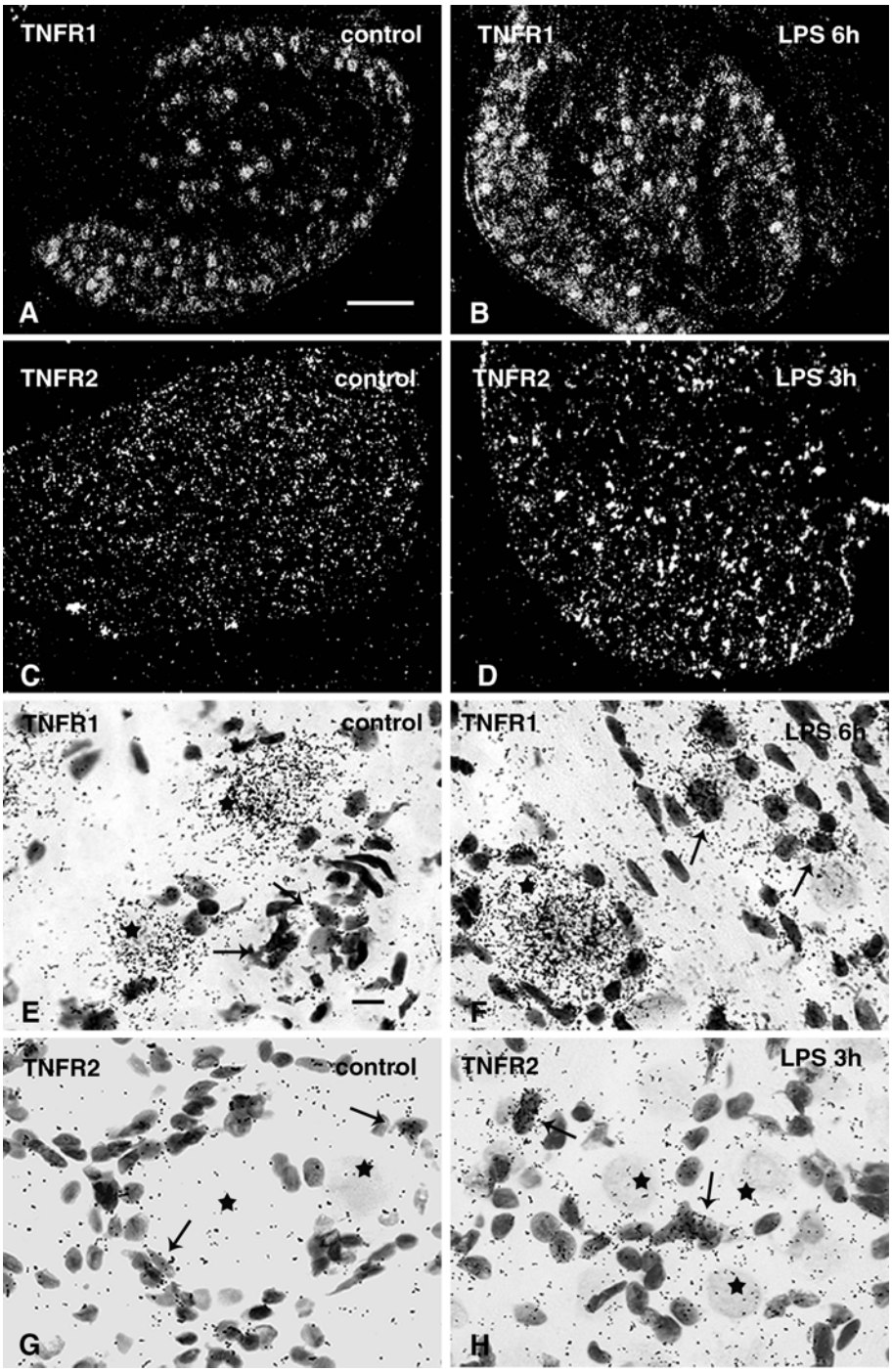

Fig. 9 Cellular distribution of TNFR1 and TNFR2 mRNAs in rat DRG

Low power darkfield images: (**A**) Strong hybridization signals for TNFR1 mRNA were found in a DRG section of a control rat. (**B**) TNFR1 hybridization signals appeared to be increased at 6 h after LPS. (**C**) Weak hybridization signals for TNFR2 mRNA were found in a DRG section of a control rat. (**D**) Hybridization signals for TNFR2 were found to be increased at 3 h after LPS.

High resolution brightfield images: (**E**) Strong labeling over neurons, which were recognized by their large faintly-stained nucleus (asterisks) and weak labeling over non-neuronal cells, which were recognized by their small dark-stained nucleus (arrows). (**F**) Increased labeling intensity for TNFR1 at 6 h after LPS both in neurons (asterisks) and in non-neuronal cells (arrows). (**G**) Hybridization signals for TNFR2 were found only over non-neuronal cells (arrows), but not over neurons (asterisks). (**H**) Systemic LPS treatment increased the hybridization signals only in non-neuronal cells (arrows). Exposure times: 7 days for TNFR1, 10 days for TNFR2. Scale bar in A: 200 μm and in E: 10 μm.

3.2.6 Relationship of TNFR1 expression with putative nociceptive neurons expressing SP, CGRP or VR1

To investigate whether TNFR1 is expressed in putative nociceptive neurons of rat DRG double labeling in situ hybridization studies were performed using VR1 as a marker for a subset of nociceptive primary afferents and the neuropeptides SP and CGRP as markers for the peptidergic subpopulations involved in the transmission of inflammatory pain (3, 4, 7-9). TNFR1 mRNA was found in nociceptive neurons expressing CGRP (Fig. 10A), SP (Fig. 10B) and VR1 (Fig. 10C). However, TNFR1 mRNA was also found in DRG neurons not expressing CGRP, SP or VR1.

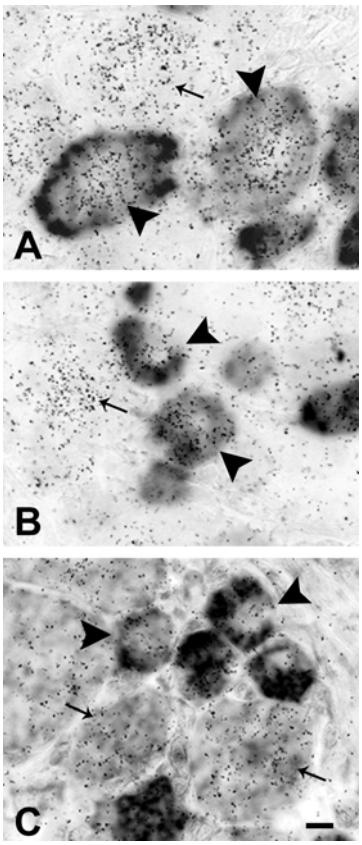

Fig. 10 Colocalization of TNFR1 and CGRP, SP or VR1

Double labeling in situ hybridization demonstrates double labeled DRG neurons (arrow heads) by the probes for (**A**) TNFR1 and αCGRP; (**B**) TNFR1 and SP; (**C**) TNFR1 and VR1. Digoxigenin labeling for the detection of αCGRP, SP and VR1 is recognized as dark reaction product and ^{35}S-labeling for the detection of TNFR1 mRNA is seen as grains. Note that many neurons were also present with labeling only for TNFR1 probes (arrows in **A** - **C**). Exposure time: 7 days. Size bar in C: 10 μm.

3.3 Constitutive and LPS-induced cell-specific expression of TNFα mRNA in rat dorsal root ganglion

To examine whether TNFα is synthesized in primary afferent neurons, the expression pattern of the TNFα gene at the mRNA level was investigated using in situ hybridization. In DRG sections of control rats specific hybridization signals for TNFα could not be detected (Fig. 11A). However, 1 h after systemic LPS treatment, the hybridization signals for TNFα were observed in many small cells scattered throughout

DRG sections (Fig. 11B). Microscopic analysis revealed that the silver grains representing TNFα mRNA were located in non-neuronal cells (Fig. 11C). To confirm the non-neuronal expression and to exclude a low basal expression of TNFα in primary sensory neurons, the sensitive technique of RT-PCR was used to analyze the RNA extracts of microdissected DRG neurons (Fig. 11D - F) and non-neuronal cells (Fig.11G - I). TNFα could be detected neither in neuronal RNA extract of control rats nor in that of LPS treated rats (Fig. 11J). However, 1 h after LPS treatment, TNFα was detected in RNA extract of microdissected non-neuronal cells, while TNFα transcripts remained undetectable in the RNA extract of microdissected neurons (Fig. 11J).

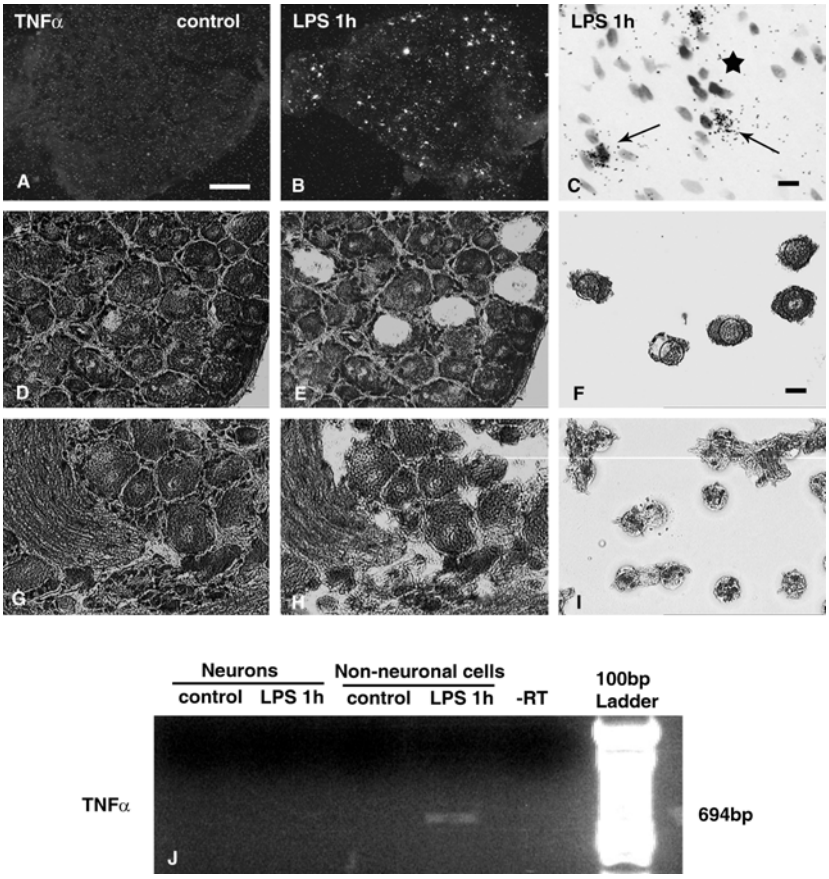

Fig. 11 Detection of TNFα mRNA in rat DRG by in situ hybridization and in microdissected cells by RT-PCR

ISH: Darkfield images showing (**A**) absence of positive hybridization signals for TNFα mRNA from a lumbar DRG section of an untreated rat and (**B**) strong hybridization signals for TNFα mRNA in a lumbar DRG section of a rat 1h after LPS. (**C**) High resolution brightfield image showing the silver grains representing TNFα mRNA over non-neuronal cells at 1h after LPS treatment (arrows) and the absence of specific hybridization signals over neuronal perikarya (asterisk).

LCM: (**D** and **G**) before LCM, (**E** and **H**) after LCM, (**F** and **I**) microdissected materials. From each sample about 200 microdissected neurons and the microdissected non-neuronal cells from approximately 200 laser pulses were subjected to RT-PCR analysis. (**J**) Specific PCR products for TNFα were amplified only from the RNA extracts of microdissected non-neuronal cells at 1 h after LPS. Scale bar in A: 200 μm, in C and F: 10 μm.

3.4 Expression of IL-1R1 and IL-1β in rat dorsal root ganglion

3.4.1 RT-PCR detection of IL-1R1 and IL-1β in RNA extracts of rat dorsal root ganglion

To investigate whether IL-1R1 and IL-1β are expressed in rat DRG and whether their expression is regulated by systemic application of LPS, total RNAs of DRG from untreated rats and from LPS treated rats were analyzed by RT-PCR. Both IL-1R1 and IL-1β could be detected in the RNA extracts of DRG from untreated rats after 40 cycles of amplification. LPS had no apparent effect on IL-1R1 transcript levels at 6 h after i.p. application (Fig. 12 upper panel). However, 3 h after LPS, IL-1β transcripts appeared to be significantly increased (Fig. 12 middle panel).

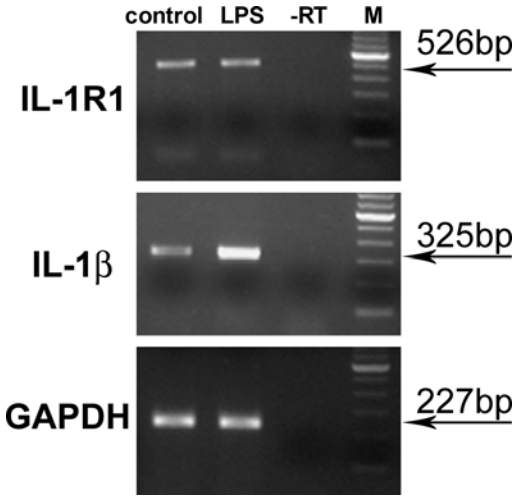

Fig. 12 RT-PCR analysis of IL-1R1 and IL-1β in rat DRG

Photographs of agarose gel stained with ethidium bromide show RT-PCR products for IL-1R1 and for IL-1β amplified from DRG total RNA extracts. LPS seems to have no effects on the levels of IL-1R1 mRNA in rat DRG at 6 h after LPS (upper panel), while IL-1β mRNA levels have dramatically increased at 3 h after LPS treatment as compared with control (middle panel). GAPDH as house-keeping gene exhibits no difference between the samples (lower panel). The size of PCR products is indicated. –RT: RT-PCR without reverse transcriptase as negative control. M: 100 bp ladder.

3.4.2 RT-PCR analysis of IL-1R1 and IL-1β expression in microdissected dorsal root ganglion neurons

In order to investigate whether IL-1R1 and IL-1β are expressed in rat DRG neurons, RT-PCR analysis on RNA extracts of microdissected DRG neurons was performed. In RNA extracts of microdissected neuronal perikarya specific PCR products for IL-1R1 but not for IL-1β could be detected after 45 cycles of amplification (Fig. 13D).

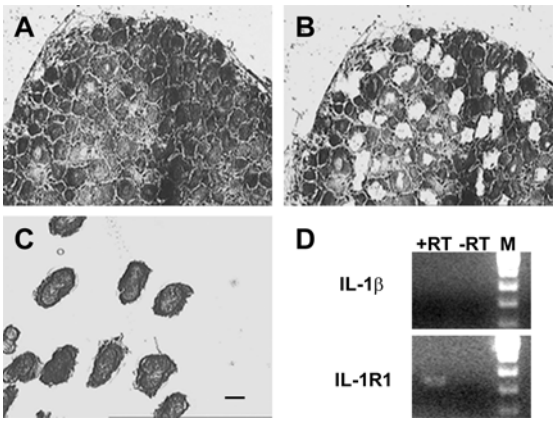

Fig. 13 RT-PCR analysis of IL-1β and IL-1R1 on RNA extracts of microdissected rat DRG neurons

Photographs show: (**A**) before microdissection (**B**) after microdissection (**C**) microdissected material (**D**) RT-PCR analysis on the RNA extracts from about 400 neuronal perikarya microdissected from the sections of a rat 3 h after LPS treatment. –RT: RT-PCR without reverse transcriptase as negative control. M: 100 bp ladder.

3.4.3 Northern blot analysis of IL-1R1 expression in rat dorsal root ganglion and in the F11 cell line

To further prove the neuronal expression of IL-1R1 Northern blot analysis was carried out on the poly(A)$^+$ RNA extracts of rat DRG and of the sensory cell line F11. As shown in Fig. 14, a single distinct band of 5.7 kb for rat IL-1R1 mRNA similar to that in rat parietal cells (119) was observed in the poly(A)$^+$ RNA extract of F11 cells and in that of rat DRG as well.

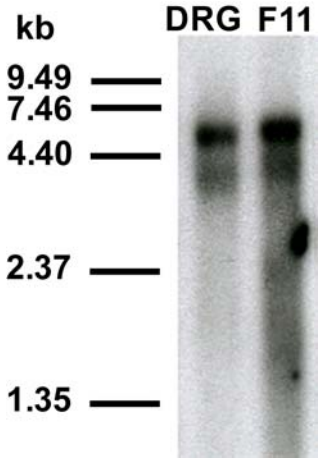

Fig. 14 Detection of IL-1R1 in rat DRG and in the F11 cell line by Northern blot

A distinct band of 5.7 kb for rat IL-1R1 mRNA was detected in poly(A)$^+$ RNA extract (5μg) of rat DRG and in that of F11 cells. Exposure time: 48 h. RNA size marker is indicated.

3.4.4 Cell-specific expression of IL-1R1 mRNA in rat dorsal root ganglion

To localize IL-1R1 mRNA in rat DRG, ISH was performed on the sections of rat L4 DRG. Hybridization signals for rat IL-1R1 mRNA were observed in a subset of cells through a section (Fig. 15A). Under brightfield illumination, the silver grains representing for IL-1R1 mRNA were found in a subset of DRG neurons (asterisks in Fig. 15C), which were recognized with large faint-stained nucleus and in non-neuronal cells (arrows in Fig. 15C) as well, which were recognized with small dark-stained

nucleus. Cell counting showed approximately 60% of rat DRG neurons expressing IL-1R1 mRNA. Most of these neurons were found to be small to medium size in diameter. LPS treatment had no effect on the levels of IL-1R1 mRNA (data not shown).

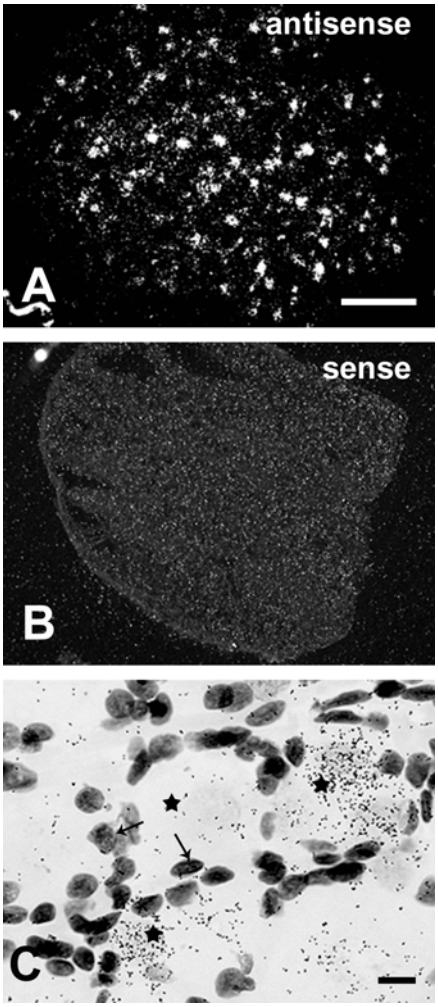

Fig. 15 Localization of IL-1R1 mRNA in rat DRG

Low power darkfield images show (**A**) hybridization signals for IL-1R1 mRNA in a subset of cells through a rat DRG section and (**B**) no specific hybridization signal in a section hybridized with sense probes. (**C**) High power bright field image show the neuronal (asterisks) and non-neuronal (arrows) localization of the hybridization signals for IL-1R1 in a DRG section. RNA probes for IL-1R1 were labeled with both ^{35}S-UTP and ^{35}S-CTP. Exposure time: 6 weeks. Scale bar in A: 200 μm and in C: 10 μm.

3.4.5 Relationship of IL-1R1 expression with putative nociceptive neuronal populations expressing SP, CGRP and VR1

To determine the neuronal subpopulations expressing IL-1R1, the expression of IL-1R1 mRNA in pain related neurons was examined. αCGRP and SP were used as markers for peptidergic neurons involved in the nociceptive transmission and VR1 was used as a marker for polymodal nociceptive neurons. Double labeling ISH was performed. As shown in Fig. 16 and table 2, approximately 64% of αCGRP positive cells were found to express IL-1R1 mRNA and about 38% of IL-1R1 mRNA expressing neurons were found to express αCGRP (Fig. 16A). Approximately 48% of substance P positive cells were found to express IL-1R1 and about 30% of IL-1R1 expressing neurons were found

to express SP (Fig. 16B). Approximately 77% of VR1 mRNA positive cells were found to express IL-1R1 and about 51% of IL-1R1 mRNA expressing neurons were found to express VR1 (Fig. 16C).

Table 2 Percentage of neurons coexpressing IL-R1 with CGRP, SP or VR1 mRNAs in rat DRG

	Number of single labeled neurons per section*	Number of double labeled neurons per section	Percetage of double labeled neurons in single labeled neurons
αCGRP	78	50	64%
IL-1R1	132		38%
SP	61	29	48%
IL-1R1	95		30%
VR1	139	107	77%
IL-1R1	209		51%

* Note: For coexpression of IL-1R1 with CGRP or SP, 6 sections were counted. For coexpression of IL-1R1 with VR1, one section was counted.

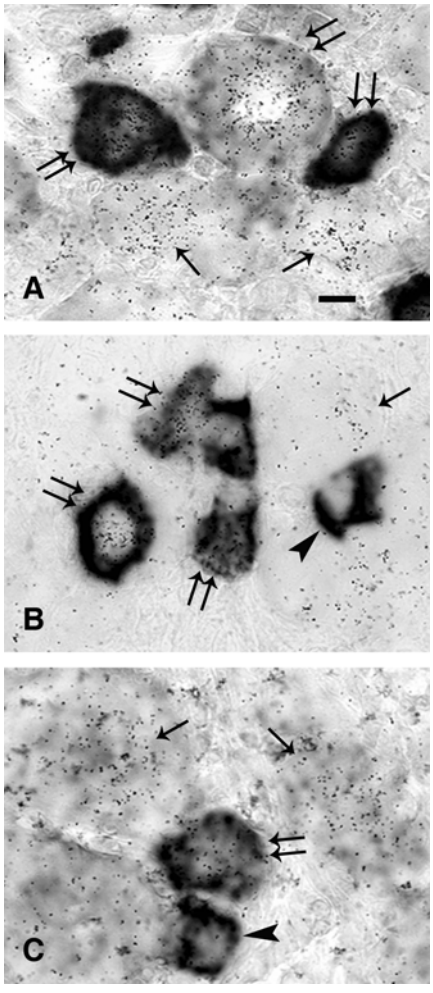

Fig. 16 Colocalization of IL-1R1 and αCGRP, SP or VR1 in rat DRG

Brightfield images show (**A**) colocalization of IL-1R1 and αCGRP, (**B**) colocalization of IL-1R1 and SP, (**C**) colocalization of IL-1R1 and VR1. Digoxigenin-labeling is recognized as dark reaction products and radioactive-labeling is seen as grains. Double labeled cells are indicated by double arrows. The neuronal cells expressing IL-1R1 mRNA but not expressing αCGRP, SP or VR1 are indicated by single arrows. The neuronal cells expressing αCGRP, SP or VR1 but not expressing IL-1R1 mRNA are indicated by arrow heads. Scale bar in A: 10 μm.

3.4.6 Constitutive and LPS-induced cellular distribution of IL-1β in rat dorsal root ganglion

To detect the cellular distribution of IL-1β mRNA in rat DRG under untreated conditions and under LPS treatment ISH was carried out. The sections of rat L4 DRG from untreated rats and from rats 3 h after LPS treatment were investigated. No specific hybridization signals for IL-1β mRNA were observed in DRG sections of untreated rats (Fig. 17A). However, IL-1β could be detected in the RNA extract of DRGs from untreated rats by RT-PCR (see Fig. 12). This suggests that IL-1β mRNA is expressed at very low levels, which can not be detected by ISH at current exposure conditions. Strong hybridization signals for IL-1β mRNA were detected in DRG sections of rats 3 h after LPS treatment (Fig. 17B). This is in agreement with RT-PCR results. When the sections were analyzed at high magnification the silver grains representing IL-1β mRNA were found over non-neuronal cells. No specific labeling for IL-1β was found over neurons (Fig. 17C).

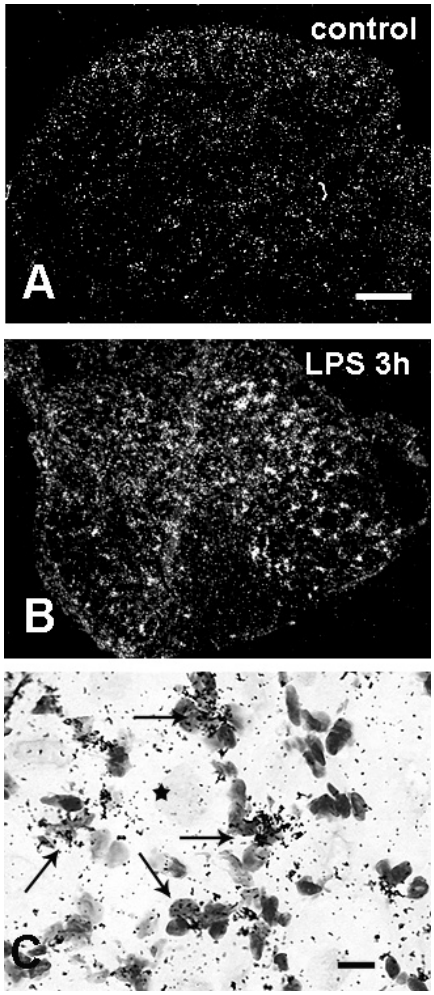

Fig. 17 Localization of IL-1β mRNA in rat DRG

Low power darkfield images show (**A**) no specific hybridization signal for IL-1β in a DRG section of an untreated rat and (**B**) specific hybridization signals for IL-1β in a DRG section of a rat 3 h after LPS treatment. High power brightfield image show (**C**) the silver grains representing hybrids for IL-1β mRNA over non-neuronal cells (arrows) but not over neurons (asterisk). The non-neuronal cells are recognized with small dark-stained nucleus. The neurons are recognized with large faint-stained nucleus. Exposure time: 1 week. Scale bar in A: 200 μm and in C: 10 μm.

3.5 Expression of LPS receptors in rat dorsal root ganglion

3.5.1 RT-PCR detection of TLR4 and CD14 in RNA extracts of rat dorsal root ganglion

To investigate whether the LPS related receptors TLR4 and CD14 are expressed in rat DRG and whether TLR4 and CD14 are regulated by systemic injection of LPS, RT-PCR analysis was performed. As shown in Fig. 18, TLR4 could be detected after 40 cycles of amplification in DRG RNA extracts both from untreated rats and from rats 6 h after LPS treatment. LPS had no apparent effect on TLR4 transcript levels at 6 h after i.p. application. CD14 was also detectable in RNA extracts of DRG both from untreated rats and from rats 6 h after LPS treatment after 35 cycles of amplification. However, CD14 transcripts appeared to be significantly increased at 6 h after LPS injection.

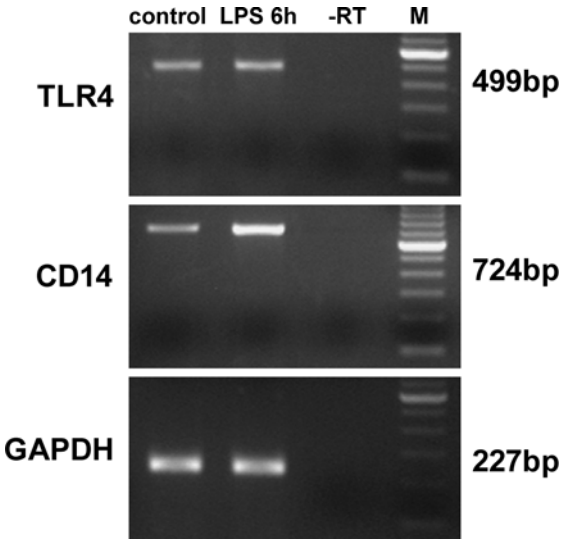

Fig. 18 RT-PCR analysis of TLR4 and CD14 in rat DRG

Photographs of agarose gel stained with ethidium bromide show RT-PCR products for TLR4 and for CD14 amplified from DRG RNA extracts. LPS seems to have no effects on the levels of TLR4 mRNA in rat DRG at 6 h after LPS (upper panel), while CD14 mRNA levels have dramatically increased at 6 h after LPS treatment as compared with control (middle panel). GAPDH as house-keeping gene exhibits no difference between the samples (lower panel). The size of PCR products is indicated. – RT: RT-PCR without reverse transcriptase as negative control. M: 100 bp ladder.

3.5.2 Northern blot analysis of TLR4 and CD14 expression in rat dorsal root ganglion

RT-PCR suggests that TLR4 is constitutively expressed in rat DRG and that LPS has no apparent effect on TLR4 expression. In order to further confirm the constitutive expression of TLR4 mRNA in rat DRG, Northern blot analysis was performed on the poly(A)$^+$ RNA of DRGs pooled from untreated rats. As shown in Fig. 19A, a single band of 3.4 kb for rat TLR4 similar to that in cardiac myocytes (120) was observed. RT-PCR also indicates that CD14 mRNA is dramatically upregulated by LPS in rat DRG at 6h after intraperitoneal application. In order to quantify the increase of CD14 mRNA levels in rat DRG after LPS injection, Northern blot analysis was performed. A single band of

1.6 kb for rat CD14 similar to that in hepatocytes (121) was observed in DRG total RNA extracts both from untreated rats and from rats 6 h after LPS treatment. In agreement with the result of RT-PCR, CD14 mRNA levels were found to be significantly increased at 6 h after LPS administration. Density analysis revealed an approximately 300-fold increase of CD14 mRNA levels at 6 h after LPS as compared with untreated control (Fig.19B).

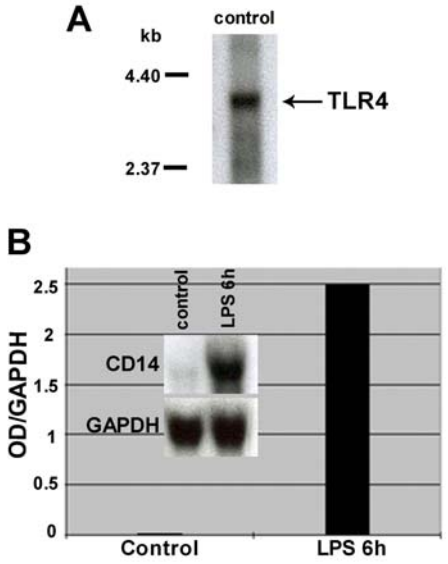

Fig. 19 Northern blot analysis of TLR4 and CD14 mRNA in rat DRG

(**A**) Photograph shows a single band of 3.4 kb for rat TLR4 mRNA in the poly(A)$^+$ RNA (5 μg) of DRGs pooled from untreated rats. RNA size marker is indicated. (**B**) A single band of 1.6 kb for rat CD14 mRNA in DRG total RNA extracts (20 μg) both from an untreated rat and from a rat 6h after LPS treatment. Densitometry shows an approximately 300-fold increase of CD14 mRNA levels in rat DRG at 6 h after LPS. Exposure time: 17 h for TLR4, 15 h for CD14 and 2.5 h for GAPDH.

3.5.3 RT-PCR analysis of TLR4 expression in microdissected dorsal root ganglion neurons

In order to examine whether TLR4 mRNA is expressed in rat DRG neurons, RT-PCR analysis was performed on the total RNA extract of the microdissected DRG neurons. As shown in Fig. 20D, specific PCR products for TLR4 could be detected after 45 cycles of amplification. This suggests that the mRNA encoding TLR4 is constitutively expressed in rat DRG neuronal cells.

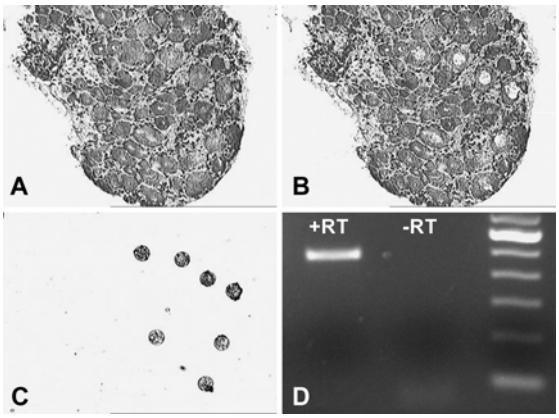

Fig. 20 Detection of TLR4 transcripts in RNA extracts of microdissected DRG neurons

(**A**) Before microdissection. (**B**) After microdissection. (**C**) Microdissected material. (**D**) A specific band of PCR products for TLR4 was detected after 45 cycles of amplification on the RNA extract of about 400 microdissected neurons. –RT: RT-PCR without reverse transcriptase as negative control.

3.5.4 Cellular distribution of constitutive TLR4 expression in rat dorsal root ganglion

RT-PCR analysis of the RNA extract of microdissected DRG neurons suggested that TLR4 mRNA is constitutively expressed in rat DRG neurons. To investigate the cellular distribution of TLR4 mRNA and to clarify whether the neuronal expression of TLR4 is in all DRG neurons or restricted to a subset of DRG neurons, ISH studies were performed. As shown in Fig. 21A, specific hybridization signals for TLR4 were observed in rat DRG. Under brightfield illumination, the silver grains representing rat TLR4 mRNA were found in a subset of DRG neurons (asterisks in Fig. 21C), which were recognized by their large faintly-stained nucleus and in non-neuronal cells (arrows in Fig. 21C) as well, which were recognized by their small dark-stained nucleus. Cell counts showed that approximately 62% of rat DRG neurons expressed TLR4 mRNA. Most of these neurons were found to be small to medium size in diameter. LPS treatment had no effect on the levels of TLR4 mRNA (data not shown).

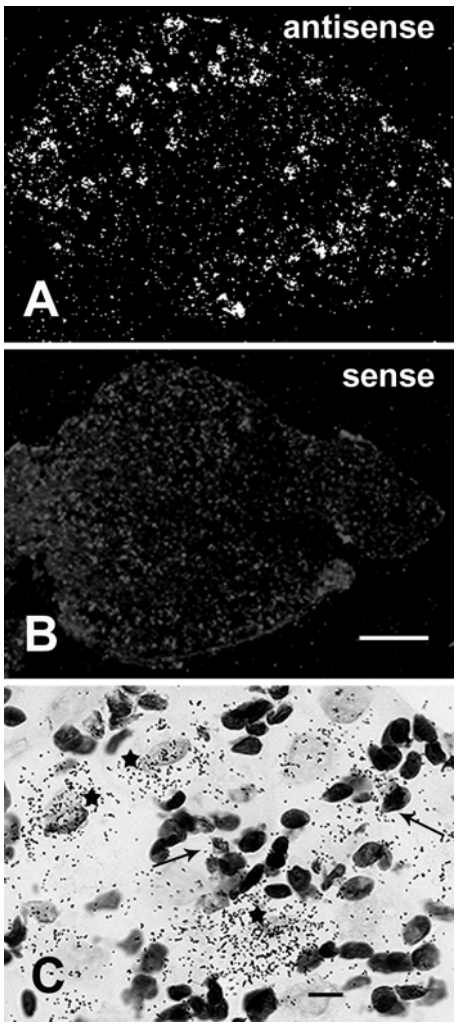

Fig. 21 Cellular distribution of TLR4 mRNA in rat dorsal root ganglion

Low power darkfield images illustrate (**A**) specific hybridization signals for TLR4 mRNA in a section of a rat L4 DRG and (**B**) no specific hybridization signal in a section hybridized with sense probes. High power brightfield image show (**C**) the neuronal (asterisks) and non-neuronal (arrows) localization of the hybridization signals for TLR4 in a DRG section. RNA probes for TLR4 were labeled with both ^{35}S-UTP and ^{35}S-CTP. Exposure time: 40 days. Scale bar in B: 200 μm and in C: 10 μm.

3.5.5 Relationship of TLR4 expression with putative nociceptive neuronal populations expressing SP, CGRP or VR1

To determine the neuronal subpopulations expressing TLR4, the expression of IL-1R1 mRNA in pain related neurons was examined. αCGRP and SP were used as markers for peptidergic neurons involved in the nociceptive transmission and VR1 was used as a marker for polymodal nociceptive neurons. Double labeling ISH was performed using radioactive labeled probes for the detection of TLR4 mRNA and digoxigenin labeled probes for the detection of the mRNAs coding αCGRP, SP or VR1. As shown in Fig. 22 and table 3, approximately 50% of αCGRP positive cells were found to express TLR4 mRNA and about 24% of TLR4 mRNA expressing neurons were found to express αCGRP (Fig. 22A). Approximately 50% of substance P positive cells were found to express TLR4 and about 15% of TLR4 expressing neurons were found to express SP (Fig. 22B). Approximately 51% of VR1 mRNA positive cells were found to express TLR4 and about 24% of TLR4 mRNA expressing neurons were found to express VR1 (Fig. 22C).

Table 3 Percentage of neurons coexpressing TLR4 with CGRP, SP or VR1 mRNAs in rat DRG

	Number of single lebeled neurons per section*	Number of double labeled neurons per section	Percentage of double labeled neurons in single labeled neurons
αCGRP	116	58	50%
TLR4	236		24%
SP	74	37	50%
TLR4	243		15%
VR1	68	35	51%
TLR4	144		24%

* Note: For coexpression of TLR4 with CGRP or VR1, 5 sections were counted. For coexpression of TLR4 with SP, 4 sections were counted.

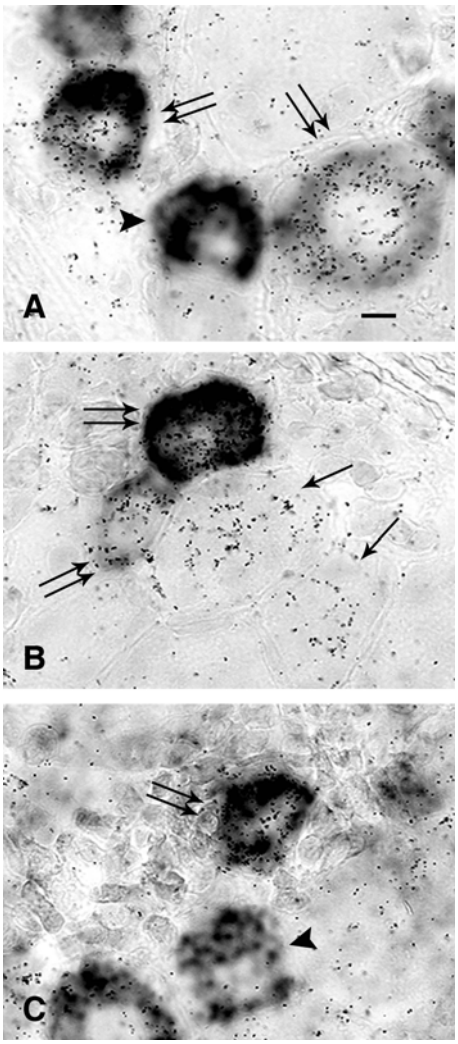

Fig. 22 Colocalization of TLR4 and αCGRP, SP or VR1

Brightfield images show (**A**) colocalization of TLR4 and αCGRP, (**B**) colocalization of TLR4 and SP, (**C**) colocalization of TLR4 and VR1. Digoxigenin-labeling is recognized as dark reaction product and radioactive-labeling is seen as grains. Double labeled cells are indicated by double arrows. The neuronal cells expressing TLR4 mRNA but not expressing αCGRP, SP or VR1 are indicated by single arrows. The neuronal cells expressing αCGRP, SP or VR1 but not expressing TLR4 mRNA are indicated by arrow heads. Scale bar in A: 10 μm.

3.5.6 Constitutive and LPS-induced cellular distribution of CD14 in rat dorsal root ganglion

To examine the cellular distribution of CD14 mRNA in DRG from controls and after LPS treatment, ISH was performed on sections of rat L4 DRG. No specific hybridization signals for CD14 mRNA were observed in DRG sections of untreated rats (Fig. 23A). However, CD14 could be detected in DRG RNA extracts of untreated rats by RT-PCR (see Fig. 18) and by Northern blot (see Fig. 19B). These results suggest that CD14 mRNA is expressed at very low levels and could not be detected by ISH at current exposure conditions. Strong specific hybridization signals for CD14 mRNA in DRG were detected 6 h after LPS treatment (Fig. 23B). This is in agreement with the results of RT-PCR and Northern blot. As shown at high magnification in Fig. 23C, the

silver grains representing CD14 mRNA were found only over non-neuronal cells. No specific labeling for CD14 was found over neurons.

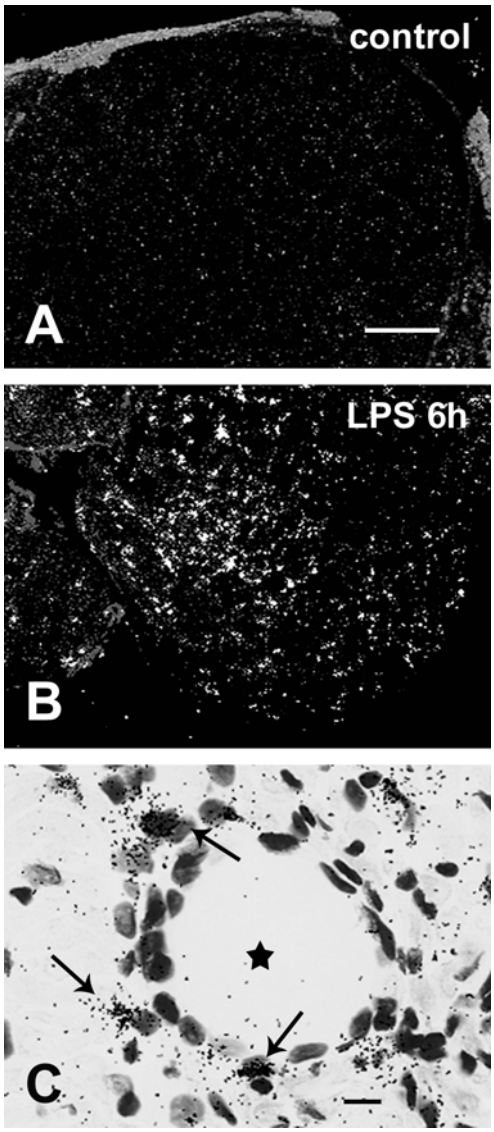

Fig. 23 Cellular distribution of CD14 mRNA in rat DRG

Low power darkfield images show (**A**) no specific hybridization signal for CD14 in a DRG section of an untreated rat and (**B**) strong specific hybridization signals for CD14 in a DRG section of a rat 6 h after LPS treatment. High power brightfield image (**C**) shows the silver grains for CD14 mRNA over non-neuronal cells (arrows) but not over neurons (asterisk). The non-neuronal cells are recognized by their small dark-stained nucleus. The neurons are recognized by their large faintly-stained nucleus. Exposure time: 2 weeks. Scale bar in A: 200 μm and in C: 10 μm.

4 Discussion

The following essential new findings have been obtained in this thesis.

(1) For the first time, the structure and the organization of the rat TNFR2 gene has been identified and the tissue-specific distribution and LPS-induced regulation of its three variants have been characterized.

(2) TNFR1 mRNA is expressed in all DRG neurons including presumed nociceptive neurons coding for VR1, SP and CGRP whereas TNFR2 mRNA is totally absent from DRG neurons; TNFR1 mRNA and TNFR2 mRNA are constitutively expressed in DRG non-neuronal cells and their expression is increased after systemic LPS.

(3) Like DRG neurons, the sensory cell line F-11 expresses TNFR1 but not TNFR2 and thus, is uniquely suited to study TNFR1-mediated intracellular signaling and cellular functions independent from that of TNFR2 effects.

(4) There is no evidence for but strong evidence against constitutive or LPS-induced expression of TNFα and IL-1β mRNAs in DRG neurons.

(5) IL-1R1 and TLR4 mRNAs are expressed in a major subpopulation of DRG neurons and exhibit substantial coincidence with presumed nociceptive neurons expressing VR1, SP or CGRP. In addition, IL-1R1 and TLR4 mRNAs exhibit constitutive expression in non-neuronal cells of the rat DRG.

(6) In contrast to the functional LPS receptor TLR4, the LPS receptor accessory protein CD14 is totally absent from DRG neurons under normal and LPS stimulated conditions. However, in DRG non-neuronal cells CD14 expression is induced by LPS.

4.1 Identification, structural characterization, tissue-specific distribution and LPS-induced regulation of the rat TNFR2 gene

This thesis describes the complete characterization of the cDNA sequence and the structure of the rat TNFR2 gene. Three cDNAs encoded by the rat TNFR2 gene have been identified. They contain the same 5'-untranslated sequence and the same full coding region. The rat TNFR2 gene is demonstrated to contain 10 exons and 9 introns that are located on chromosome 5q36. Therefore, the overall organization of the rat TNFR2 gene is identical to that of human and mouse, which also contain 10 exons and 9 introns as reported previously (35, 36).

Northern blot analysis performed in this thesis has revealed that three different transcripts for the rat TNFR2 gene exist in all tissues examined including DRG, spinal cord, brain, spleen, lung and kidney. These data conform to previous observations of three mRNAs of the rat TNFR2 gene found in microglia (37). Comparing the mRNA transcripts of the rat TNFR2 gene with those of the human (122) and mouse TNFR2 gene (36) revealed that the rat TNFR2 gene transcribes three mRNAs, while the human and mouse TNFR2 genes transcribe only two mRNAs. This indicates that the TNFR2 gene transcription occurs in a species-specific manner. The possible functional implications of three TNFR2 transcripts in the rat as compared with two TNFR2 transcripts in the mouse and human remain to be shown.

Multiple transcripts from the same gene can be due to alternative splicing of exons, different cleavage with subsequent polyadenylation at the 3'-end and different initial transcription sites. For example, the two transcripts of human TNFR2 are due to different initial transcription sites (122). Like the two mouse TNFR2 transcripts (36), multiple transcripts of the rat TNFR2 gene are due to different 3'-end cleavage.

The relative abundance of the three transcripts of the rat TNFR2 gene differs. The 4.4 kb transcript is most abundant followed by the 3.1 kb and 5.4 kb transcripts. Comparing the 3'-UTR of the three transcripts of the rat TNFR2 gene, three typical polyadenylation signals (AATAAA) (123, 124) have been found within 45 nucleotides upstream of the 3'-end cleavage site in the 4.4 kb transcript (see Fig. 2), but only one relatively commonly used polyadenylation signal (ATTAAA) in the 5.4 kb transcript and only one shortened version (ATAAA) of the consensus polyadenylation signal sequence in the 3.1 kb transcript is encountered. This may account for the more abundant expression of the 4.4 kb mRNA as compared with that of the 3.1 kb and 5.4 kb transcripts.

LPS-induced regulation of the three rat TNFR2 mRNAs in the spleen and DRG is different. In the spleen, systemic LPS treatment predominantly increases the 3.1 kb transcript, while the 4.4 kb and the 5.4 kb transcripts are only marginally increased by LPS. In DRG, however, systemic LPS treatment causes a greater increase of the 4.4 kb transcript than of the 3.1 kb and 5.4 kb transcripts. This suggests tissue-specific or cell-specific regulation of individual transcripts of the rat TNFR2 gene after systemic LPS. The evidence obtained in the present study that TNFR2 transcripts exhibit tissue-specific and cell-specific expression and regulation pattern needs to be further elaborated in other tissues, cell types and conditions of stimulation. The possible role of

differential regulation of TNFR2 transcripts in the peripheral nervous system (i.e. DRG) and in the immune system (i.e. spleen) is a matter of speculation at present.

4.2 Functional implications of TNFR1 and TNFR2 expression in rat dorsal root ganglion

4.2.1 Expression of TNFR1 but not of TNFR2 in dorsal root ganglion neurons and the sensory F-11 cell line

Based on sensitive methods of ISH and of RT-PCR in combination with LCM, this study provides strong evidence that TNFR1 but not TNFR2 is expressed in DRG neurons and that all DRG neurons express TNFR1. Previously, neuronal TNFR1 expression has been found in trigeminal ganglia of the mouse (40) and in primary sensory neurons of the trigeminal mesencephalic nucleus of the mouse (125). The total lack of neuronal expression of TNFR2 in rat DRG demonstrated in the present study is in contrast to the reported presence of TNFR2 expression in mouse trigeminal ganglia, though at very low levels (40). The presence of TNFR1 but absence of TNFR2 expression in DRG neurons corresponds well to the observation that TNFR1 but not TNFR2 was found to be expressed in the sensory cell line F-11 as revealed by RT-PCR and Western blot analysis in the present study. There is no previous report on TNF receptor expression in the F-11 cell line. Thus, the present study is the first to provide evidence that the F-11 cell line represents a new tool to study TNFR1-mediated intracellular signaling and cellular functions independent from that of TNFR2-mediated effects.

The neuronal expression of TNFR1 may suggest that TNFα-induced hyperalgesia is at least partially dependent on TNFR1. Indeed, neutralizing antibodies against TNFR1 but not against TNFR2 reduce thermal hyperalgesia and mechanical allodynia in the CCI mouse (126). Intrathecally applied antisense oligodeoxynucleotides to TNFR1 decrease not only TNFR1 protein expression in peripheral nerve terminals of DRG neurons but also reduce inflammatory hyperalgesia in the rat (56).

Taken together, the present data in conjunction with studies on TNF receptor mediated functions of primary sensory neurons by others provide strong evidence that TNFR1 but not TNFR2 is the neuronal TNF receptor of primary sensory neurons of the rat DRG with functional significance for nociceptive signaling.

In contrast to these results, several recent studies of others have demonstrated positive immunostaining for TNFR2 in DRG neurons of rats and mice (27, 38, 39). However, TNF receptor immunostaining likely to occur in DRG non-neuronal cells has not been observed by these authors. Analysis of the cellular expression of TNFR1 and TNFR2 in DRG at the mRNA level was not performed. In light of the absence of TNFR2 mRNA from DRG neurons but presence of TNFR2 mRNA in DRG non-neuronal cells shown in this study, it seems very unlikely that TNFR2 protein is truly expressed in DRG neurons. The reported TNFR2 immunostaining in DRG neurons (27, 38, 39) is probably due to non-specific immunostaining which cannot be explained at present, however. Therefore, the view of TNFR2 expression in DRG neurons should be dismissed.

4.2.2 Cell-specific plasticity of TNFR1 and TNFR2 expression in the dorsal root ganglion after LPS treatment

The present study has shown that systemic application of LPS enhances the expression of TNFR1 mRNA in DRG neurons and that of both TNFR1 and TNFR2 in DRG non-neuronal cells. It has been demonstrated previously that LPS causes an increase of TNFR1 and TNFR2 expression in the rat brain but the cells involved have not been clearly identified (127). In the mouse brain, LPS-induced TNFR2 mRNA is restricted to non-neuronal cells while TNFR1 mRNA occurs both in neurons and some non-neuronal cells (125). As the present study demonstrated that a specific subpopulation of DRG neurons is endowed with the LPS receptor TLR4 but not with the LPS receptor accessory protein CD14 (see below) it is concluded that the LPS-induced increase of TNF receptor expression in DRG neurons is at least in part directly mediated by neuronal TLR4. As its shown in this thesis that TNFR1 and TNFR2 expression in non-neuronal DRG cells is increased after LPS and that non-neuronal cells express CD14 and TLR4 it is conceivable that both CD14 and TLR4 mediate the LPS-induced regulation of non-neuronal TNFR1 and TNFR2. In addition concomitant induction of TNFα in and release from DRG non-neuronal cells has to be taken into account (see below). The LPS-induced enhancement of TNFR1 expression in DRG neurons is suggested to amplify TNFα signaling in primary afferents resulting in increased sensitization to inflammatory cytokines.

4.2.3 Possible roles of TNFR1 in DRG neurons and of TNFR1 and TNFR2 in DRG non-neuronal cells in pain and other sensory functions

The expression of TNFR1 in small diameter presumed nociceptive neurons expressing SP, CGRP or VR1 demonstrated in this thesis is in line with a large body of evidence for an involvement of TNFα in nociceptive responses (43, 45, 50, 128, 129). TNFα is known to induce the release of SP and CGRP from peripheral terminals (9, 130, 131). Recombinant TNFα excites nociceptors and enhances heat-evoked release of CGRP from peripheral nerve terminals (55). Acute application of TNFα to peripheral axons induces ectopic activity in nociceptive primary afferent fibers (44). Blockade of TNFα or TNFR1 reduces pain behavior (56, 126, 132). By revealing expression of TNFR1 on peptidergic and VR1 positive nociceptive neurons, the possible molecular and cellular mechanisms for direct activation of primary sensory neurons of DRG by TNFα in the course of inflammatory pain and of neuropathic pain have been identified in this thesis.

The finding that the expression of the TNFR1 gene is virtually pan-neuronal and not restricted to presumed nociceptive neurons in the rat DRG clearly implies a much broader role of TNFα in primary sensory functions than nociception alone. The most obvious possibility is that TNFR1 expressing neurons function as immunosensors (2, 133) by sensing any TNFα released in the periphery during the immune response and during inflammation, either by being in contact with TNFα secreting cells or by being exposed to circulating TNFα. For example, TNFα contributes to nerve growth factor (NGF)-dependent neuronal cell death during development (134). Neutralizing antibodies against either TNFα or TNFR1 rescued many sensory neurons following NGF deprivation in vitro (134). Continuous presence of TNFα is required for preservation of synaptic strength at excitatory synapses. TNFα enhances synaptic efficacy by increasing surface expression of AMPA receptors (135). Preventing the actions of endogenous TNFα has the opposite effects. Through its effects on AMPA receptor trafficking, TNFα may play a role in synaptic plasticity and modulating responses to neural injury (135). Very recently, however, a neuronal protective effect of TNFα in glutamate-induced neuronal cell death has been demonstrated in neuron-microglia cocultures (136).

Taken together, the neuronal expression of TNFR1 but not of TNFR2 in DRG strongly suggests that endogenous and exogenous TNFα are likely to influence primary

sensory functions and neurotransmission directly by acting on TNFR1, both at the level of cell bodies and at the terminals in DRG and periphery. Similar considerations apply to the spinal cord where TNFα can be synthesized by and released from glial cells (50, 137, 138). The non-neuronal expression of both TNFR1 and TNFR2 in DRG and their plasticity after LPS indicate that endogenous and exogenous TNFα would activate the non-neuronal cells via both TNFR1 and TNFR2. The activation of these non-neuronal cells is likely to result in the release of TNFα and other mediators, which can be expected to directly act in a paracrine manner on primary sensory neurons (Fig. 24 and Fig. 26).

4.2.4 Cellular source of TNFα in rat dorsal root ganglion

In this study it was shown that systemic application of LPS induces the expression of TNFα mRNA in DRG non-neuronal cells. These TNFα expressing cells most likely represent resident macrophages or dendritic cells but may also include mast cells, i.e. cell types known to occur in DRG and shown to be capable of TNF synthesis (25, 139-142). In the peripheral nervous system TNFα has been demonstrated in macrophages (139), mast cells (142), Schwann cells (25, 141) and fibroblasts (140). To unequivocally determine the cellular identity of the non-neuronal cells expressing TNFα double labeling studies at the mRNA and protein level need to be performed.

Several studies have described the presence and axonal transport of TNFα in DRG neurons (27-29). Based on immunocytochemistry, TNFα has been reported to be present in a subpopulation of primary afferents after chronic constriction injury (CCI) of the sciatic nerve (27, 28) and neuronal biosynthesis of TNFα has been proposed. An increase of TNFα mRNA in rat DRG after nerve injury has been reported but the cellular source of TNFα synthesis has not been determined (143). If the view that TNFα protein is synthesized by DRG sensory neurons is correct, TNFα mRNA should be expressed by DRG neurons. Contrary to the assumptions in the literature that DRG neurons synthesize TNFα the present study provides no evidence for but major evidence against TNFα gene expression in DRG neurons. Sensitive and specific radioactive ISH revealed neither constitutive nor LPS-induced expression of TNFα mRNA in rat DRG neurons. Using the sensitive RT-PCR method on RNA extracts of microdissected DRG cells, TNFα transcripts were easily detected in DRG non-neuronal cells of the rats 3h after LPS treatment but not in DRG neurons of normal or LPS-

treated rats. This conforms well to similar expression pattern as revealed by in situ hybridization in this study which demonstrated TNFα to be clearly restricted to non-neuronal cells. There is a theoretical possibility that the presence of immunostained TNFα protein in DRG neurons as reported by Schäfers et al. (28, 29) and by Shubayev and Myers (27) could be due to neuronal uptake of TNFα. However, direct evidence for TNFα uptake by DRG neurons is missing. TNFα originating from the circulation or from juxtaneuronal non-neuronal cells could bind to neuronal TNFR1 with subsequent internalization resulting in the presence of immunostainable TNFα in DRG neurons. Surprisingly, the authors claiming the presence of specific TNFα immunoreactivity did not comment on TNFα immostaining in non-neuronal cells. Therefore, the total lack of TNFα mRNA from DRG neurons as unequivocally revealed in this study may rather point to the conclusion that the reported TNFα immunostaining in DRG neurons is non-specific. Therefore, the view of TNFα biosynthesis in DRG neurons should be dismissed.

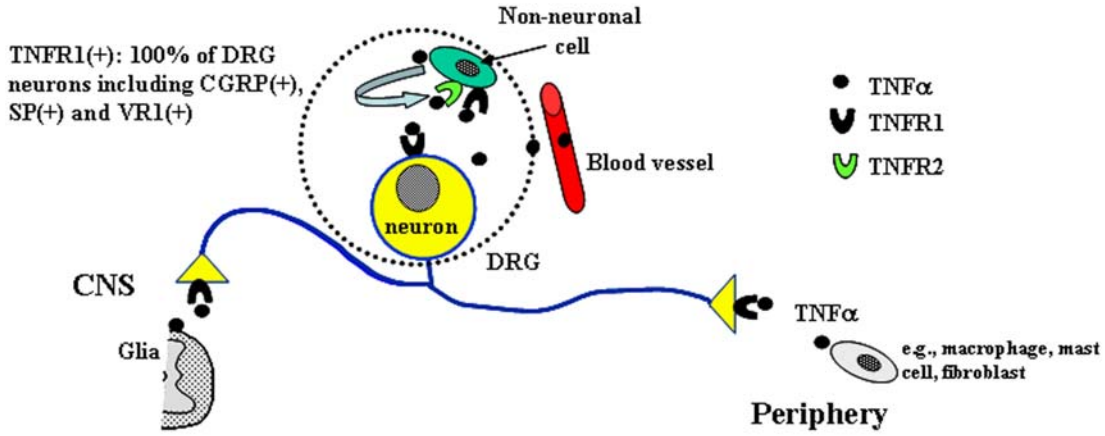

Fig. 24 Schematic diagram demonstrating the cellular and molecular basis of TNFα-mediated signaling in primary sensory neurons and non-neuronal cells in rat DRG

TNFR1 is expressed in all DRG neurons. Both TNFR1 and TNFR2 are expressed in DRG non-neuronal cells. LPS induces expression of TNFα that occurs exclusively in non-neuronal cells. Endogenous or exogenous TNFα is likely to directly act on DRG neurons via TNFR1, both at the level of cell bodies and at the terminals inside DRG and in the periphery. Similar considerations apply to the spinal cord where TNFα can be synthesized by and released from glial cells. In addition, endogenous and exogenous TNFα can be expected to act on DRG non-neuronal cells by acting on TNFR1 and/or TNFR2. TNFR1 expressing DRG neurons may function as immunosensors to sense TNF during immune responses or inflammation. For more details and references see related text.

4.3 Functional implications of IL-1β and IL-1R1 expression in rat dorsal root ganglion

4.3.1 Cellular source of IL-1β in rat dorsal root ganglion

The present study clearly shows that LPS-induced expression of IL-1β mRNA occurs in DRG non-neuronal cells and provides strong evidence against expression of IL-1β mRNA in DRG neurons. Previously, using less sensitive in situ hybridization with non-radioactive (digoxigenin) labeled probes and immunocytochemistry, Copray and coworkers have reported that IL-1β mRNA and IL-1β protein are expressed in about 70% of rat DRG neurons but did not comment on IL-1β expression in DRG non-neuronal cells (82). This is in contrast to the present study, which demonstrated by very sensitive ISH with radioactive labeled probes, that hybridization signals for IL-1β could be detected neither in DRG neurons of control rats nor in DRG neurons of LPS-treated rats. Further evidence for absence of IL-1β expression in DRG neurons was provided by the highly sensitive method of RT-PCR analysis of extracts of microdissected DRG neurons of both control rats and LPS-treated rats which consistently failed to detect IL-1β transcripts. Therefore, it is concluded that LPS-induced expression of IL-1β mRNA in rat DRG occurs exclusively in non-neuronal cells with no constitutive or LPS-inducible expression of IL-1β mRNA in DRG neurons. This obvious discrepancy to the data by Copray et al. (82) can be explained by the following considerations. It is conceivable that IL-1β immunostaining demonstrated by Copray and coworkers (82) is due to uptake of IL-1β by DRG neurons from the circulation or non-neuronal local cells. On the other hand, non-radioactive in situ hybridization involves a step of immunocytochemistry to visualize digoxigenin-labeled probes with anti-digoxigenin antibodies which imply the possibility for non-specific overstaining of DRG neurons. Given the proven absence of IL-1β mRNA from DRG neurons in this study, however, the view of DRG neurons expressing IL-1β should be dismissed.

4.3.2 Possible roles of IL-1R1 expression in neuronal and non-neuronal cells of rat dorsal root ganglion

The present study is the first to clearly show that IL-1R1 mRNA is constitutively expressed in a subpopulation of rat DRG neurons and in some DRG non-neuronal cells, too. Previously, Copray and coworkers have demonstrated that IL-1R1 is expressed in

virtually all DRG neurons and all non-neuronal DRG cells using ISH with non-radioactive (digoxigenin) labeled probes (82). In this study, however, IL-1R1 mRNA could be detected neither in DRG neurons nor in DRG non-neuronal cells when using ISH with single radioactive (^{35}S-UTP) labeled probes (data not shown). It was necessary to use the more sensitive method of ISH with double radioactive (^{35}S-CTP and ^{35}S-UTP) labeled probes, to reveal IL-1RI mRNA in a specific subset of DRG neurons and DRG non-neuronal cells. In contrast to the data by Copray et al. (82), there was no evidence for pan-neuronal and pan-non-neuronal expression of IL-1R1 in DRG.

By demonstrating substantial coincidence of IL-1R1 expressing neurons with presumed nociceptive neurons expressing VR1, SP or CGRP in rat DRG, the present study has provided a possible mechanism for a direct influence of endogenous and exogenous IL-1β on DRG neurons to evoke nociceptive responses. Indeed, blocking of IL-1R1 reduces pain associated behavior (59, 60, 90-92, 144, 145). Using IL-1ra it has been demonstrated that endogenous IL-1β is involved in inflammatory hyperalgesia produced by intraplantar injection of complete Freund's adjuvant, or endotoxin in rats (93, 146). Peripheral administration of IL-1β causes hyperalgesia, presumably due to activation of peripheral sensory fibers (92). Electrophysiological studies have shown that small diameter cutaneous nerves are activated by local injection of IL-1β in rats (92).

Furthermore, coexpression of IL-1R1 with CGRP and SP in presumed nociceptive DRG neurons suggests that endogenous and exogenous IL-1β stimulated the release of these neuropeptides from DRG neurons and modulated neurogenic inflammation by direct actions on IL-1R1 bearing sensory neurons. Indeed, IL-1β has been shown to cause the releasing of CGRP (55) and SP (61, 62). A recent report by Opree and Kress suggests that IL-1β can induce a pronounced and transient sensitization of the heat-evoked CGRP release from nociceptors *in vitro* in the rat skin model (55). IL-1β in skin can induce the release of substance P (SP) from peripheral nerve terminals (147). SP is able to degranulate mast cells (148), stimulates macrophages to release TNFα, IL-1β, and IL-6 (149), and induces inflammatory responses in the skin (150). In cultured DRG neurons, IL-1β appeared to induce the release of substance P (61, 62). Coexpression of IL-1R1 with VR1 in the presumed nociceptive DRG neurons suggests the possibility that endogenous and exogenous IL-1β directly sensitizes the VR1 positive neurons to mediate noxious heat in nociceptors

during inflammation. It has been shown that capsaicin-induced vasodilatation is enhanced by IL-1β (151). However, according to the percentage of IL-1R1 expressing DRG neurons and the percentage of DRG neurons simultaneously expressing IL-1R1 and CGRP, SP or VR1 (Fig. 25), there are some DRG neurons expressing IL-1R1 but not expressing CGRP, SP or VR1. This indicates that the neuronally expressed IL-1R1 may be involved in a broder role than pain.

Moreover, presumed central terminals of IL-1R1 expressing DRG neurons could be the target of IL-1β synthesized by and released from spinal glial cells during spinal cord injury or inflammation (50, 152). However, both nociceptive (50, 137) and antinociceptive (153) effects of spinal IL-1β have been reported. Therefore, nociceptive and antinociceptive roles of spinal IL-1β need to be further clarified.

The non-neuronal expression of IL-1R1 in DRG demonstrated in this study also suggests the possibility of indirect effects of IL-1β on primary sensory neurons. IL-1β has been shown to enhance the neurite regeneration from transected nerve terminals in cultured adult DRG explants via stimulating surrounding non-neuronal cells to secrete neurotrophic factors (60). The cutaneous levels of nerve growth factor (NGF) are increased after intraplantar injection of IL-1β in rats (60, 93). NGF is known to play a major role in the development of inflammatory hyperalgesia (154, 155).

Taken together, the evidence provided by this study strongly suggests that endogenous and exogenous IL-1β is likely to influence primary sensory neurotransmission especially that related to nociception and neurogenic inflammation by directly acting on IL-1R1 expressing DRG neurons or by indirectly acting on IL-1R1 expressing non-neuronal cells which then release other mediators to act on primary sensory neurons. Endogenous and exogenous IL-1β is likely to act on primary sensory neurons in a paracrine manner and the non-neuronal cells in an autocrine and/or paracrine manner (Fig. 25 and Fig. 26).

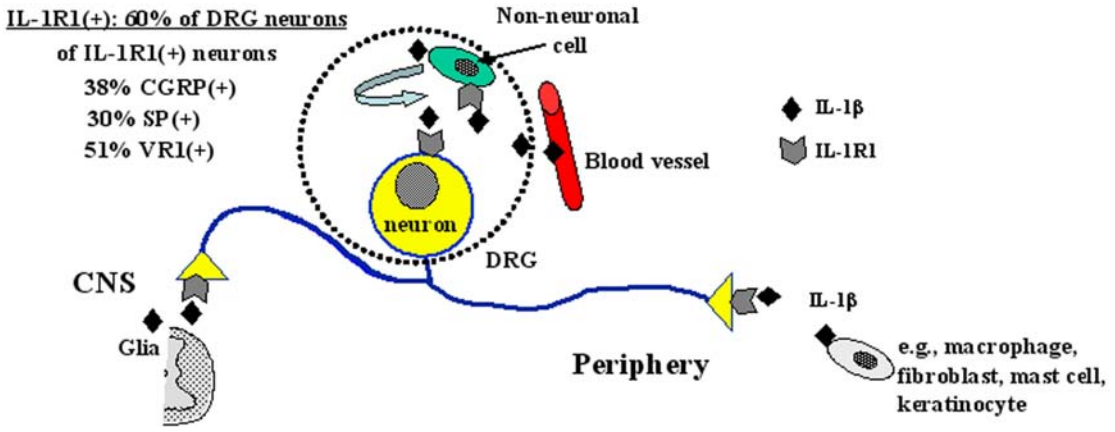

Fig. 25 Schematic diagram demonstrating the cellular and molecular basis of IL-1β-mediated signaling in primary sensory neurons and non-neuronal cells in rat DRG

IL-1R1 is expressed in a subset of rat DRG neurons and in non-neuronal cells as well. LPS induces expression of IL-1β that occurs exclusively in non-neuronal cells. Endogenous or exogenous IL-1β may directly act on DRG neurons via the neuronally expressed IL-1R1, both at the level of cell bodies and at the terminals inside DRG, in the periphery and in the CNS especially in the spinal cord, where IL-1β can be synthesized by and released from glial cells. In the periphery multiple sources for the synthesis and release of IL-1β are known, especially macrophages. In addition, endogenous and exogenous IL-1β can be expected to act on DRG non-neuronal cells via IL-1R1 expressed by non-neuronal cells. For more details and references see related text.

4.4 Functional implications of TLR4 and CD14 expression in rat dorsal root ganglion

For the first time, this study has shown that the LPS receptor TLR4 is expressed in a subset of DRG neurons and that the LPS receptor accessory protein CD14 is totally absent from DRG neurons both in control rats and in LPS-treated rats. TLR4 and CD14 are the components of the receptor complex for bacterial endotoxin (LPS) (103, 104, 156, 157). Recent studies suggest that TLR4 is the functional receptor for LPS (103-106). This discovery was made by positional cloning of the *Lps* gene in the LPS-non-responsive C3H/HeJ mouse strain (105, 106), and was confirmed in TLR4 knockout mice (104). The expression of TLR4 in DRG neurons and the absence of CD14 from DRG neurons suggest that LPS may directly activate primary DRG sensory neurons via TLR4. As DRG neurons were shown to lack CD14 the question arises whether soluble CD14 (sCD14) that could be provided from the serum is required. The sCD14 has been shown to be required for TLR4-dependent recognition of lipopolysaccharide by

epithelial cells (158). Whether activation of primary sensory neurons by LPS really requires sCD14 remains to be investigated.

By demonstrating the expression of TLR4 on presumed nociceptive neurons coding for CGRP, SP or VR1 the present study provides substantial evidence for the possibility that LPS directly activates nociceptive DRG neurons and thus can directly cause nociceptive behavior. Furthermore, LPS could directly influence neuropeptide release from peripheral nerve endings of peptidergic sensory neurons during the course of neurogenic inflammation. In fact LPS has been shown to induce hyperalgesia associated with inflammation (14, 50, 91, 107-110). Additionally, LPS has been reported to be a potent stimulus for the systemic release of CGRP in rat and pig (159-161). Accumulation of plasma CGRP is greatly diminished in endotoxin-tolerant rats exposed to endotoxin (161). LPS-induced release of CGRP from cultured rat DRG neurons has also been reported (99). LPS has been shown to induce the release of SP in experimental cystitis in mice (162). The coexpression of TLR4 and VR1 demonstrated in this thesis suggests that LPS may influence heat sensation of DRG neurons perhaps by interference with intracellular signal transduction cascades of TLR4 and VR1. In fact LPS has been shown to reduce the thermal nociceptive thresholds in rats (108).

The constitutive expression of TLR4 in non-neuronal DRG cells and the LPS-induced expression of CD14 in non-neuronal DRG cells revealed in this study indicate that indirect actions of LPS resulting in activation of primary DRG sensory neurons are also possible. LPS may act on DRG non-neuronal cells via TLR4 and CD14 to cause increased synthesis and release of TNFα and IL-1β as well as of many other mediators. These mediators may then directly act on DRG sensory neurons. Apparently both IL-1β and TNFα are crucial for the induction of LPS hyperalgesia (14, 59, 109, 110, 129). LPS-induced hyperalgesia is blocked either by IL-1 receptor antagonist (IL-1ra) or by TNF binding protein, which functionally acts as a TNFα antagonist (14, 91). Therefore, the LPS-induced pain or hyperalgesia is partially contributed by endogenous IL-1β and TNFα. The presence of IL-1R1 and TNFR1 in primary nociceptive sensory neurons in rat DRG provides a reasonable explaination for these effects.

The enhanced expression of CD14 by LPS in DRG non-neuronal cells may facilitate the responses of primary sensory neurons to LPS. In fact a priming effect of LPS to enhance endotoxin-induced thermal hyperalgesia and mechanical allodynia after a second application of LPS as compared with a single dose of LPS has been reported

(108). Intraperitoneal administration of LPS had no significant effect on either thermal or mechanical thresholds in the first few hours after injection; however, priming rats by i.p. LPS produced a reduction in both thermal nociceptive thresholds and mechanical response thresholds in rats given a subsequent i.p. injection of LPS (108).

Taken together, the neuronal expression of TLR4 in DRG strongly suggests that LPS can directly activate primary sensory neurons resulting in increased nociceptive behavior and neurogenic inflammation. This implicates that the primary sensory neurons may directly sense LPS liberated during bacterial infections. These data together with a recent report showing *E. coli*-induced sickness at a time with no detectable increases in circulating cytokines or endotoxin (96) suggests a neural pathway from the periphery to the brain during gram-negative bacterial infection. In addition indirect effects via non-neuronal DRG cells endowed with TLR4 have to be taken into account (Fig.26).

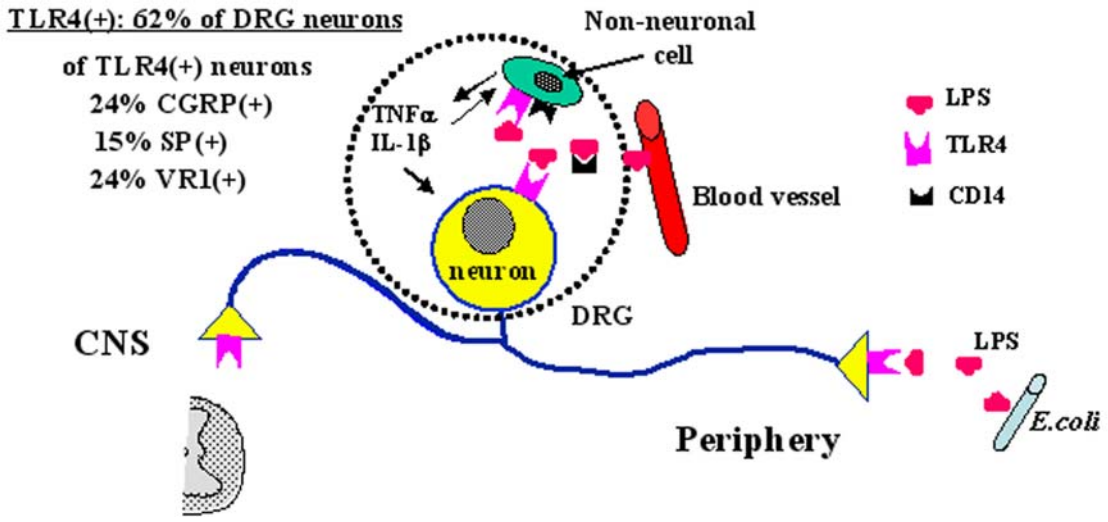

Fig. 26 Schematic diagram demonstrating the cellular and molecular basis of LPS-mediated effects on primary sensory neurons and non-neuronal cells in rat DRG

The LPS receptor TLR4 is expressed in a subset of rat DRG neurons while the LPS accessory protein CD14 is absent from neurons. Both TLR4 and CD14 are expressed in DRG non-neuronal cells. LPS entering from the blood stream is likely to directly act on DRG neurons via TLR4, both at the level of cell bodies and at the terminals. In addition, LPS can be expected to act on DRG non-neuronal cells by acting on TLR4 and CD14. This is likely to result in the induction or enhancement of biosynthesis and release of TNFα and IL-1β in the non-neuronal cells. These mediators would then act on DRG neurons in a paracrine manner and act on DRG non-neuronal cells in a paracrine and/or autocrine manner.

5 Summary

The proinflammatory cytokines tumor necrosis factor alpha (TNFα) and interleukin 1 beta (IL-1β) as well as bacterial lipopolysaccharide (LPS) are known to affect primary afferent functions related to pain and neurogenic inflammation. However, it is not completely understood how these molecules signal to primary sensory neurons of the dorsal root ganglion (DRG). In order to clarify this question RT-PCR, Northern blot, Western blot, RT-PCR in combination with laser capture microdissection (LCM) and in situ hybridization (ISH) with radioactive-labeled probes as well as double ISH were employed. These methods were used to determine the cell-specific expression pattern of TNFα, IL-1β and their functional receptors as well as of LPS-related receptors in neuronal and non-neuronal cells of rat DRG as well as in the sensory cell line F11.

The following essential new findings and conclusions have been obtained.

(1) For the first time, the rat TNFR2 gene was characterized with 10 exons and 9 introns, which are located in chromosome 5q36. Three cDNAs for the rat TNFR2 gene were identified. Their full coding region was found to be identical. Three transcripts of the rat TNFR2 gene were observed in neural tissues (i.e. DRG, spinal cord and brain) and in peripheral tissues (i.e. spleen, lung and kidney). The regulation of TNFR2 transcripts by LPS seemed to occur in a tissue- and cell-specific manner as demonstrated for the spleen and DRG.

(2) TNFR1 mRNA was found to be constitutively expressed in all DRG neurons including presumed nociceptive neurons coding for neuropeptides calcitonin gene-related peptide (CGRP), substance P (SP) or vanilloid receptor 1 (VR1) and to be increased after LPS. In contrast to the literature, TNFR2 mRNA was found to be totally absent from DRG neurons of control rats and of rats after LPS challenge. TNFR1 mRNA and TNFR2 mRNA were found to be constitutively expressed in DRG non-neuronal cells and to be increased after systemic LPS. The data provided by this study suggest that TNFα may influence DRG sensory functions by directly acting on TNFR1 in neurons or by indirectly acting on both TNFR1 and TNFR2 in non-neuronal cells.

(3) Like DRG neurons, the sensory cell line F-11 was found to express TNFR1 but not TNFR2. Therefore, the F11 cell line is uniquely suited to study TNFR1-mediated intracellular signaling and cellular functions independent from that of TNFR2 effects.

(4) There was no evidence for but strong evidence against constitutive or LPS-induced expression of TNFα and IL-1β mRNAs in DRG neurons. LPS-induced expression of TNFα and IL-1β mRNAs in DRG occurred exclusively in DRG non-neuronal cells. Thus, the previously reported concept that TNFα and IL-1β are synthesized by DRG neurons should be dismissed. To the contrary, the present data indicate that endogenous TNFα and IL-1β in DRG are exclusively synthesized by non-neuronal cells implicating that they may act on DRG neurons in a paracrine manner.

(5) In contrast to a previous report indicating that IL-1R1 is expressed in all DRG cells, the present study demonstrated that IL-1R1 mRNA is expressed only in a subpopulation of DRG neurons and in some DRG non-neuronal cells as well. IL-1R1 exhibited substantial coincidence with presumed nociceptive neurons expressing VR1, SP or CGRP. The results of the present study suggest that endogenous and exogenous IL-1β may directly activate DRG neurons via IL-1R1 to preferentially modulate nociceptive functions. In addition, IL-1β may act on DRG non-neuronal cells to cause further release of IL-1β.

(6) For the first time, the functional LPS receptor-TLR4 was demonstrated to be expressed in DRG neuronal and non-neuronal cells at the mRNA level. The neuronal expression of TLR4 was limited to a subset of DRG neurons where it exhibited substantial coincidence with presumed nociceptive neurons expressing VR1, SP or CGRP. The mRNA coding for the LPS receptor accessory protein CD14 was totally absent from DRG neurons of control rats and of rats after systemic LPS. LPS-induced expression of CD14 occurred in DRG non-neuronal cells. The present data indicate that LPS may directly act on primary sensory neurons via TLR4 or indirectly act on primary sensory neurons via TLR4 and CD14. This implies that primary sensory neurons of DRG may detect an infectious state by directly sensing LPS via TLR4.

Taken together, this study provides new insights into the cellular and molecular basis of TNFα, IL-1β and LPS mediated primary sensory neurotransmission related to pain and neurogenic inflammation. In addition, the present study provides new evidence that the primary sensory neurons of DRG may have an important role as immunosensors to detect and control microbial infection and inflammation.

6 References

1. Esther P. Gardner, J. H. M., Thomas M. Jessell. 2000. The Bodily Senses. *Principles of neural science 4th Edition Edited by Kandel, Eric R. Schwartz, James H. Jessell, Thomas M. (New York, McGraw-Hill):430*.

2. Weihe, E., M. Bette, T. Fink, H. E. Romeo, and M. K.-H. Schaefer. 1999. Molecular Anatomical Basis of Interactions between Nervous and immune Systems in Health and Disease. *Psychoneuroimmunology : an interdisciplinary introduction edited by Manfred Schedlowski and Uwe Tewes. (New York, Kluwer Academic/Plenum Publishers):167*.

3. Julius, D., and A. I. Basbaum. 2001. Molecular mechanisms of nociception. *Nature 413:203*.

4. Scholz, J., and C. J. Woolf. 2002. Can we conquer pain? *Nat Neurosci 5 Suppl:1062*.

5. Hokfelt, T., J. O. Kellerth, G. Nilsson, and B. Pernow. 1975. Substance p: localization in the central nervous system and in some primary sensory neurons. *Science 190:889*.

6. Lee, Y., Y. Kawai, S. Shiosaka, K. Takami, H. Kiyama, C. J. Hillyard, S. Girgis, I. MacIntyre, P. C. Emson, and M. Tohyama. 1985. Coexistence of calcitonin gene-related peptide and substance P-like peptide in single cells of the trigeminal ganglion of the rat: immunohistochemical analysis. *Brain Res 330:194*.

7. Caterina, M. J., and D. Julius. 2001. The vanilloid receptor: a molecular gateway to the pain pathway. *Annu Rev Neurosci 24:487*.

8. Caterina, M. J., M. A. Schumacher, M. Tominaga, T. A. Rosen, J. D. Levine, and D. Julius. 1997. The capsaicin receptor: a heat-activated ion channel in the pain pathway. *Nature 389:816*.

9. Davis, J. B., J. Gray, M. J. Gunthorpe, J. P. Hatcher, P. T. Davey, P. Overend, M. H. Harries, J. Latcham, C. Clapham, K. Atkinson, S. A. Hughes, K. Rance, E. Grau, A. J. Harper, P. L. Pugh, D. C. Rogers, S. Bingham, A. Randall, and S. A. Sheardown. 2000. Vanilloid receptor-1 is essential for inflammatory thermal hyperalgesia. *Nature 405:183*.

10. Srinivasa N. Raja, R. A. Meyer, M. Ringkamp, and J. N. Campbell. 1999. Peripheral neural mechanisms of nociception. *Textbook of pain. 4th, edited by Wall, Patrick D. Melzack, Ronald (Churchill Livingstone, Edinburgh):11*.

11. Levine, J. D., and D. B. Reichling. 1999. Peripheral mechanisms of inflammatory pain. *Textbook of pain. 4th, edited by Wall, Patrick D. Melzack, Ronald (Churchill Livingstone, Edinburgh):59*.

12. Cunha, F. Q., S. Poole, B. B. Lorenzetti, and S. H. Ferreira. 1992. The pivotal role of tumour necrosis factor alpha in the development of inflammatory hyperalgesia. *Br J Pharmacol 107:660*.

13. Ferreira, S. H., B. B. Lorenzetti, A. F. Bristow, and S. Poole. 1988. Interleukin-1 beta as a potent hyperalgesic agent antagonized by a tripeptide analogue. *Nature 334:698*.

14. Watkins, L. R., E. P. Wiertelak, L. E. Goehler, K. P. Smith, D. Martin, and S. F. Maier. 1994. Characterization of cytokine-induced hyperalgesia. *Brain Res 654:15*.

15. Watkins, L. R., L. E. Goehler, J. Relton, M. T. Brewer, and S. F. Maier. 1995. Mechanisms of tumor necrosis factor-alpha (TNF-alpha) hyperalgesia. *Brain Res 692:244*.

16. Ashkenazi, A., and V. M. Dixit. 1999. Apoptosis control by death and decoy receptors. *Curr Opin Cell Biol 11:255*.

17. Abbas, A. K., A. H. Lichtman, and J. S. Pober. 2000. *Cellular and molecular immunology*. W.B. Saunders, Philadelphia ; London.

18. Bette, M., M. K. Schafer, N. van Rooijen, E. Weihe, and B. Fleischer. 1993. Distribution and kinetics of superantigen-induced cytokine gene expression in mouse spleen. *J Exp Med 178:1531*.

19. Bianchi, M., P. Sacerdote, P. Ricciardi-Castagnoli, P. Mantegazza, and A. E. Panerai. 1992. Central effects of tumor necrosis factor alpha and interleukin-1 alpha on nociceptive thresholds and spontaneous locomotor activity. *Neurosci Lett 148:76*.

20. Hopkins, S. J., and N. J. Rothwell. 1995. Cytokines and the nervous system. I: Expression and recognition. *Trends Neurosci 18:83*.

21. Szelenyi, J. 2001. Cytokines and the central nervous system. *Brain Res Bull 54:329*.

22. Sei, Y., L. Vitkovic, and M. M. Yokoyama. 1995. Cytokines in the central nervous system: regulatory roles in neuronal function, cell death and repair. *Neuroimmunomodulation 2:121*.

23. Rothwell, N. J., G. Luheshi, and S. Toulmond. 1996. Cytokines and their receptors in the central nervous system: physiology, pharmacology, and pathology. *Pharmacol Ther 69:85*.

24. La Fleur, M., J. L. Underwood, D. A. Rappolee, and Z. Werb. 1996. Basement membrane and repair of injury to peripheral nerve: defining a potential role for macrophages, matrix metalloproteinases, and tissue inhibitor of metalloproteinases-1. *J Exp Med 184:2311*.

25. Wagner, R., and R. R. Myers. 1996. Schwann cells produce tumor necrosis factor alpha: expression in injured and non-injured nerves. *Neuroscience 73:625*.

26. Shubayev, V. I., and R. R. Myers. 2002. Anterograde TNF alpha transport from rat dorsal root ganglion to spinal cord and injured sciatic nerve. *Neurosci Lett 320:99*.

27. Shubayev, V. I., and R. R. Myers. 2001. Axonal transport of TNF-alpha in painful neuropathy: distribution of ligand tracer and TNF receptors. *J Neuroimmunol 114:48*.

28. Schafers, M., C. Geis, C. I. Svensson, Z. D. Luo, and C. Sommer. 2003. Selective increase of tumour necrosis factor-alpha in injured and spared myelinated primary afferents after chronic constrictive injury of rat sciatic nerve. *Eur J Neurosci 17:791*.

29. Schafers, M., C. Geis, D. Brors, T. L. Yaksh, and C. Sommer. 2002. Anterograde transport of tumor necrosis factor-alpha in the intact and injured rat sciatic nerve. *J Neurosci 22:536*.

30. Arnett, H. A., J. Mason, M. Marino, K. Suzuki, G. K. Matsushima, and J. P. Ting. 2001. TNF alpha promotes proliferation of oligodendrocyte progenitors and remyelination. *Nat Neurosci 4:1116*.

31. Fontaine, V., S. Mohand-Said, N. Hanoteau, C. Fuchs, K. Pfizenmaier, and U. Eisel. 2002. Neurodegenerative and neuroprotective effects of tumor Necrosis factor (TNF) in retinal ischemia: opposite roles of TNF receptor 1 and TNF receptor 2. *J Neurosci 22:RC216*.

32. Smith, C. A., T. Davis, D. Anderson, L. Solam, M. P. Beckmann, R. Jerzy, S. K. Dower, D. Cosman, and R. G. Goodwin. 1990. A receptor for tumor necrosis factor defines an unusual family of cellular and viral proteins. *Science 248:1019*.

33. Lewis, M., L. A. Tartaglia, A. Lee, G. L. Bennett, G. C. Rice, G. H. Wong, E. Y. Chen, and D. V. Goeddel. 1991. Cloning and expression of cDNAs for two distinct murine tumor necrosis factor receptors demonstrate one receptor is species specific. *Proc Natl Acad Sci U S A 88:2830*.

34. Goodwin, R. G., D. Anderson, R. Jerzy, T. Davis, C. I. Brannan, N. G. Copeland, N. A. Jenkins, and C. A. Smith. 1991. Molecular cloning and expression of the type 1 and type 2 murine receptors for tumor necrosis factor. *Mol Cell Biol 11:3020*.

35. Beltinger, C. P., P. S. White, J. M. Maris, E. P. Sulman, S. J. Jensen, D. LePaslier, B. J. Stallard, D. V. Goeddel, F. J. de Sauvage, and G. M. Brodeur. 1996. Physical mapping and genomic structure of the human TNFR2 gene. *Genomics 35:94*.

36. Hurle, B., F. Segade, R. Rodriguez, S. Ramos, and P. S. Lazo. 1998. The mouse tumor necrosis factor receptor 2 gene: genomic structure and characterization of the two transcripts. *Genomics 52:79*.

37. Dopp, J. M., A. Mackenzie-Graham, G. C. Otero, and J. E. Merrill. 1997. Differential expression, cytokine modulation, and specific functions of type-1 and type-2 tumor necrosis factor receptors in rat glia. *J Neuroimmunol 75:104*.

38. Pollock, J., S. M. McFarlane, M. C. Connell, U. Zehavi, P. Vandenabeele, D. J. MacEwan, and R. H. Scott. 2002. TNF-alpha receptors simultaneously activate Ca2+ mobilisation and stress kinases in cultured sensory neurones. *Neuropharmacology 42:93*.

39. Schafers, M., L. S. Sorkin, C. Geis, and V. I. Shubayev. 2003. Spinal nerve ligation induces transient upregulation of tumor necrosis factor receptors 1 and 2 in injured and adjacent uninjured dorsal root ganglia in the rat. *Neurosci Lett 347:179*.

40. Cunningham, E. T., Jr., A. K. Stalder, P. P. Sanna, S. S. Liu, F. E. Bloom, E. L. Howes, Jr., I. L. Campbell, and T. P. Margolis. 1997. Distribution of tumor necrosis factor receptor messenger RNA in normal and herpes simplex virus infected trigeminal ganglia in the mouse. *Brain Res 758:99*.

41. Empl, M., S. Renaud, B. Erne, P. Fuhr, A. Straube, N. Schaeren-Wiemers, and A. J. Steck. 2001. TNF-alpha expression in painful and nonpainful neuropathies. *Neurology 56:1371*.

42. Aloe, L., R. Moroni, F. Angelucci, and M. Fiore. 1997. Role of TNF-alpha but not NGF in murine hyperalgesia induced by parasitic infection. *Psychopharmacology (Berl) 134:287*.

43. Wagner, R., and R. R. Myers. 1996. Endoneurial injection of TNF-alpha produces neuropathic pain behaviors. *Neuroreport 7:2897*.

44. Sorkin, L. S., W. H. Xiao, R. Wagner, and R. R. Myers. 1997. Tumour necrosis factor-alpha induces ectopic activity in nociceptive primary afferent fibres. *Neuroscience 81:255*.

45. Sorkin, L. S., and C. M. Doom. 2000. Epineurial application of TNF elicits an acute mechanical hyperalgesia in the awake rat. *J Peripher Nerv Syst 5:96*.

46. Sommer, C., C. Schmidt, and A. George. 1998. Hyperalgesia in experimental neuropathy is dependent on the TNF receptor 1. *Exp Neurol 151:138*.

47. Sommer, C., T. Lindenlaub, P. Teuteberg, M. Schafers, T. Hartung, and K. V. Toyka. 2001. Anti-TNF-neutralizing antibodies reduce pain-related behavior in two different mouse models of painful mononeuropathy. *Brain Res 913:86*.

48. Schafers, M., J. Brinkhoff, S. Neukirchen, M. Marziniak, and C. Sommer. 2001. Combined epineurial therapy with neutralizing antibodies to tumor necrosis factor-alpha and interleukin-1 receptor has an additive effect in reducing neuropathic pain in mice. *Neurosci Lett 310:113*.

49. Sacerdote, P., M. Bianchi, P. Ricciardi-Castagnoli, and A. E. Panerai. 1992. Tumor necrosis factor alpha and interleukin-1 alpha increase pain thresholds in the rat. *Ann N Y Acad Sci 650:197*.

50. Reeve, A. J., S. Patel, A. Fox, K. Walker, and L. Urban. 2000. Intrathecally administered endotoxin or cytokines produce allodynia, hyperalgesia and

changes in spinal cord neuronal responses to nociceptive stimuli in the rat. *Eur J Pain 4:247*.

51. Hori, T., T. Oka, M. Hosoi, and S. Aou. 1998. Pain modulatory actions of cytokines and prostaglandin E2 in the brain. *Ann N Y Acad Sci 840:269*.

52. Hori, T., T. Oka, M. Hosoi, M. Abe, and K. Oka. 2000. Hypothalamic mechanisms of pain modulatory actions of cytokines and prostaglandin E2. *Ann N Y Acad Sci 917:106*.

53. George, A., M. Marziniak, M. Schafers, K. V. Toyka, and C. Sommer. 2000. Thalidomide treatment in chronic constrictive neuropathy decreases endoneurial tumor necrosis factor-alpha, increases interleukin-10 and has long-term effects on spinal cord dorsal horn met-enkephalin. *Pain 88:267*.

54. Oka, T., Y. Wakugawa, M. Hosoi, K. Oka, and T. Hori. 1996. Intracerebroventricular injection of tumor necrosis factor-alpha induces thermal hyperalgesia in rats. *Neuroimmunomodulation 3:135*.

55. Opree, A., and M. Kress. 2000. Involvement of the proinflammatory cytokines tumor necrosis factor- alpha, IL-1 beta, and IL-6 but not IL-8 in the development of heat hyperalgesia: effects on heat-evoked calcitonin gene-related peptide release from rat skin. *J Neurosci 20:6289*.

56. Parada, C. A., J. J. Yeh, E. K. Joseph, and J. D. Levine. 2003. Tumor necrosis factor receptor type-1 in sensory neurons contributes to induction of chronic enhancement of inflammatory hyperalgesia in rat. *Eur J Neurosci 17:1847*.

57. Dinarello, C. A. 1991. Interleukin-1 and interleukin-1 antagonism. *Blood 77:1627*.

58. Dinarello, C. A. 1996. Biologic basis for interleukin-1 in disease. *Blood 87:2095*.

59. Bianchi, M., B. Dib, and A. E. Panerai. 1998. Interleukin-1 and nociception in the rat. *J Neurosci Res 53:645*.

60. Horie, H., I. Sakai, Y. Akahori, and T. Kadoya. 1997. IL-1 beta enhances neurite regeneration from transected-nerve terminals of adult rat DRG. *Neuroreport 8:1955*.

61. Morioka, N., K. Takeda, K. Kumagai, T. Hanada, K. Ikoma, I. Hide, A. Inoue, and Y. Nakata. 2002. Interleukin-1beta-induced substance P release from rat cultured primary afferent neurons driven by two phospholipase A2 enzymes: secretory type IIA and cytosolic type IV. *J Neurochem 80:989*.

62. Inoue, A., K. Ikoma, N. Morioka, K. Kumagai, T. Hashimoto, I. Hide, and Y. Nakata. 1999. Interleukin-1beta induces substance P release from primary afferent neurons through the cyclooxygenase-2 system. *J Neurochem 73:2206*.

63. Cunningham, E. T., Jr., and E. B. De Souza. 1993. Interleukin 1 receptors in the brain and endocrine tissues. *Immunol Today 14:171*.

64. Ilyin, S. E., D. Gayle, M. C. Flynn, and C. R. Plata-Salaman. 1998. Interleukin-1beta system (ligand, receptor type I, receptor accessory protein and receptor antagonist), TNF-alpha, TGF-beta1 and neuropeptide Y mRNAs in specific brain regions during bacterial LPS-induced anorexia. *Brain Res Bull 45:507*.

65. Loddick, S. A., C. Liu, T. Takao, K. Hashimoto, and E. B. De Souza. 1998. Interleukin-1 receptors: cloning studies and role in central nervous system disorders. *Brain Res Brain Res Rev 26:306*.

66. Alheim, K., and T. Bartfai. 1998. The interleukin-1 system: receptors, ligands, and ICE in the brain and their involvement in the fever response. *Ann N Y Acad Sci 840:51*.

67. Sims, J. E., M. A. Gayle, J. L. Slack, M. R. Alderson, T. A. Bird, J. G. Giri, F. Colotta, F. Re, A. Mantovani, K. Shanebeck, and et al. 1993. Interleukin 1 signaling occurs exclusively via the type I receptor. *Proc Natl Acad Sci U S A 90:6155*.

68. Liege, S., S. Laye, K. S. Li, E. Moze, and P. J. Neveu. 2000. Interleukin 1 receptor accessory protein (IL-1RAcP) is necessary for centrally mediated neuroendocrine and immune responses to IL-1beta. *J Neuroimmunol 110:134*.

69. Touzani, O., H. Boutin, R. LeFeuvre, L. Parker, A. Miller, G. Luheshi, and N. Rothwell. 2002. Interleukin-1 influences ischemic brain damage in the mouse independently of the interleukin-1 type I receptor. *J Neurosci 22:38*.

70. Laye, S., S. Liege, K. S. Li, E. Moze, and P. J. Neveu. 2001. Physiological significance of the interleukin 1 receptor accessory protein. *Neuroimmunomodulation 9:225*.

71. Zetterstrom, M., A. K. Sundgren-Andersson, P. Ostlund, and T. Bartfai. 1998. Delineation of the proinflammatory cytokine cascade in fever induction. *Ann N Y Acad Sci 856:48*.

72. Cremona, S., E. Goujon, K. W. Kelley, R. Dantzer, and P. Parnet. 1998. Brain type I but not type II IL-1 receptors mediate the effects of IL-1 beta on behavior in mice. *Am J Physiol 274:R735*.

73. Cremona, S., S. Laye, R. Dantzer, and P. Parnet. 1998. Blockade of brain type II interleukin-1 receptors potentiates IL1beta-induced anorexia in mice. *Neurosci Lett 246:101*.

74. Ericsson, A., C. Liu, R. P. Hart, and P. E. Sawchenko. 1995. Type 1 interleukin-1 receptor in the rat brain: distribution, regulation, and relationship to sites of IL-1-induced cellular activation. *J Comp Neurol 361:681*.

75. French, R. A., R. W. VanHoy, R. Chizzonite, J. F. Zachary, R. Dantzer, P. Parnet, R. M. Bluthe, and K. W. Kelley. 1999. Expression and localization of p80 and p68 interleukin-1 receptor proteins in the brain of adult mice. *J Neuroimmunol 93:194*.

76. Gayle, D., S. E. Ilyin, and C. R. Plata-Salaman. 1997. Interleukin-1 receptor type I mRNA levels in brain regions from male and female rats. *Brain Res Bull 42:463*.

77. Parker, L. C., D. A. Rushforth, N. J. Rothwell, and G. N. Luheshi. 2000. IL-1beta induced changes in hypothalamic IL-1R1 and IL-1R2 mRNA expression in the rat. *Brain Res Mol Brain Res 79:156.*

78. Van Dam, A. M., H. E. De Vries, J. Kuiper, F. J. Zijlstra, A. G. De Boer, F. J. Tilders, and F. Berkenbosch. 1996. Interleukin-1 receptors on rat brain endothelial cells: a role in neuroimmune interaction? *Faseb J 10:351*.

79. Wong, M. L., P. B. Bongiorno, A. al-Shekhlee, A. Esposito, P. Khatri, and J. Licinio. 1996. IL-1 beta, IL-1 receptor type I and iNOS gene expression in rat brain vasculature and perivascular areas. *Neuroreport 7:2445*.

80. Wong, M. L., and J. Licinio. 1994. Localization of interleukin 1 type I receptor mRNA in rat brain. *Neuroimmunomodulation 1:110*.

81. Yabuuchi, K., M. Minami, S. Katsumata, and M. Satoh. 1994. Localization of type I interleukin-1 receptor mRNA in the rat brain. *Brain Res Mol Brain Res 27:27*.

82. Copray, J. C., I. Mantingh, N. Brouwer, K. Biber, B. M. Kust, R. S. Liem, I. Huitinga, F. J. Tilders, A. M. Van Dam, and H. W. Boddeke. 2001. Expression of interleukin-1 beta in rat dorsal root ganglia. *J Neuroimmunol 118:203*.

83. Oka, T., S. Aou, and T. Hori. 1993. Intracerebroventricular injection of interleukin-1 beta induces hyperalgesia in rats. *Brain Res 624:61*.

84. Oka, T., S. Aou, and T. Hori. 1994. Intracerebroventricular injection of interleukin-1 beta enhances nociceptive neuronal responses of the trigeminal nucleus caudalis in rats. *Brain Res 656:236*.

85. Oka, T., K. Oka, M. Hosoi, and T. Hori. 1996. Inhibition of peripheral interleukin-1 beta-induced hyperalgesia by the intracerebroventricular administration of diclofenac and alpha- melanocyte-stimulating hormone. *Brain Res 736:237*.

86. Yabuuchi, K., A. Nishiyori, M. Minami, and M. Satoh. 1996. Biphasic effects of intracerebroventricular interleukin-1 beta on mechanical nociception in the rat. *Eur J Pharmacol 300:59*.

87. Oka, T., K. Oka, M. Hosoi, S. Aou, and T. Hori. 1995. The opposing effects of interleukin -1 beta microinjected into the preoptic hypothalamus and the ventromedial hypothalamus on nociceptive behavior in rats. *Brain Res 700:271*.

88. Sellami, S., and R. de Beaurepaire. 1995. Hypothalamic and thalamic sites of action of interleukin-1 beta on food intake, body temperature and pain sensitivity in the rat. *Brain Res 694:69*.

89. Falchi, M., F. Ferrara, C. Gharib, and B. Dib. 2001. Hyperalgesic effect of intrathecally administered interleukin-1 in rats. *Drugs Exp Clin Res 27:97*.

90. Sweitzer, S., D. Martin, and J. A. DeLeo. 2001. Intrathecal interleukin-1 receptor antagonist in combination with soluble tumor necrosis factor receptor exhibits an anti-allodynic action in a rat model of neuropathic pain. *Neuroscience 103:529*.

91. Maier, S. F., E. P. Wiertelak, D. Martin, and L. R. Watkins. 1993. Interleukin-1 mediates the behavioral hyperalgesia produced by lithium chloride and endotoxin. *Brain Res 623:321*.

92. Fukuoka, H., M. Kawatani, T. Hisamitsu, and C. Takeshige. 1994. Cutaneous hyperalgesia induced by peripheral injection of interleukin-1 beta in the rat. *Brain Res 657:133*.

93. Safieh-Garabedian, B., S. Poole, A. Allchorne, J. Winter, and C. J. Woolf. 1995. Contribution of interleukin-1 beta to the inflammation-induced increase in nerve growth factor levels and inflammatory hyperalgesia. *Br J Pharmacol 115:1265*.

94. Cunha, J. M., F. Q. Cunha, S. Poole, and S. H. Ferreira. 2000. Cytokine-mediated inflammatory hyperalgesia limited by interleukin-1 receptor antagonist. *Br J Pharmacol 130:1418*.

95. Holst, O., A. J. Ulmer, H. Brade, H. D. Flad, and E. T. Rietschel. 1996. Biochemistry and cell biology of bacterial endotoxins. *FEMS Immunol Med Microbiol 16:83*.

96. Campisi, J., M. K. Hansen, K. A. O'Connor, J. C. Biedenkapp, L. R. Watkins, S. F. Maier, and M. Fleshner. 2003. Circulating cytokines and endotoxin are not necessary for the activation of the sickness or corticosterone response produced by peripheral E. coli challenge. *J Appl Physiol 95:1873*.

97. Filogamo, G., S. Biasol, E. Recluta, and A. Vercelli. 2002. Increase in the number of NADPH-diaphorase-positive neurons in the lumbar dorsal root ganglia following lipopolysaccharide exposure of the sciatic nerve. *Morphologie 86:27*.

98. Xing, L., L. Hou, and X. Wang. 2002. Comparison of calcitonin gene-related peptide release from rat lymphocytes and dorsal root ganglia neurons. *Brain Behav Immun 16:17*.

99. Hou, L., and X. Wang. 2001. PKC and PKA, but not PKG mediate LPS-induced CGRP release and [Ca(2+)](i) elevation in DRG neurons of neonatal rats. *J Neurosci Res 66:592*.

100. Wright, S. D., P. S. Tobias, R. J. Ulevitch, and R. A. Ramos. 1989. Lipopolysaccharide (LPS) binding protein opsonizes LPS-bearing particles for recognition by a novel receptor on macrophages. *J Exp Med 170:1231*.

101. Wright, S. D., R. A. Ramos, P. S. Tobias, R. J. Ulevitch, and J. C. Mathison. 1990. CD14, a receptor for complexes of lipopolysaccharide (LPS) and LPS binding protein. *Science 249:1431*.

102. Schutt, C. 1999. Cd14. *Int J Biochem Cell Biol 31:545*.

103. Akira, S., K. Takeda, and T. Kaisho. 2001. Toll-like receptors: critical proteins linking innate and acquired immunity. *Nat Immunol 2:675*.

104. Hoshino, K., O. Takeuchi, T. Kawai, H. Sanjo, T. Ogawa, Y. Takeda, K. Takeda, and S. Akira. 1999. Cutting edge: Toll-like receptor 4 (TLR4)-deficient mice are hyporesponsive to lipopolysaccharide: evidence for TLR4 as the Lps gene product. *J Immunol 162:3749.*

105. Poltorak, A., X. He, I. Smirnova, M. Y. Liu, C. V. Huffel, X. Du, D. Birdwell, E. Alejos, M. Silva, C. Galanos, M. Freudenberg, P. Ricciardi-Castagnoli, B. Layton, and B. Beutler. 1998. Defective LPS signaling in C3H/HeJ and C57BL/10ScCr mice: mutations in Tlr4 gene. *Science 282:2085*.

106. Qureshi, S. T., L. Lariviere, G. Leveque, S. Clermont, K. J. Moore, P. Gros, and D. Malo. 1999. Endotoxin-tolerant mice have mutations in Toll-like receptor 4 (Tlr4). *J Exp Med 189:615*.

107. Borovikova, L. V., S. Ivanova, M. Zhang, H. Yang, G. I. Botchkina, L. R. Watkins, H. Wang, N. Abumrad, J. W. Eaton, and K. J. Tracey. 2000. Vagus nerve stimulation attenuates the systemic inflammatory response to endotoxin. *Nature 405:458*.

108. Cahill, C. M., A. Dray, and T. J. Coderre. 1998. Priming enhances endotoxin-induced thermal hyperalgesia and mechanical allodynia in rats. *Brain Res 808:13*.

109. Mason, P. 1993. Lipopolysaccharide induces fever and decreases tail flick latency in awake rats. *Neurosci Lett 154:134*.

110. Wiertelak, E. P., K. P. Smith, L. Furness, K. Mooney-Heiberger, T. Mayr, S. F. Maier, and L. R. Watkins. 1994. Acute and conditioned hyperalgesic responses to illness. *Pain 56:227*.

111. Meller, S. T., C. Dykstra, D. Grzybycki, S. Murphy, and G. F. Gebhart. 1994. The possible role of glia in nociceptive processing and hyperalgesia in the spinal cord of the rat. *Neuropharmacology 33:1471*.

112. Platika, D., M. H. Boulos, L. Baizer, and M. C. Fishman. 1985. Neuronal traits of clonal cell lines derived by fusion of dorsal root ganglia neurons with neuroblastoma cells. *Proc Natl Acad Sci U S A 82:3499.*

113. Schmidt, W. M., and M. W. Mueller. 1999. CapSelect: a highly sensitive method for 5' CAP-dependent enrichment of full-length cDNA in PCR-mediated analysis of mRNAs. *Nucleic Acids Res 27:e31*.

114. Sambrook, J., and D. W. Russell. 2001. *Molecular cloning : a laboratory manual*. Cold Spring Harbor Laboratory Press, Cold Spring Harbor, N.Y.

115. Schafer, M. K.-H., J. P. Herman, and S. J. Watson. 1993. In situ Hybridization Histochemistry. *Imaging drug action in the brain:337*.

116. Schafer, M. K.-H., and R. Day. 1995. In Situ Hybridization Techniques to Map Processing Enzymes. *Methods in Neurosciences 23:16*.

117. Chomczynski, P. 1992. One-hour downward alkaline capillary transfer for blotting of DNA and RNA. *Anal Biochem 201:134*.

118. Tannenbaum, C. S., J. A. Major, and T. A. Hamilton. 1993. IFN-gamma and lipopolysaccharide differentially modulate expression of tumor necrosis factor receptor mRNA in murine peritoneal macrophages. *J Immunol 151:6833*.

119. Schepp, W., K. Dehne, H. Herrmuth, K. Pfeffer, and C. Prinz. 1998. Identification and functional importance of IL-1 receptors on rat parietal cells. *Am J Physiol 275:G1094*.

120. Frantz, S., L. Kobzik, Y. D. Kim, R. Fukazawa, R. Medzhitov, R. T. Lee, and R. A. Kelly. 1999. Toll4 (TLR4) expression in cardiac myocytes in normal and failing myocardium. *J Clin Invest 104:271*.

121. Liu, S., L. S. Khemlani, R. A. Shapiro, M. L. Johnson, K. Liu, D. A. Geller, S. C. Watkins, S. M. Goyert, and T. R. Billiar. 1998. Expression of CD14 by hepatocytes: upregulation by cytokines during endotoxemia. *Infect Immun 66:5089*.

122. Seitz, C., P. Muller, R. C. Krieg, D. N. Mannel, and T. Hehlgans. 2001. A novel p75TNF receptor isoform mediating NFkappa B activation. *J Biol Chem 276:19390*.

123. Wahle, E., and U. Ruegsegger. 1999. 3'-End processing of pre-mRNA in eukaryotes. *FEMS Microbiol Rev 23:277*.

124. Edwalds-Gilbert, G., K. L. Veraldi, and C. Milcarek. 1997. Alternative poly(A) site selection in complex transcription units: means to an end? *Nucleic Acids Res 25:2547*.

125. Bette, M., O. Kaut, M. K. Schafer, and E. Weihe. 2003. Constitutive expression of p55TNFR mRNA and mitogen-specific up-regulation of TNF alpha and p75TNFR mRNA in mouse brain. *J Comp Neurol 465:417*.

126. Sommer, C., C. Schmidt, and A. George. 1998. Hyperalgesia in experimental neuropathy is dependent on the TNF receptor 1. *Exp Neurol 151:138*.

127. Nadeau, S., and S. Rivest. 1999. Effects of circulating tumor necrosis factor on the neuronal activity and expression of the genes encoding the tumor necrosis factor receptors (p55 and p75) in the rat brain: a view from the blood-brain barrier. *Neuroscience 93:1449*.

128. Watkins, L. R., L. E. Goehler, J. Relton, M. T. Brewer, and S. F. Maier. 1995. Mechanisms of tumor necrosis factor-alpha (TNF-alpha) hyperalgesia. *Brain Res 692:244*.

129. Junger, H., and L. S. Sorkin. 2000. Nociceptive and inflammatory effects of subcutaneous TNFalpha. *Pain 85:145*.

130. Hua, X. Y., P. Chen, A. Fox, and R. R. Myers. 1996. Involvement of cytokines in lipopolysaccharide-induced facilitation of CGRP release from capsaicin-sensitive nerves in the trachea: studies with interleukin-1beta and tumor necrosis factor-alpha. *J Neurosci 16:4742*.

131. Ding, M., R. P. Hart, and G. M. Jonakait. 1995. Tumor necrosis factor-alpha induces substance P in sympathetic ganglia through sequential induction of interleukin-1 and leukemia inhibitory factor. *J Neurobiol 28:445*.

132. Sommer, C., T. Lindenlaub, P. Teuteberg, M. Schafers, T. Hartung, and K. V. Toyka. 2001. Anti-TNF-neutralizing antibodies reduce pain-related behavior in two different mouse models of painful mononeuropathy. *Brain Res 913:86*.

133. Weihe, E., D. Nohr, S. Michel, S. Muller, H. J. Zentel, T. Fink, and J. Krekel. 1991. Molecular anatomy of the neuro-immune connection. *Int J Neurosci 59:1*.

134. Barker, V., G. Middleton, F. Davey, and A. M. Davies. 2001. TNFalpha contributes to the death of NGF-dependent neurons during development. *Nat Neurosci 4:1194*.

135. Beattie, E. C., D. Stellwagen, W. Morishita, J. C. Bresnahan, B. K. Ha, M. Von Zastrow, M. S. Beattie, and R. C. Malenka. 2002. Control of synaptic strength by glial TNFalpha. *Science 295:2282*.

136. Suzuki, T., I. Hide, K. Ido, S. Kohsaka, K. Inoue, and Y. Nakata. 2004. Production and release of neuroprotective tumor necrosis factor by P2X7 receptor-activated microglia. *J Neurosci 24:1*.

137. Watkins, L. R., D. Martin, P. Ulrich, K. J. Tracey, and S. F. Maier. 1997. Evidence for the involvement of spinal cord glia in subcutaneous formalin induced hyperalgesia in the rat. *Pain 71:225*.

138. Watkins, L. R., E. D. Milligan, and S. F. Maier. 2001. Spinal cord glia: new players in pain. *Pain 93:201*.

139. Wesselingh, S. L., K. Takahashi, J. D. Glass, J. C. McArthur, J. W. Griffin, and D. E. Griffin. 1997. Cellular localization of tumor necrosis factor mRNA in neurological tissue from HIV-infected patients by combined reverse transcriptase/polymerase chain reaction in situ hybridization and immunohistochemistry. *J Neuroimmunol 74:1*.

140. Sommer, C., and M. Schafers. 1998. Painful mononeuropathy in C57BL/Wld mice with delayed wallerian degeneration: differential effects of cytokine production and nerve regeneration on thermal and mechanical hypersensitivity. *Brain Res 784:154*.

141. Murwani, R., S. Hodgkinson, and P. Armati. 1996. Tumor necrosis factor alpha and interleukin-6 mRNA expression in neonatal Lewis rat Schwann cells and a neonatal rat Schwann cell line following interferon gamma stimulation. *J Neuroimmunol 71:65*.

142. Gordon, J. R., and S. J. Galli. 1991. Release of both preformed and newly synthesized tumor necrosis factor alpha (TNF-alpha)/cachectin by mouse mast cells stimulated via the Fc epsilon RI. A mechanism for the sustained action of mast cell-derived TNF-alpha during IgE-dependent biological responses. *J Exp Med 174:103*.

143. Murphy, P. G., J. Grondin, M. Altares, and P. M. Richardson. 1995. Induction of interleukin-6 in axotomized sensory neurons. *J Neurosci 15:5130*.

144. Konsman, J. P., P. Parnet, and R. Dantzer. 2002. Cytokine-induced sickness behaviour: mechanisms and implications. *Trends Neurosci 25:154*.

145. Sommer, C., S. Petrausch, T. Lindenlaub, and K. V. Toyka. 1999. Neutralizing antibodies to interleukin 1-receptor reduce pain associated behavior in mice with experimental neuropathy. *Neurosci Lett 270:25*.

146. Safieh-Garabedian, B., S. A. Kanaan, J. J. Haddad, P. A. Jaoude, S. J. Jabbur, and N. E. Saade. 1997. Involvement of interleukin-1 beta, nerve growth factor and prostaglandin E2 in endotoxin-induced localized inflammatory hyperalgesia. *Br J Pharmacol 121:1619*.

147. Perretti, M., A. Ahluwalia, R. J. Flower, and S. Manzini. 1993. Endogenous tachykinins play a role in IL-1-induced neutrophil accumulation: involvement of NK-1 receptors. *Immunology 80:73*.

148. Mousli, M., T. E. Hugli, Y. Landry, and C. Bronner. 1994. Peptidergic pathway in human skin and rat peritoneal mast cell activation. *Immunopharmacology 27:1*.

149. Lotz, M., J. H. Vaughan, and D. A. Carson. 1988. Effect of neuropeptides on production of inflammatory cytokines by human monocytes. *Science 241:1218*.

150. Walsh, D. T., V. B. Weg, T. J. Williams, and S. Nourshargh. 1995. Substance P-induced inflammatory responses in guinea-pig skin: the effect of specific NK1 receptor antagonists and the role of endogenous mediators. *Br J Pharmacol 114:1343*.

151. Herbert, M. K., and P. Holzer. 1994. Interleukin-1 beta enhances capsaicin-induced neurogenic vasodilatation in the rat skin. *Br J Pharmacol 111:681*.

152. Sweitzer, S. M., R. W. Colburn, M. Rutkowski, and J. A. DeLeo. 1999. Acute peripheral inflammation induces moderate glial activation and spinal IL-1beta expression that correlates with pain behavior in the rat. *Brain Res 829:209*.

153. Souter, A. J., M. G. Garry, and D. L. Tanelian. 2000. Spinal interleukin-1beta reduces inflammatory pain. *Pain 86:63*.

154. Lewin, G. R., and L. M. Mendell. 1994. Regulation of cutaneous C-fiber heat nociceptors by nerve growth factor in the developing rat. *J Neurophysiol 71:941*.

155. Lewin, G. R., A. Rueff, and L. M. Mendell. 1994. Peripheral and central mechanisms of NGF-induced hyperalgesia. *Eur J Neurosci 6:1903*.

156. Laflamme, N., and S. Rivest. 2001. Toll-like receptor 4: the missing link of the cerebral innate immune response triggered by circulating gram-negative bacterial cell wall components. *Faseb J 15:155*.

157. Haziot, A., E. Ferrero, F. Kontgen, N. Hijiya, S. Yamamoto, J. Silver, C. L. Stewart, and S. M. Goyert. 1996. Resistance to endotoxin shock and reduced dissemination of gram- negative bacteria in CD14-deficient mice. *Immunity 4:407*.

158. Backhed, F., L. Meijer, S. Normark, and A. Richter-Dahlfors. 2002. TLR4-dependent recognition of lipopolysaccharide by epithelial cells requires sCD14. *Cell Microbiol 4:493*.

159. Griffin, E. C., N. Aiyar, M. J. Slivjak, and E. F. Smith, 3rd. 1992. Effect of endotoxicosis on plasma and tissue levels of calcitonin gene-related peptide. *Circ Shock 38:50*.

160. Arden, W. A., R. R. Fiscus, X. Wang, L. Yang, R. Maley, M. Nielsen, S. Lanzo, and D. R. Gross. 1994. Elevations in circulating calcitonin gene-related peptide correlate with hemodynamic deterioration during endotoxic shock in pigs. *Circ Shock 42:147*.

161. Wang, X., C. Han, S. B. Jones, L. Yang, and R. R. Fiscus. 1995. Calcitonin gene-related peptide release in endotoxicosis may be mediated by prostaglandins. *Shock 3:34*.

162. Saban, M. R., R. Saban, T. G. Hammond, M. Haak-Frendscho, H. Steinberg, M. W. Tengowski, and D. E. Bjorling. 2002. LPS-sensory peptide communication in experimental cystitis. *Am J Physiol Renal Physiol 282:F202*.

7 Abbreviations

All units of measurement are abbreviated according to the International System of units (SI).

A	Adenosine
ATP	Adenosine triphosphate
BCIP	5-bromo-4-chloro-3-indolyl-phosphate
bp	Base pairs
BSA	Bovine serum albumin
C	Cytosine
cDNA	Complementary DNA
CNS	central nervous system
DEPC	Diethyl pyrocarbonate
DMEM	Dulbecco's Minimal Essential Medium
DNA	Deoxyribonucleic acid
DNase	Deoxyribonuclease
dNTPs	2-deoxynucleoside-5-triphosphates
DTT	Dithiothreitol
et al.	and others
EDTA	Ethylene diaminetetraacetic acid
EST	Expressed Sequence Tags
EtBr	Ethidium bromide
FBS	Fetal bovine serum
G	Guanosine
GPI	glycol-sylphosphatidylinositol
HEPES	(2-Hydroxyethyl)-1-piperazineethanesulphonic acid
HRP	Horse radish peroxidase
IL-1	Interleukin 1
IL-1α	Alpha interleukin 1
IL-1β	Beta interleukin 1
IL-1R1	IL-1 receptor type 1;
IL-1R2	IL-1 receptor type 2
IL-1ra	IL-1 receptor antagonist;
IPTG	Isopropyl-β-D-thiogalactoside
JNK	c-Jun N-terminal kinase
kb	Kilobase pairs
kD	Kilodaltons
LBP	LPS-binding protein
LPS	lipopolysaccharide
LRR	leucine-rich repeats
mCD14	membrane CD14
MyD88	myeloid differentiation primary response gene
NBT	Nitroblue tetrazolium salt
NFκB	Nuclear factor kappa B
p38	p38 MAPK
PAGE	Polyacrylamide gel electrophoresis
PBS	Phosphate buffered saline
PCR	Polymerase chain reaction

PMSF	Phenylmethylsulfonyl fluoride
RNA	Ribonucleic acid
RNase	Ribonuclease
rpm	Revolutions per minute
RT-PCR	Reverse transcription PCR
sCD14	soluble CD14
SDS	Sodium-dodecyl-sulphate
SSC	Standard sodium citrate buffer
T	Thymine
TAE	Tris-acetate-EDTA buffer
TBE	Tris-borate-EDTA buffer
TE	Tris-EDTA
TEA	Triethanolamine
TESAP	3-(Triethoxysilyl) propylamine
TLR	toll-like receptor
TNF	tumor necrosis factor
TNFR	TNF receptor
Tris	Tris(hydroxymethyl)-amino-methane
U	Unit
UV	Ultraviolet
X-gal	5-Bromo-4-chloro-3-indolyl-β-D-galactopyranoside

8 Addendum

8.1 Financial support

This project is supported in part by grants to Prof. Weihe and Dr. Schäfer from the German Research Community DFG SFB297 project B1 and from the BMBF 01GS01118.

8.2 Publications

Articles

1. Mika J, **Li Y**, Weihe E, Schafer MK (2003) Relationship of pronociceptin/orphanin FQ and the nociceptin receptor ORL1 with substance P and calcitonin gene-related peptide expression in dorsal root ganglion of the rat. Neurosci Lett 348:190-194.
2. **Li Y**, Ji A, Weihe E, Schafer MK (2004) Cell-specific expression and LPS-induced regulation of TNFα and TNF receptors in rat dorsal root ganglion. J Neurosci submitted.

Abstracts

1. **Li Y**; Ji A; Bender F; Bette M; Weihe E; Schafer MK (2001) Neuronal and non-neuronal expression of TNF receptors in rat dorsal root ganglion: effects of LPS. Soc Neurosci Abstr 27:52.2
2. **Li Y**; Ji A; Bender F; Weihe E; Schafer MK (2001) Use of Laser Capture Microdissection to Identify Cytokine- and Cytokine receptor expressing cells in rat dorsal root ganglion. 1st European Laser-Capture-Microdissection Symposium, Marburg, P10.
3. Schafer MK, **Li Y**; Ji A; Ulke C, Weihe E (2002) Relevance of presynaptic IL-1 and TNF receptors on rat DRG neurons for immuno-nociceptive signaling. 10th World Congress of Pain, San Diego, 1090-P6
4. Dorazil-Dudzik M, Mika J, **Li Y**, Schafer MK, Garlicki J, Wordliczek J, Obara I, Przewlocka B (2002) Effect of local pentoxifyline treatment on inflammatory pain and TNFα mRNA level in inflamed tissue in rats. 10th World Congress of Pain, 805-P75
5. **Li Y**, Ji A, Schafer MK (2002) Toll-like receptor 4 is expressed by peptidergic presumed nociceptive neurons in rat dorsal root ganglion. Program No. 46.19. *2002 Abstract Viewer/Itinerary Planner*. Washington, DC: Society for Neuroscience, Online

Submissions to GenBank

1. **Li Y**, Ji A, Schafer MK (2002) Rattus norvegicus TNFR2 mRNA, transcript variant 1, complete cds. GenBank AF498039
2. **Li Y**, Ji A, Schafer MK (2002) Rattus norvegicus TNFR2 mRNA, transcript variant 2, complete cds. GenBank AY191268
3. **Li Y**, Ji A, Schafer MK (2002) Rattus norvegicus TNFR2 mRNA, transcript variant 3, complete cds. GenBank AY191269

8.3 Akademische Lehrer

Meine akademischen Lehrer in Marburg waren die Damen und Herren:

Aumüller, Beato, Besedovsky, Cetin, Gemsa, Heeg, Krieg, Müller, Oertel, Schäfer,

Seitz, Steiniger, Suske, Voigt, Weihe, Westermann.

8.4 Acknowledgements

I would like to express my deep gratitude to my mentor, Dr. Martin K.-H. Schäfer, both for his intellectual input and practical help, not only concerning academic matters but also the living in Marburg. He has always been ready to give advice founded in his broad professional knowledge and wealth of technical expertise. I appreciate the care and thought he has taken to ensure my professional development and my successful integration here in Marburg.

I am particularly grateful to Dr. Reiner Westmann for his friendly support in all adminstrative matters concerning my status as student of the Philipps University Marburg.

I also would like to thank Dr. Annette Bieller for very helpful discussions about technical problems with molecular biology methods.

For the generous gift of some of the primers used to characterize the TNFα system and IL-1 system my thanks go to Dr. Micheal Bette and Dr. Christian Ulke.

Special thanks should go to Herrn Uwe Schneider and Dr. Ulrich Rausch for their efforts to manage the internet network and keep me online. This was extremely helpful for preparing this thesis.

My deep gratitude goes to Frau Barbara Wiegand for her day to day suppport in the laboratory work and for managing the ordering of reagents.

I would like to thank Frau Heike Reichert-Preibsch for her assistance in the cell culture laboratory and teaching me good laboratory practice.

For the tissue dissection, I would like to give special thanks to Dr. Johannes Tebbe who first taught me how to dissect the rat dorsal root ganglion and to Herrn Michael Schneider for his help not only with tissue preparation but also for the organization of the animal experiments.

I am grateful to Frau Marion Zibuschka and Frau Elke Rodenberg-Frank for teaching me immunohistochemical procedures, to Frau Heidi Hlawaty for teaching me cutting cryosections and to Frau Heidemarie Schneider for support in the photographic documentation.

Last not least I would like to say a very special thank you to the head of the department of Molecular Neuroscience, Herrn Professor Dr. E. Weihe, not only for giving me the privilege to work with him and learn from him, but also for his most generous support, his valuable scientific advice and his critical, but most constructive comments of preparing this thesis. I consider myself very fortunate that he taught me critical scientific thinking and that he was willing to share with me his scientific visions on the neuroimmune connection in the pain pathway.